

https://dspace.org/

Experimental investigations into a passive auto-tuning mass damper

Carlisle, Meaghan

2014-03-11
http://hdl.handle.net10539/14095

Downloaded from a DSpace repository. https://dspace.org/

Experimental Investigations into a Passive Auto-Tuning Mass Damper

Meaghan Carlisle

A research report submitted to the Faculty of Civil and Environmental Engineering, University of the Witwatersrand, Johannesburg, in partial fulfilment of the requirements for the degree of Master of Science in Engineering.

Johannesburg, July 2013

DECLARATION

I declare that this research report is my own unaided work. It is being submitted to the Degree of Master of Science to the University of the Witwatersrand, Johannesburg. It has not been submitted before for any degree or examination to any other University.

……

Meaghan Carlisle

…… day of …… 2013

ABSTRACT

A passive auto-tuning mass damper (PATMD) is a vibration control device that consists of a mass which is suspended in the top region of a structure and is forced into motion, due to inertia, when the structure is excited. A steel test structure is used to carry out the experimental investigation. The PATMD is connected to the structure to be controlled by a group of inelastic ropes and is free to move in any translational direction. It moves relative to the structure, utilising and dissipating large amounts of energy as it swings from side to side, and in this way, the vibrational energy of the structure is absorbed and consequently the vibrations of the structure are controlled.

First, the 'PATMD efficiency tests' are carried out, whereby the test model is subjected to translational, torsional and coupled free vibration tests, initially without the PATMD and then with the PATMD, in order to determine the damping effects of the PATMD. The test model is then subjected to forced harmonic vibration tests similar to those described above and the damping effects are again analysed. These tests aim to demonstrate the PATMD's effectiveness in controlling the translational vibration in two directions, torsional vibration and coupled vibration, under both free and forced excitation, without being tuned.

Secondly, a parameter study is carried out whereby the dynamic properties of the primary test model are varied whilst the PATMD is left unchanged. The free and forced vibration tests are repeated. Finally, the properties of the PATMD are varied whilst the primary model remains unaltered. Again, the tests described above are repeated, without any tuning of the system taking place.

The results of the 'PATMD efficiency tests' demonstrate its capability of providing significant control to translational, torsional and coupled vibrations of the structure without being tuned in any way. Furthermore, the parameter study demonstrates the PATMD's effectiveness under very different conditions of the system, without having undergone any tuning or specific adjustment. The tests reveal that the PATMD is robust, uncomplicated and versatile making it an ideal application for engineering structures.

ACKNOWLEDGEMENTS

I would like to thank my supervisor, Dr Li for his support, encouragement, expert guidance and patience throughout this study. I would also like to thank Kenneth Harman and the laboratory staff at the School of Civil and Environmental Engineering for their help in setting up my test model for my research. Thanks to my parents, Janet and Paul for funding my studies and for the continual support. Thanks also to P.D. Naidoo and Associates for contributing to the funding of my Master's degree. Lastly, I would like to thank Wesley, Rebecca and Marc for being boss-dogs.

TABLE OF CONTENTS

Declaration ..... **i**

Abstract ..... **ii**

Acknowledgements ..... **iii**

Table of Contents ..... **iv**

List of Figures ..... **viii**

1. INTRODUCTION **1**

1.1 General 1

1.2 Objectives of Study 2

1.3 Scope 3

2. LITERATURE REVIEW **4**

2.1 An Introduction to Vibration Control 4

2.1.1 Different Vibration Control Techniques 8

2.1.2 The History of Dampers 12

2.2 Dampers and Detuning 15

2.2.1 Passive Vibration Control with Applications 15

2.2.1.1 Tuned Mass Damper (TMD) 15

2.2.1.2 Multiple Tuned Mass Damper (MTMD) 19

2.2.1.3 Impact Damper 23

2.2.1.4 Base Isolation 24

2.2.2 Active Vibration Control with Applications 25

2.2.3 Semi-Active Vibration Control with Applications 27

2.3 Dampers and Torsional Vibration 31

3. EXPERIMENTAL METHOD **34**

3.1 Introduction 34

3.2 Experimental Structure and Set-up 34

3.2.1 PATMD Efficiency Tests 34

3.2.2 Changing the Model's Stiffness 38

3.2.3 Changing the Model's Mass 39

3.2.4 Changing the PATMD's Mass Ratio 41

3.2.5 Changing the PATMD's Connection to the Test Model 41

3.3 Experimental Procedure 43

3.3.1 Free Vibration Tests 43

3.3.2 Forced Vibration Tests 44

4. PATMD EFFICIENCY TESTS **45**

4.1 Free Vibration 45

4.1.1 Translational Vibration in the X-Direction 45

4.1.2 Translational Vibration in the Y-Direction 47

4.1.3 Torsional Vibration 48

4.1.4 Coupled Vibration (Translation in X-Direction and Torsion) 50

4.1.5 Coupled Vibration (Translation in Y-Direction and Torsion) 51

4.2 Forced Vibration 53

4.2.1 Translational Vibration in the X-Direction 53

4.2.2 Translational Vibration in the Y-Direction 53

4.3 Summary and Conclusions 54

5. EFFECTS OF CHANGING MODEL'S STIFFNESS **55**

5.1 Free Vibration 55

5.1.1 Translational Vibration in the X-Direction 55

5.1.2 Translational Vibration in the Y-Direction 57

5.1.3 Torsional Vibration 59
5.1.4 Coupled Vibration (Translation in the X-Direction and Torsion) 60
5.1.5 Coupled Vibration (Translation in the Y-Direction and Torsion) 62
5.2 Forced Vibration 63
5.2.1 Translational Vibration in the X-Direction 63
5.2.2 Translational Vibration in the Y-Direction 64
5.3 Summary and Conclusions 64

6. EFFECTS OF CHANGING THE MODEL'S MASS 65

6.1 Free Vibration 65
6.1.1 Translational Vibration in the X-Direction 65
6.1.2 Translational Vibration in the Y-Direction 67
6.1.3 Torsional Vibration 68
6.1.4 Coupled Vibration (Translation in the X-Direction and Torsion) 69
6.1.5 Coupled Vibration (Translation in the Y-Direction and Torsion) 71
6.2 Forced Vibration 72
6.2.1 Translational Vibration in the X-Direction 72
6.2.2 Translational Vibration in the Y-Direction 73
6.3 Summary and Conclusions 73

7. EFFECTS OF CHANGING THE MASS RATIO 74

7.1 Free Vibration 74
7.1.1 Translational Vibration in the X-Direction 74
7.1.2 Translational Vibration in the Y-Direction 75
7.1.3 Torsional Vibration 76
7.1.4 Coupled Vibration (Translation in the X-Direction and Torsion) 76
7.1.5 Coupled Vibration (Translation in the Y-Direction and Torsion) 77
7.2 Forced Vibration 78

7.2.1 Translational Vibration in the X-Direction 78
7.2.2 Translational Vibration in the Y-Direction 79
7.3 Summary and Conclusions 80

8. EFFECTS OF CHANGING THE PATMD CONNECTION 81

8.1 Free Vibration 81
8.1.1 Translational Vibration in the X-Direction 81
8.1.2 Translational Vibration in the Y-Direction 82
8.1.3 Torsional Vibration 83
8.1.4 Coupled Vibration (Translation in the X-Direction and Torsion) 84
8.1.5 Coupled Vibration (Translation in the Y-Direction and Torsion) 85
8.2 Forced Vibration 86
8.2.1 Translational Vibration in the X-Direction 86
8.2.2 Translational Vibration in the Y-Direction 87
8.3 Summary and Conclusions 88

9. CONCLUSIONS 89

10. FURTHER RESEARCH 91

BIBLIOGRAPHY 92

APPENDIX A: Prokon Simulations A-1

APPENDIX B: Photographs B-1

LIST OF FIGURES

CHAPTER 2

Figure 1. The 'world's first skyscraper', the Home Insurance Building, Chicago, 1884. ____5
Figure 2. The similar looking (a) Chrysler Building (1930); (b) 40 Wall Street Building (1930) and (c) the Empire State Building (1931). _____6
Figure 3. The Burj Khalifa compared to other well-known tall structures._____8
Figure 4. (a) The Wallace F. Bennett building and (b) the building without glazing, showing the buckling restrained bracing. _____9
Figure 5. The various aerodynamic alterations to corner geometry (Kareem, Kijewski and Tamura, 1999). _____10
Figure 6. The Shanghai World Financial Center b) The Burj Khalifa. _____11
Figure 7. The Petronas Towers in Kuala Lumpur. _____12
Figure 8. One of the first dampers used in structural engineering (Taylor, 2003). _____14
Figure 9. A schematic representation of a TMD system. _____16
Figure 10. The tuned mass damper (TMD) situated in the Taipei 101 building, Taiwan. ___17
Figure 11. A TMD on the roof of a multi-story building._____17
Figure 12. The bi-TMD system proposed by Ok, Song and Park, 2008. _____20
Figure 13. Three types of tuned mass dampers: (a) series MTMDs (b) parallel MTMDs, and (c) multiple DOF TMD (Zou, 2009). _____21
Figure 14. The Burj Al Arab contains an MTMD in its exoskeleton. _____22
Figure 15. The buffered impact damper proposed by Li and Darby (2006). _____24
Figure 16. A base isolation system. _____25
Figure 17. An active control system. _____26
Figure 18. The Hankyu Chayamachi Building which utilises the heliport as the damper mass. _____27
Figure 19. The AVS system proposed by Kobori and Sakamoto (1996). _____29
Figure 20. The SAIVS-TMD device proposed by Nagarajaiah and Varadarajan (2004). ___30
Figure 21. The SMTD in use in the Citicorp Center. _____30
Figure 22. The Capella Tower. _____32
Figure 23. The Kyobashi Seiwa Building in Tokyo (Soong and Spencer, 2002). _____33

CHAPTER 3

Figure 24. (a) The primary test model (b) The test model containing the PATMD (c) A view from above. 36
Figure 25. The primary model's first three natural frequencies and corresponding mode shapes. 36
Figure 26. The experimental setup showing the test model, accelerometer, data logger and computer. 37
Figure 27. A schematic diagram of the experimental setup. 37
Figure 28. A Prokon illustration of the three heights at which the model was tested in order to vary the model's stiffness- 0.5m, 0.75m and 1m respectively. 38
Figure 29. Photographs of the three heights at which the model was tested in order to vary the model's stiffness- 0.5m, 0.75m and 1m respectively. 39
Figure 30. A Prokon illustration of the three masses at which the model was tested – 14kg, 20kg and 32kg respectively. 40
Figure 31. Photographs of the three masses at which the model was tested – 14kg, 20kg and 32kg respectively. 41
Figure 32. A photograph of the three different damper masses used to create different mass ratios–2.5%, 5% and 7.5% respectively. 41
Figure 33. An illustration of the different PATMD connection configurations that were tested. 43

CHAPTER 4

Figure 34. Power spectral density (PSD) of the acceleration response for free vibration in the X-direction. 46
Figure 35. Time history of acceleration response for free vibration in the X-direction. 46
Figure 36. Power spectral density (PSD) of the acceleration response for free vibration in the Y-direction. 47
Figure 37. Time history of acceleration response for free vibration in the Y-direction. 48
Figure 38. Power spectral density (PSD) of the acceleration response for free torsional vibration. 49
Figure 39. Time history of acceleration response for free torsional vibration. 49

Figure 40. Power spectral density (PSD) of the acceleration response for free coupled vibration (translation in the X-direction and torsion). 50
Figure 41. Time history of acceleration response for free coupled excitation (translation in the X-direction and torsion). 51
Figure 42. Power spectral density (PSD) of the acceleration response for free coupled excitation (translation in the Y-direction and torsion). 52
Figure 43. Time history of acceleration response for free coupled excitation (translation in the Y-direction and torsion). 52
Figure 44. Power spectral density (PSD) of the acceleration response of the model under forced excitation in the X-direction. 53
Figure 45. Power spectral density (PSD) of the acceleration response of the model under forced excitation in the Y-direction. 54

CHAPTER 5

Figure 46. The PSD and time-history of acceleration graphs for free translational vibration in the X-direction for model heights of 0.5m, 0.75m and 1m respectively. 57
Figure 47. The PSD and time-history of acceleration graphs for free translational vibration in the Y-direction for model heights of 0.5m, 0.75m and 1m respectively. 58
Figure 48. The PSD and time-history of acceleration graphs for free torsional vibration for model heights of 0.5m, 0.75m and 1m. 60
Figure 49. The PSD and time-history of acceleration graphs for free coupled vibration (translation in the X-direction and torsion) for model heights of 0.5m, 0.75m and 1m. 61
Figure 50. The PSD and time-history of acceleration graphs for free coupled vibration (translation in the Y-direction and torsion) for model heights of 0.5m, 0.75m and 1m respectively. 63
Figure 51. The PSD graphs for forced vibration in the translational X-direction for model heights of 0.5m, 0.75m and 1m respectively. 63
Figure 52. The PSD graphs for forced vibration in the translational Y-direction for model heights of 0.5m, 0.75m and 1m respectively. 64

CHAPTER 6

Figure 53. The PSD and time-history of acceleration graphs for free translation in the X-direction for model masses of 14kg, 20kg and 32kg respectively. 66
Figure 54. The PSD and time-history of acceleration graphs for free translation in the Y-direction for model masses of 14kg, 20kg and 32kg respectively. 68
Figure 55. The PSD and time-history of acceleration graphs for free torsional vibration for model masses of 14kg, 20kg and 32kg respectively. 69
Figure 56. The PSD and time-history of acceleration graphs for free coupled vibration (translation in the Y-direction and torsion) for model masses of 14kg, 20kg and 32kg respectively. 70
Figure 57. The PSD and time-history of acceleration graphs for free coupled vibration (translation in the X-direction and torsion) for model masses of 14kg, 20kg and 32kg respectively. 72
Figure 58. The PSD graphs for forced translational vibration in the X-direction for model masses of 14kg, 20kg and 32kg respectively. 72
Figure 59. The PSD graphs for forced translational vibration in the Y-direction for model masses of 14kg, 20kg and 32kg respectively. 73

CHAPTER 7

Figure 60. The PSD graphs for free translational vibration in the X-direction for mass ratios of 2.5%, 5% and 7.5%. 75
Figure 61. The PSD graphs for free translational vibration in the Y-direction for mass ratios of 2.5%, 5% and 7.5%. 75
Figure 62. The PSD graphs for free torsional vibration for mass ratios of 2.5%, 5% and 7.5%. 76
Figure 63. The PSD graphs for free coupled vibration (translation in the X-direction and torsion) for mass ratios of 2.5%, 5% and 7.5%. 77
Figure 64. The PSD graphs for free coupled vibration (translation in the Y-direction and torsion) for mass ratios of 2.5%, 5% and 7.5%. 78
Figure 65. The PSD graphs for forced translational vibrations in the X-direction for mass ratios of 2.5%, 5% and 7.5%. 79

Figure 66. The PSD graphs for forced translational vibrations in the Y-direction for mass ratios of 2.5%, 5% and 7.5%. _____80

CHAPTER 8

Figure 67. The PSD graphs for free translational vibration in the X-direction for the different connecting configurations of the PATMD._____82
Figure 68. The PSD graphs for free translational vibration in the Y-direction for the different connecting configurations of the PATMD._____83
Figure 69. The PSD graphs for free torsional vibration for the different connecting configurations of the PATMD. _____84
Figure 70. The PSD graphs for free coupled vibration (translation in the X-direction and torsion) for the different connecting configurations of the PATMD._____85
Figure 71. The PSD graphs for free coupled vibration (translation in the Y-direction and torsion) for the different connecting configurations of the PATMD._____86
Figure 72. The PSD graphs for forced translational vibration in the X-direction for the different connecting configurations of the PATMD. _____87
Figure 73. The PSD graphs for forced translational vibration in the Y-direction for the different connecting configurations of the PATMD. _____88

Chapter 1

INTRODUCTION

1.1 General

The control of the dynamic response of structures to certain loads is an important focus of study in Civil Engineering, aiming to eliminate unwanted vibrations and to maintain a safe and comfortable environment for the inhabitants of a structure. Vibrations can occur in floor systems of tall, flexible buildings, due, most commonly, to excitation from human activity, wind, and seismic activity. The dynamic nature of these loads can cause vibrations which are not usually a safety concern but rather a serviceability issue, causing discomfort to the occupants. One way of decreasing the vibrations in an existing structure is to change the building's stiffness or mass; however this may not be a viable solution due to space limitations, construction disruptions and cost.

In relatively recent years, the research of vibration control on Civil Engineering structures has increased with the development of active and passive control devices. Passive control devices are those which are activated by the excitation of the structure and possess no feedback capability. They seem to be favoured due to the fact that they do not require power for their use as well as their mechanical simplicity and efficiency. A common passive control device which is frequently featured in the literature is the Tuned Mass Damper (TMD). The World Trade Center Towers (1973) in New York and the John Hancock Tower (1976) in Boston were among the first practical applications of this type of control device. Since then,

a number of high-rise buildings, towers, bridges, chimneys and mast structures have been fitted with a TMD in order to suppress wind induced vibrations.

Although TMDs have been widely successful in many applications around the world, they possess two main shortfalls, their sensitivity to detuning and their lack of efficiency in controlling torsional and coupled vibration. For this reason, a passive auto-tuning mass damper (PATMD) is proposed, which aims to eliminate these shortcomings and create a vibration control device which is simple, yet also feasible and effective.

1.2 Objectives of Study

It is obvious from observing the results of TMD applications that this system of vibration control for the protection of Civil Engineering structures has been an effective solution. As stated above, although TMDs have achieved a great amount of success, the main shortfall of their use is their need to be tuned to a particular modal frequency and the fact that their efficiency depends strictly on this frequency. Unfortunately, the structure's frequencies can change with time due to changes in the building's use or occupancy and changes to non-structural elements. These modifications may adjust the building's mass or stiffness and therefore alter its modal frequencies. Furthermore, errors in predicting the natural frequency of the structure are inevitable as well as inaccuracies in the fabrication of the TMD.

Generally, a TMD is used only to control one frequency of the structure – the frequency to which it has been tuned. However, a real-life structure will clearly contain more than one natural frequency as it can vibrate in a few translational directions (all with different frequencies), as well as in torsional and coupled directions (also with separate frequencies). Theoretically, each frequency to be controlled would require its own TMD. The proposed PATMD aims to independently control multiple frequencies of the structure.

A further shortcoming of typical TMDs is that they do not effectively control torsional and coupled vibration which could be present in tall, slender buildings.

The objective of this research is therefore to come up with a passive vibration control device which can control more than one frequency of the structure. It should be robust, so that if the

conditions of the system change for some reason, it does not run the risk of becoming detuned. It must be capable of controlling torsional and coupled vibrations, as well as translational vibrations on tall structures. Furthermore, it must be effective, but also simple and practical, so that it can be adapted for use in real-life structures.

1.3 Scope

The research contained in this research report is presented in the following order:

Chapter 2 contains the 'Literature Review', which presents a comprehensive summary of the literature that is available on a number of different types of vibration control devices that have been developed. 'An Introduction to Vibration Control' discusses how the need for damping devices came about and documents the different ways in which vibrations on structures can be controlled. 'Dampers and Detuning' discusses the pertinent problem of the detuning of TMD systems and considers various solutions. 'Dampers and Torsional Vibration' discusses torsional vibration control.

Chapter 3 contains the 'Experimental Method', which outlines the various processes that were undertaken in carrying out this research. It describes the experimental setup used for the tests, as well as the experimental procedure followed.

Chapters 4 to 8 contain the 'Results and Discussion', which present the results in graphical form, as well as summarising the outcomes of the experimental tests and discussing any observations.

Chapters 9 and 10 contain the 'Conclusions' and 'Further Research' respectively. Chapter 9 summarises the findings that can be drawn from the experimental test results and Chapter 10 lists a few areas of the study which should be investigated further.

Chapter 2

LITERATURE REVIEW

2.1 An Introduction to Vibration Control

In recent years, many office and apartment type buildings have evolved from being relatively short, sturdy, low-rise structures to tall, slender, lightweight assemblies. There are many factors which have led to this structural evolution including the emergence of innovations such as reliable elevators; electric lights and mechanical plumbing pumps; and more importantly new construction materials and structural design and analysis techniques. An increasing population meant that more space was required to accommodate everyone, especially in business districts as economic growth took place. The emergence of the skyscraper brought with it a number of new challenges for the architects, designers and contractors.

The first generation of 'tall buildings' were no higher than 7-storeys and were built from heavy masonry walls. The loads were supported by these walls which got wider and wider towards the base as the structure got taller. Although the great amount of space taken up by the masonry walls was undesirable, they provided a considerable amount of stiffness to the building, and gave it attractive damping characteristics.

The 10-storey steel-framed Home Insurance Building in Chicago constructed in 1884 is considered to be the 'world's first skyscraper'. It was the first building to be supported by a structural steel frame, and weighed about a third of what it would have weighed had the usual heavy masonry or stone been used. This new type of construction allowed for more floor space and windows but city officials were so concerned and uncertain about this ground-breaking approach that they halted the project whilst a safety investigation was carried out (Landau and Condit, 1996).



Figure 1. The 'world's first skyscraper', the Home Insurance Building, Chicago, 1884.

The Home Insurance Building was constructed in the middle of a 'skyscraper battle' which took place in the 1880's between Chicago and New York as they fought to be the leading metropolis with the most impressive skyline. The race to be the tallest building ensued in busy business districts as skyscraper design and construction became a more viable option. A few decades later, the Chrysler Building (1930) and 40 Wall Street (1930) both in New York were also involved in a 'battle' for the coveted title (Ali, 2005). At completion, the Chrysler Building stood at the same height as its rival project, however 40 Wall Street designer, H. Craig Severance changed the originally announced height, and increased the building by 3 storeys, quickly announcing it 'the tallest building in the world' at 283m. Not to be outdone,

William Chrysler obtained permission for a 38m spire to be placed at the Chrysler Building's peak, giving it the title of world's tallest building at 319m. This title was short-lived however, as the Empire State building was completed 11 months later and stood at 443m making it the world's tallest building for the next 40 years (Ali and Moon, 2007). Although these impressive heights were accomplished through the emergence of the steel frame system and other technological advancements, excessive structural material was still being used, making these structures fairly over-designed and uneconomical.

(a) (b) (c)



Figure 2. The similar looking (a) Chrysler Building (1930); (b) 40 Wall Street Building (1930) and (c) the Empire State Building (1931).

A new generation of economical and efficient structures emerged in about the 1960s. This was due to the design of tall structures being optimised as a result of the development of sophisticated structural modelling packages and the advent of lighter materials. Advances in material science saw the development of high-performance and light weight steel, concrete-

steel composite systems, megaframes and tube systems. Walls were no longer load-bearing, as curtain walls containing glass, copper cladding and louvres emerged. The results were not all positive though. The lighter sections which were being used caused structures to have much higher flexibility and reduced damping characteristics. This is particularly a problem with skyscrapers, which are subjected to large wind loads as they travel higher. The accelerations in buildings increase rapidly with increasing height, causing unwanted vibrations in the structure's floor systems (Schmidt, 2012).

Furthermore, in areas susceptible to seismic activity, as a structure becomes taller and more flexible, the structure's natural frequencies become closer to the forcing frequencies which would be experienced in an earthquake. The structure's response would therefore be magnified as it nears resonance. The Grand Hyatt hotel in San Francisco provides guests with a note on a windy day advising them that there may be creaking noises as the building gently sways back and forth in the wind. Even with an engineer's assurance that this movement is not a structural concern but rather a serviceability issue, the inhabitants often find it disconcerting and some even suffer from motion sickness in severe cases (Feblowitz, 2010). Therefore, even if the vibrations are not a structural integrity concern, an acceptable level of comfort needs to be provided to the occupants of the building.

The world's tallest building, the Burj Khalifa is shown in red below, compared to a number of other skyscrapers. Following America's domination of skyscraper construction in the 1900's, super-tall building construction has slowed in the area and there are now only two American buildings in the top ten, the Sears Tower and the new World Trade Center. Six of the top ten are situated in Asian countries and two are in the Middle-East. The surge of super-tall structures has happened relatively quickly making the development of effective vibration control techniques imperative.

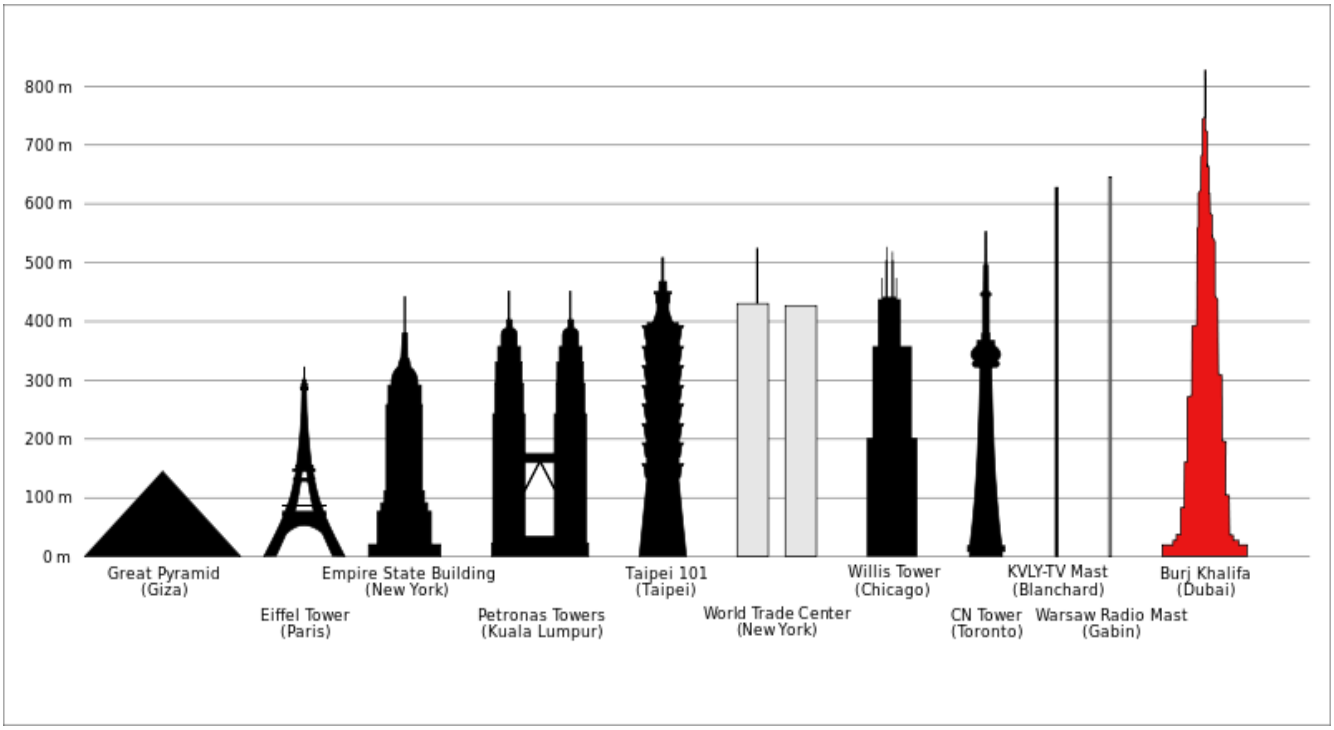

Figure 3. The Burj Khalifa compared to other well-known tall structures.

2.1.1 Different Vibration Control Techniques

There are a few ways in which the excessive vibrations on a structure can be dealt with. The first way is to alter the mass or stiffness - typically of an existing structure which is experiencing excessive vibration. In this way, the structure's dynamic properties will be modified and the structure's dynamic response can be reduced. New structural elements such as shear walls or bracing can be added to the existing building or beam/column jacketing could be performed in order to strengthen members. However, these modifications are often not feasible due to cost restraints, space restraints and aesthetic reasons.

The eight storey reinforced concrete Wallace F. Bennett Federal Building which was built in the 1960's is situated near to the Wasatch fault in Utah. There were concerns that the building would not perform well under an earthquake, and in 2001 the owner elected to rehabilitate the building in order to prevent collapse during a seismic event with a 475 year return period. In order to cause the minimum disruption to the occupants, a braced frame system to be added to the exterior of the building was selected. A total number of 344

buckling restrained braces (BRBs) were installed, each having a yield force of between 900kN and 8500kN (Brown, Aiken and Jafarzadeh, 2001).

(a)  (b) 

Figure 4. (a) The Wallace F. Bennett building and (b) the building without glazing, showing the buckling restrained bracing.

Secondly, in the case of tall, slender buildings, aerodynamic changes to the building's shape can limit the wind-induced vibrations on the building. Consideration of the wind in designing a skyscraper is paramount. Gravity loads are well understood and easy to deal with as they only act in one direction - down. However, wind loads at high altitudes are less predictable and are more complex. They can place extremely large lateral forces on tall structures, causing it to sway and twist (Mendis *et al*., 2007).

The shape of a building can significantly affect the wind forces it is subjected to and thereby its resulting motion. By changing the structure's aerodynamic properties, the vortex shedding phenomenon can be reduced (Amin and Ahuja, 2010). In buildings that are yet to be built, chamfered corners, openings in the structure and altering the buildings cross sectional shape with height can all be considered in order to reduce the wind-induced vibrations. In existing structures, the addition of fins/vented fins could have significant effects on the alongwind and crosswind response characteristics. Figure 5 below shows possible aerodynamic alterations

to a square building. Although an aerodynamically efficient plan shape can be an effective means of suppressing wind-induced loads, the size and value of saleable/rentable floor area may be reduced.

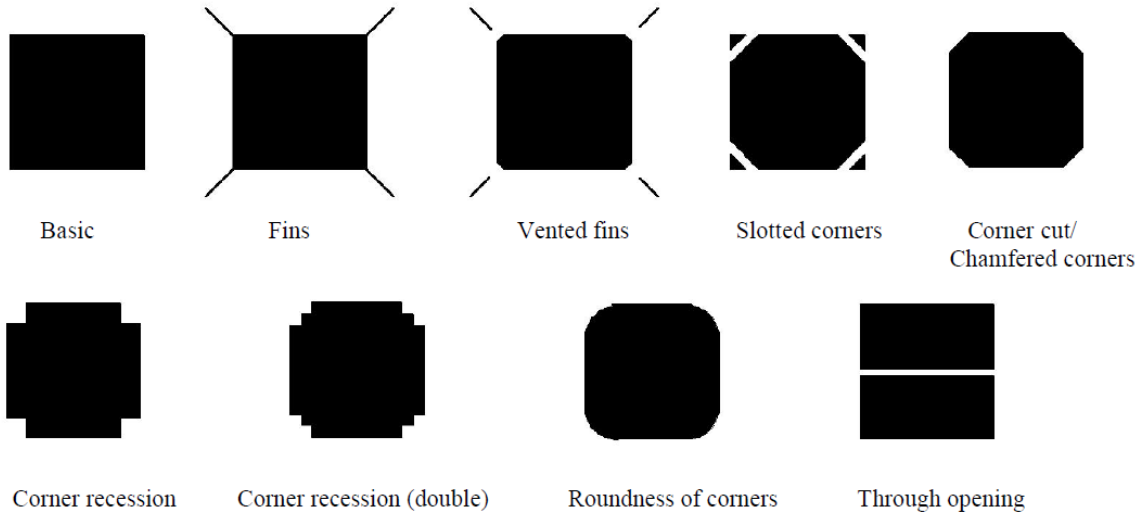

Figure 5. The various aerodynamic alterations to corner geometry (Kareem, Kijewski and Tamura, 1999).

The Shanghai World Financial Center was constructed with an opening near the top of the building in order to improve its resistance to adverse aerodynamic effects. It is often referred to as 'the bottle opener' due to its interesting shape, shown in Figure 6. The tallest building in the world, the Burj Khalifa was constructed with a tapering cross-section in order to 'confuse the wind' so that a strong flow pattern can't form (Feblowitz, 2010). The uneven cross-section prevents the wind from forming whirlpools or vortices around the building which would cause large loads on the structure. Over 40 wind tunnel tests were conducted on the Burj Khalifa in order to examine what effects the wind would have on the tower and its occupants. Tests were carried out on large structural analysis models and facade pressure tests were completed. As it stands, the Burj will still sway about 2 meters at the top. Interestingly, a new monitoring technology call *SmartSync* has been commissioned for the Burj. It will provide feedback about the building's behaviour and safety during earthquakes and wind storms, and will therefore be used to validate designer's predicted behaviours. This is a useful application in structures with vibration control in order to assess the results of this relatively new technology. Consequently, it allows appropriate changes to be made where necessary, in order to improve these applications going forward.

(a)  (b) 

Figure 6. The Shanghai World Financial Center b) The Burj Khalifa.

The third way in which excessive vibrations of buildings can be dealt with, is the addition of an auxiliary damping device. Unlike the mass and stiffness characteristics of a structure, damping is not an easily measurable physical property and is often difficult to engineer without the addition of an auxiliary damping system. There are two distinct types of vibration control devices which are commonly used. The first type converts kinetic energy into heat energy through the yielding of metals, the use of friction sliders or the deformation of viscoelastic solids and fluids such as fluid dampers, base isolators and viscoelastic dampers. The second type works by transferring energy from the building's movement, into a supplemental oscillator that absorbs the vibrations of the primary structure, such as the well-known tuned mass damper (TMD).

Professor Takuji Kobori was a pioneer in the development and implementation of structural control technology in the 1960s (Nagarajaiah, 2009). This is one of the reasons that Japan has been at the forefront of structural control applications in the past. There are currently over 2000 applications of base isolation; over 300 applications of passive dampers and over 40 applications of active dampers in Japan alone (Lynch, 1998).

Of the top ten tallest buildings in the world, four contain auxiliary damping devices – the Taipei 101 in Taiwan, the Shanghai World Financial Center in China and the two Petronas Towers in Kuala Lumpur (shown below in Figure 7). All four contain tuned mass dampers (TMDs) which will be expanded on in following sections. The six remaining buildings, the Burj Khalifa (Dubai), the Makkah Royal Clock Tower Hotel (Saudi Arabia), One World Trade Center (United Sates of America), the International Commerce Center (Hong Kong), the Zifeng Tower (China) and the Willis Tower (United States of America), do not make use of external damping mechanisms but rather use aerodynamic properties and/or structural systems (such as core and outrigger systems, tube systems and belt/bandage systems) to mitigate the structure's motion response.



Figure 7. The Petronas Towers in Kuala Lumpur.

2.1.2 The History of Dampers

The first application of dampers for vibration control occurred in the late 1800's after the development of large bore artillery and naval guns. There were several unsuccessful attempts to arrest gun recoil using coil springs and rubber blocks, which instigated research into the

use of hydraulic dampers. The first reported use of this type of control was by the British Army, who used hydraulic recoil dampers on gun carriages in 1862. The 75mm French field gun, model M1897, was the first gun containing the hydraulic recoil damper that was mass produced. This gun was considered to be a true 'technological marvel' and the first modern artillery piece. Thousands of these dampers were being used in guns by the end of World War I – some were even semi-active, meaning that the damping force was altered by changing the gun's elevation angle (Taylor, 2003).

The fluid damper then found fame in the automobile industry in the 1920's and 1930's. Automotive engineers found it particularly difficult to produce a car with a smooth ride over all road surfaces. Friction and rubber dampers produced marginal improvement and required a lot of maintenance; and the fluid damper was therefore introduced. The automotive shock absorbers that are used today are configured very similarly to the gun recoil buffers of WWI, except that they have a much greater life span (Taylor, 2003).

The fluid damper was also used extensively during the Cold War in missile isolators; however companies that manufactured them found few opportunities for their use after the war ended and therefore had to look for other possible applications of their damping products. One such company, Taylor Devices, connected with the National Centre for Earthquake Engineering Research (NCEER) in order to carry out joint research on fluid damped buildings and bridges. Existing military fluid dampers were installed onto small models of buildings which were placed on a shaking table and subjected to a dynamic load. It was found that the dampers were highly effective in increasing the structure's earthquake resistance. In 1993, 186 of these dampers were used on the five buildings of the Arrowhead Regional Medical Center in California which is located 3.2 kilometres away from the San Jacinto and 15 kilometres from the San Andreas active fault lines. One of the dampers is shown in Figure 8 below.

Viscoelastic dampers were first used structurally in the World Trade Centre buildings in New York in 1973. Ten thousand viscoelastic dampers were installed so as to limit the sway in the top floors to about 3 feet. The viscoelastic material absorbed the energy by being slightly displaced and then returning to its original position. These dampers have since been used in a

number of tall structures as an energy dissipating system, and are often used for structural retrofits due to their ability to easily be incorporated into an existing structure.



Figure 8. One of the first dampers used in structural engineering (Taylor, 2003).

Tuned mass dampers (TMDs) were first investigated in 1909 by Frahm to reduce the rolling motion of ships as well as for vibrations in ship hulls. He invented the undamped Dynamic Vibration Absorber (DVA). Den Hartzog introduced damping into Frahm's absorber in 1928, significantly improving its performance.

The John Hancock building in Boston (1973) was the first structural application of the TMD. It is 60 storeys high and consists of conventional steel framing. Not even a year after the completion of the building, a number of glass panes from the curtain wall started falling off of the structure, and during a particularly windy season in 1973, one third of the glass panes fell to the ground creating a danger for pedestrians below and causing damage to adjacent buildings. It was found that the glass pane connections had developed fatigue which caused cracks to develop, which in turn caused the glass panes to fail. The fatigue was attributed to an excessive swaying motion caused by wind loading. Analytical studies, including wind tunnel tests concluded that the sway was unacceptable, was causing serious discomfort to the

inhabitants and an immediate solution needed to be found. The tests showed that the building lacked stiffness in one direction, subjecting it to the 'P-delta' effect which could cause serious failure of the building. The building was stiffened by the addition of steel stiffeners, which doubled the stiffness in the weak direction. A longer term solution was needed to stabilise the building further, and two tuned mass dampers were installed (Nazario, 2000).

Since the development and early applications of the different types of dampers, much research has been done on each and they have subsequently been improved upon and used successfully in more recent applications, as will be described in the following sections.

2.2 Dampers and Detuning

2.2.1 Passive Vibration Control with Applications

2.2.1.1 Tuned Mass Damper (TMD)

Passive control devices have been around for a relatively long time when compared with active and semi-active control devices and have been successfully used in a number of structural applications. Many active and semi-active devices are still being researched, with several positive theoretical results being achieved but there are a few practical applications worldwide. The most common type of passive damper is the tuned mass damper (TMD). It is, in its basic configuration, a single degree-of-freedom (SDOF) auxiliary mechanism consisting of a mass, spring and a dashpot which is connected to the main structure. The TMD's natural frequency is tuned to the natural frequency of the fundamental mode of the structure and therefore, under excitation, the damper will resonate out of phase with the structure's motion due to inertia. In this way, a portion of the structure's vibratory energy is transferred to the TMD and is dissipated. In general, the TMD is tuned to the first modal frequency of the structure to be controlled since this frequency is dominant in the structure's behaviour after excitation.

The figure below shows a TMD attached to the structure to be damped. The terms m_1, K_1, C_1 and X_1 represent the mass, stiffness, damping and displacement of the structure respectively. The terms m_2, K_2, C_2, X_2 represent the mass, stiffness, damping and displacement of the TMD respectively. F(t) represents the excitation force acting on the structure and f(t) represents the force on the TMD (Abdelraheem Farghaly, 2012)

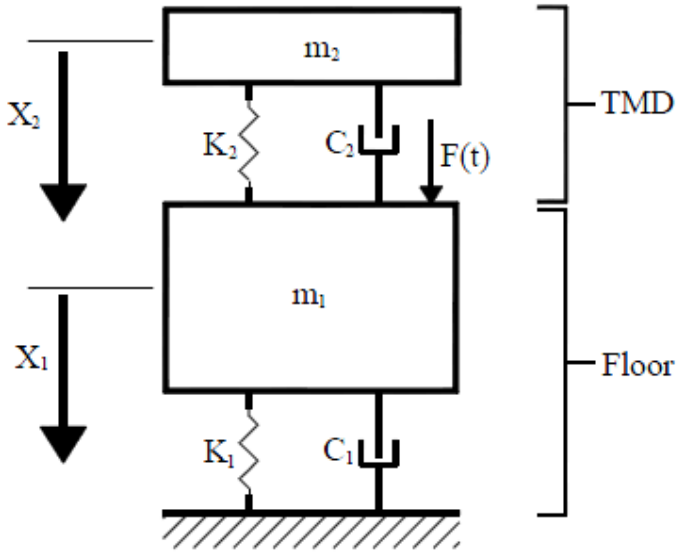

Figure 9. A schematic representation of a TMD system.

The equations of motion of this SDOF structure-TMD system were derived by Den Hartog (1928) and are given as:

$$m_1\ddot{X}_1(t) + C_1\dot{X}_1(t) + K_1X(t) - \left[C_2\{\dot{X}_2(t) - \dot{X}_1(t)\} + K_2\{X_2(t) - X_1(t)\}\right] = F(t) \quad (1)$$

$$m_2\ddot{X}_2(t) + \left[C_2\{\dot{X}_2(t) - \dot{X}_1(t)\} + K_2\{X_2(t) - X_1(t)\}\right] = f(t) \quad (2)$$

The Taipei 101, Figure 10, contains the world's most famous example of a TMD. The building combines passive control with aerodynamic properties and an effective structural system to mitigate excessive vibrations. It contains a mega-frame with a braced central core which is connected, via out-riggers, to eight super-columns. Furthermore, belt trusses are used to stiffen the whole system. The building sits just 200m from a major fault line in the city of Taipei, making it susceptible to seismic events as well as high winds and typhoons. For this reason, it was decided that a TMD, in the form of a 730 ton, giant circular pendulum was required. The sphere, which is made up of steel plates welded together, sits between the 87th and 92nd floors and sways to reduce movements in the building by 30 to 40 percent. The structure is designed so as to withstand gale force winds of 60m/s and an earthquake with a 2500 year return period (Kourakis, 2005).

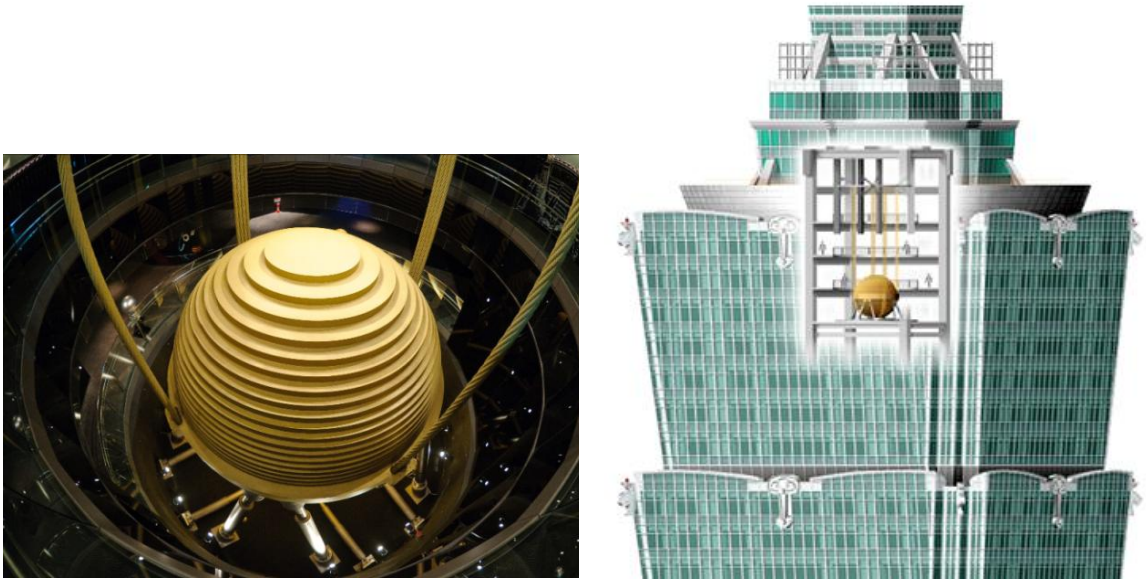

Figure 10. The tuned mass damper (TMD) situated in the Taipei 101 building, Taiwan.

TMDs can be used for the retrofitting of existing buildings, but often space is a limitation (Nawrotzki, 2006). An example of a TMD used for a structural retrofit is shown in Figure 11, where a mass has been placed on the rooftop of a multi-story building. The mass is made up of reinforced concrete and it rests on helical steel spring devices.



Figure 11. A TMD on the roof of a multi-story building.

TMDs have been proven to be effective in reducing the dynamic response of structures induced by narrow-band periodic excitation such as traffic and wind loads many times over. However, their effectiveness in mitigating earthquake induced vibrations is still a topic of controversial discussion. Some authors have reported that the seismic performance of TMDs with small mass ratios is poor (Kaynia, Veneziano and Biggs, 1981) whilst others (Hoang, Fujino and Warnitchai, 2008) found that TMD's with large mass ratios can be very effective in controlling vibrations. Nawrotzki (2006) found, in numerical simulations which he carried out, that the TMD improves the response behaviour by up to 40% for most of the investigated cases, but there are also models under seismic excitation without significant improvement. He then confirmed his positive findings by carrying out an experimental investigation in which he subjected a multi-story model to ten different earthquake signals. These include well known earthquakes such as the Kobe earthquake of 1995 (6.8 on the Richter scale) and the Mexico City earthquake of 1985 (8.1 on the Richter scale). Results showed that the peak amplitudes were reduced by more than 40% in most cases. A mass ratio of 1.5% - 4% was used, and it was concluded that a higher mass ratio contributed to higher damping.

Although, as shown above, TMDs have generally been successful in reducing the motion response of buildings under vibration excitation, it is well known that its main limitation is its capacity to become detuned. Changes to the building's mass or stiffness, which could come about due to changes in the buildings use or occupancy, or due to accidental changes or deterioration could cause a TMD to become detuned. During an earthquake, the structure could become damaged early on, thereby changing its natural frequency and rendering the TMD useless. Furthermore, there could be discrepancies between expected and actual properties of the structure. Hazra and Sadhu (2013) have proposed a structural health monitoring algorithm to assess the detuning of TMDs whilst in operation. Many existing applications of TMDs possess no feasible way of adapting their fundamental properties. Therefore, the current practice to overcome the detuning involves the determination of the primary structure's modal properties whilst inhibiting the TMD, and then 're-tuning' the TMD, which is a very expensive process.

2.2.1.2 Multiple Tuned Mass Damper (MTMD)

A number of researchers have studied multiple TMDs (MTMDs) in order to increase the TMD's effectiveness in vibration control and to reduce their sensitivity to detuning. A MTMD contains a number of dampers rather than a single damper. They can be used to control more than one mode of vibration in multiple degree-of-freedom systems (MDOF) or they can be used to control a single mode of vibration by having properties which are distributed around the single mode to be controlled.

Ok, Song and Park (2008) have proposed a bi-tuned mass damper in order to guarantee robust seismic performance of structures against detuning. The researchers explore the idea of using two small TMDs, termed a bi-TMD. The frequencies and damping ratios of the two TMDs are set to values close to the target value, which is the primary structure's fundamental frequency, rather than tuning them exactly. The performance of the bi-TMD is measured using two performance indices which evaluate its effectiveness – the 'nominal' index and the 'robust' index. The nominal index measures the bi-TMD's ability to reduce the building's motion response whilst the robust index measures the robustness of the bi-TMD under variations in the natural frequency of the structure. An optimisation process is used in order to obtain a method whereby the efficiency and the robustness can both considered in the results, as they are both equally important in the design. In order to compare the results obtained from the bi-TMD tests to the performance of a single TMD, the optimal parameters of a single TMD were determined from the Den Hartog formula given earlier which Ok *et al*. state is the most common design formula of a TMD in practical applications. It was found that the 'nominal' performance of the bi-TMD was not a significant improvement over the single TMD; however, the robustness was greatly improved.

Iwanami and Seto (1984) also proposed the use of two TMDs which they named a 'dual TMD' system. They showed that under harmonically forced vibration, the effectiveness of the dual TMD system was greater than a single TMD system, however, not significantly.

A few researchers have studied MTMDs which contain more than two TMDs. Xu and Igusa (1992) proposed a MTMD system which consists of a number of TMDs which have distributed natural frequencies close to the structure's fundamental frequency. Yamaguchi and Hampornchai (1993) found that from a given number of single TMDs, there exists an

optimum MTMD having the optimum frequency range and the optimum damping ratio. Furthermore, they found that the optimum MTMD is more effective than the optimum single TMD. They also concluded that a MTMD can be more robust than a single TMD.

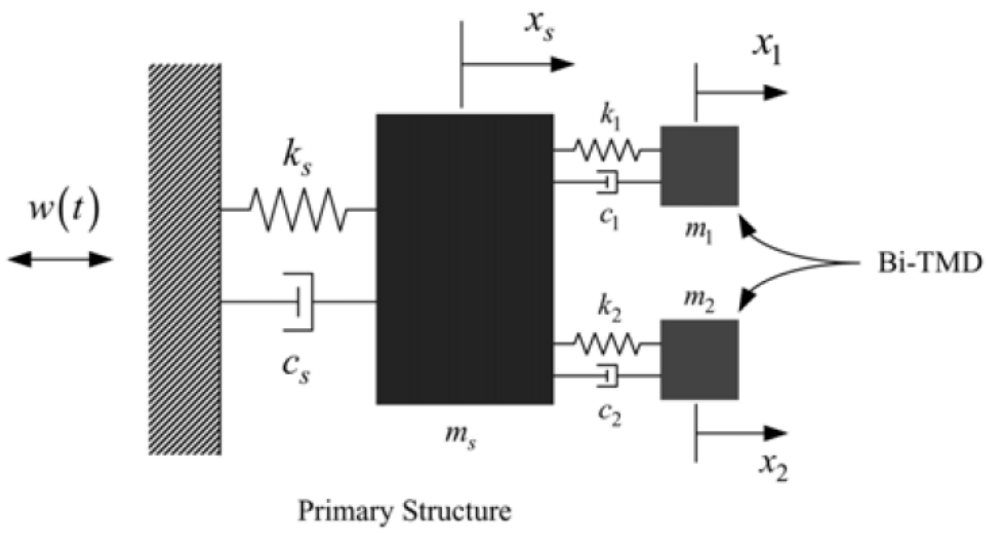

Figure 12. The bi-TMD system proposed by Ok, Song and Park, 2008.

Shariatmadar and Razavi (2010) have proposed a MTMD system which consists of one TMD placed at the top of the structure which is tuned to the first natural frequency of the structure, and a second TMD which is placed in one of the middle stories and is tuned to the second natural frequency of the structure. They found that the MTMD is more effective at suppressing the accelerations than a single TMD and furthermore, it was found to be more robust under different input motions. Lastly, they state that a MTMD is superior to a single TMD due to the fact that they occupy a much smaller space individually and can therefore be installed more easily, especially in the case of structural retrofits where available space may be limited.

An analysis by Bergman, MacFarlane and Kareem (1989) found that a main damper tuned to the structure's fundamental mode, as well as a few other strategically placed dampers with higher distributed frequencies produced the most effective results. MTMDs can be placed in one position or distributed around a building and can be designed in series or parallel configuration. Zuo (2009) researched the effectiveness of an MTMD attached to the primary

structure in series whilst Kareem and Kline (1995) researched MTMDs attached in parallel. Zuo (2009) found that series MTMDs are more effective and robust than the classic TMD; parallel MTMDs and multi-DOF TMDs under harmonic and random excitation. He found that series TMDs are virtually insensitive to changes in the mass of the primary system and that they are less sensitive to the parameter variances of the system than the other types of TMDs. Furthermore, Zuo (2009) has studied an efficient numerical algorithm to optimize the stiffness and damping of each of the TMDs in the MTMD system.

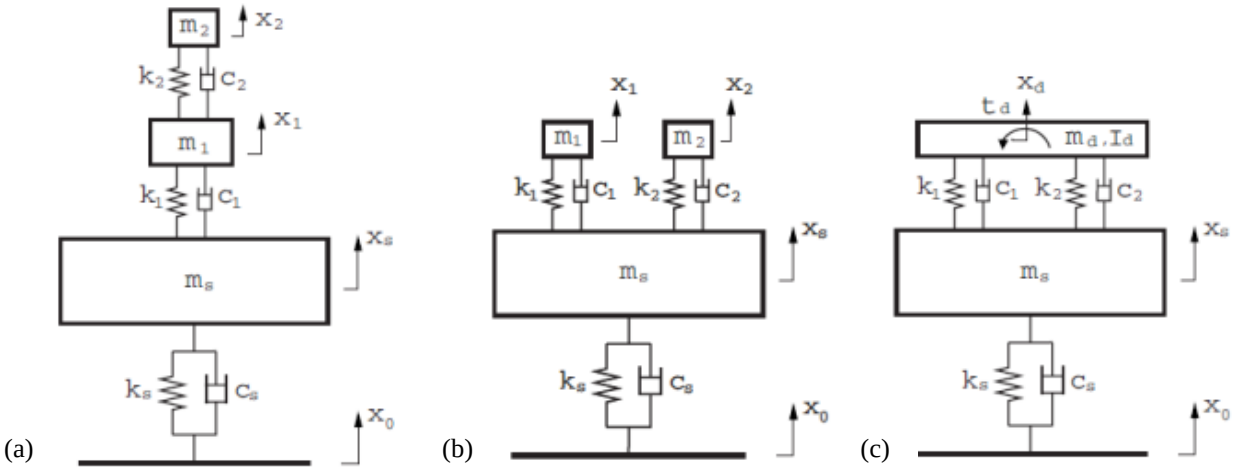

Figure 13. Three types of tuned mass dampers: (a) series MTMDs (b) parallel MTMDs, and (c) multiple DOF TMD (Zou, 2009).

In their parallel MTMD studies, Kareem and Kline (1995) warn that if the natural frequencies of the separate dampers of the MTMD are the same, the MTMD degenerates into a single TMD, which will be effective in controlling vibration motion, but will be no more robust than a single TMD. However, the distributed frequency range must not become too large either as this could impair the efficiency of the system, and the high frequencies could interfere with the higher modes of vibration of the primary system. They carried out a study to find out what effect a number of different variables have on controlling vibrations of a building which is subjected to wind loading. The variables included the number of dampers; the mass ratio of the individual dampers and the frequency range of the individual dampers in the MTMD. They found that the effect of adding more dampers to the system flattened the frequency response function. Furthermore, they found that MTMD systems with variable damper

masses were no more effective than MTMD systems with constant damper masses and they established that the frequency range of the dampers has the largest effect on the efficiency and robustness and is therefore the most important parameter. The mass and damping ratios, and the number of individual dampers play a secondary role in its performance. They also found a MTMD to be preferable to a single TMD due to portability and constructability; however the largest advantage is that the system will generally not be compromised if one of the dampers in the MTMD fails to function or becomes detuned.

The Burj Al Arab, a 322m hotel in Dubai, is equipped with a MTMD to control wind induced vibration, shown in Figure 14. It contains 11 four-ton TMDs which are attached to its exoskeleton. The TMDs are located in the columns on various storeys of the structure.



Figure 14. The Burj Al Arab contains a MTMD in its exoskeleton.

2.2.1.3 Impact Damper

A few other types of passive dampers which do not have to be tuned and therefore don't run the risk of becoming detuned have been researched and used in practice. An impact damper consists of a freely moving mass which is restricted by stops inside a 'container' which is mounted on the primary system to be controlled. The mass moves relative to the structure when it is excited, causing impacts between the mass and the stops which causes momentum to be transferred from the structure to the mass. Energy is thereby dissipated as heat, noise and high frequency vibrations. These dampers have been widely used in turbine blades, radar antenna, light poles and more recently, tall structures. However, the high noise levels, contact forces and accelerations generated in the primary structure are undesirable.

A few researchers have undertaken to reduce these unwanted results. Masri (1968) studied a 'multi-unit impact damper' which uses a number of small masses instead of one larger mass; Popplewell and Semercigil (1989) developed a 'bean-bag impact damper' which consists of a bag filled with spherical lead shots and Gharib and Ghani (2012) suggested a 'linear particle chain impact damper'.

An impact damper system however, also has its limitations. It can generally only control vibration in one direction and its performance can degenerate significantly if certain parameters are not optimised. The clearance between the stops, size of damper mass, and forcing frequency are all important parameters. A buffered impact damper studied by Li and Darby (2006), effectively reduces the accelerations, contact force and associated noise generated during the collision and is 'less sensitive to variation of excitation type, clearance and damper mass'. Hanging chain impact dampers are the most commonly used in practice and have been used in Australia and Japan in towers, masts and light poles to control wind-induced vibrations (Kareem, Kijewski and Tamura, 1999).

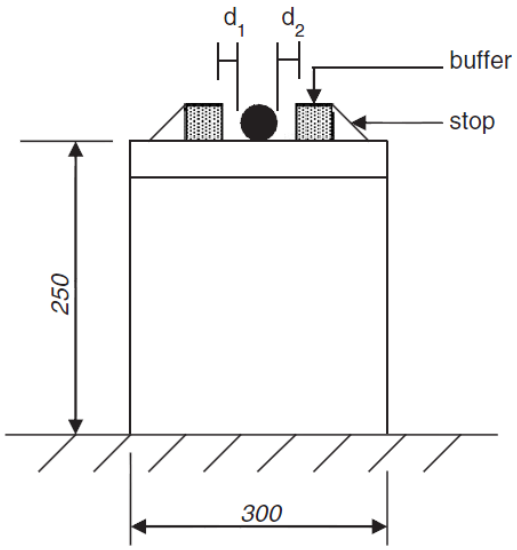

Figure 15. The buffered impact damper proposed by Li and Darby (2006).

2.2.1.4 Base Isolation

Base isolation is the most common type of passive vibration control currently in use around the world. A base isolator protects the structure from serious damage from seismic forces by decoupling the superstructure and the substructure. Base isolators were first used for structural application in 1985 in the Foothill Communities Law and Justice Center which is situated 20 kilometres from the San Andreas fault line and was designed for an earthquake measuring 8.3 on the Richter scale, which was thought to be the maximum feasible earthquake that could occur in that area. The building is supported on 98 high-damping rubber bearings (Clark, Aiken and Kelly, 1997). Base isolation can be used for both a new structure and a seismic retrofit of a structure. In the United States of America, a number of prominent monuments have been installed with base isolation in order to protect them from a major seismic event. The San Francisco City Hall is a large historical building that was severely damage in the 1989 Loma Prieta earthquake. It was 'cut from its foundation and made to float' on 530 isolators and shock absorbers which allows the building to sway up to 66cm.

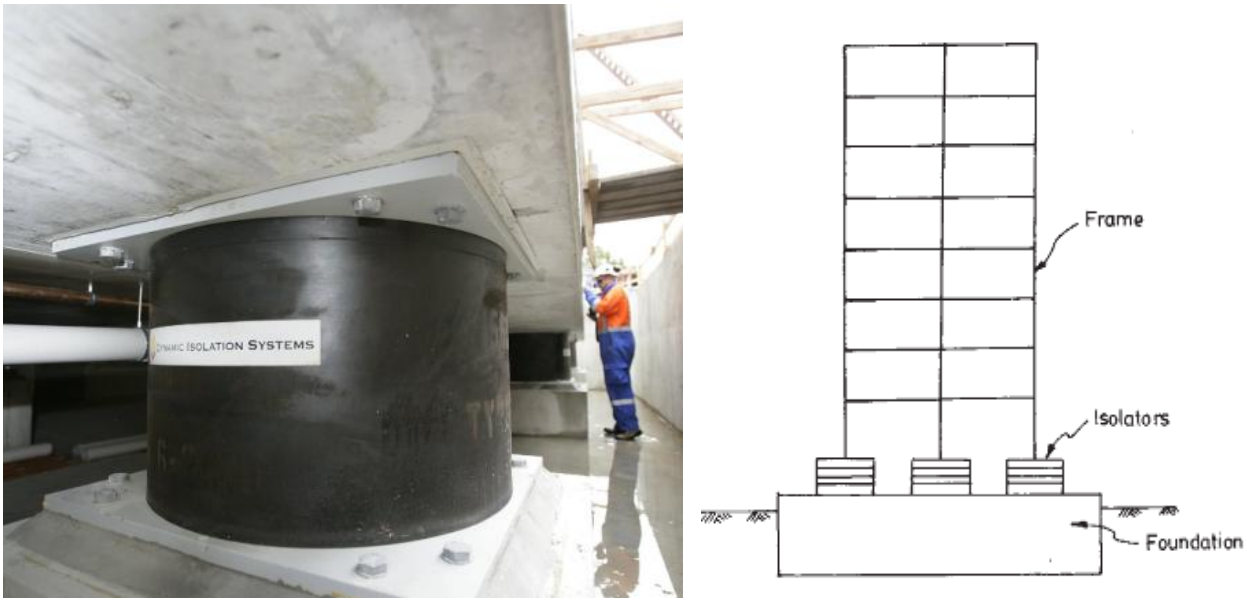

Figure 16. A base isolation system.

2.2.2 Active Vibration Control with Applications

An active TMD (AMD) is one which contains an external device (an actuator) in order to accelerate or decelerate the auxiliary mass. The activation of the auxiliary device is based on the measurement of the external disturbance. Sensors are used in order to measure this disturbance, and with the help of computers, the digital signal activates the required external force. The use of an AMD could help overcome the drawbacks of the TMD and MTMD systems, as they are more robust to tuning error if an appropriate feedback system is used. They can also provide a swifter response and have the ability to respond to changes in the system.

A number of issues have come about whilst trying to implement this type of control device in real life structures, which has prevented their wide application. Firstly, AMDs require substantial power to operate. Furthermore, it is difficult to accurately model the primary structure in order to ascertain its natural frequencies. The control algorithm is created based on the modelling, however if the model is inaccurate, it will not be able to effectively control the structure. Another issue is the time delay which occurs between the sensor picking up a motion of the structure and applying the control forces. This may cause the structure's motion and the control force to be unsynchronised, causing instability of the structure and

exacerbating the response (Datta, 2003). There are also questions relating to their reliability due to their infrequent activation and maintenance issues. Furthermore, their performance is limited by the capacity of the installed actuator (Scheller and Starossek, 2011).

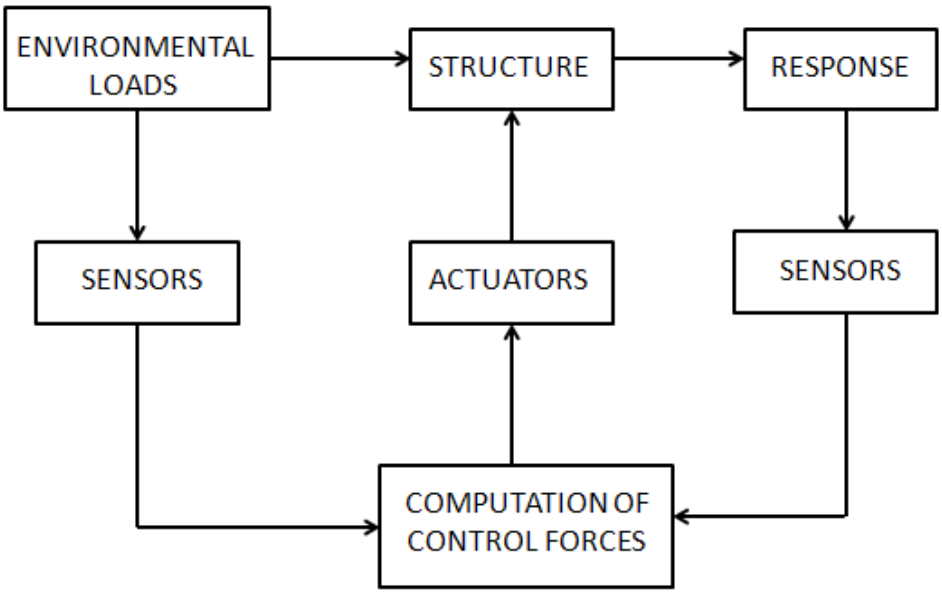

Figure 17. An active control system.

By 1998, Japan was the only country with applications of AMDs, and they had twenty at this time (Lynch, 1998). Much research was being carried out in this region due to the large number of earthquakes that affect the area. Most of these dampers worked well under wind-induced or moderate earthquake vibrations however, they would stop working when subjected to a large earthquake. Still, there have been a few notable applications of AMDs around the world. The first real building with active control technology was the Kyobashi Seiwa Building completed in 1989 in Japan and which will be discussed under 'Dampers and Torsion.' Since then, over 40 buildings in Japan have been installed with full-scale active control schemes. However, the large majority of these applications can only control small seismic events or wind excitation and the end goal is to develop an active control device which can perform successfully during a strong seismic event.

The Hankyu Chayamachi Building in Japan made use of the heliport on the roof to provide the mass of the AMD. The heliport, which rests on multi-stage rubber bearings was chosen

so as not to add any additional weight to the structure, whilst also saving money. Two 5 ton thrust actuators for the X and Y-directions increased the damping ratio by over 9% (Kareem, Kijewski and Tamura, 1999).

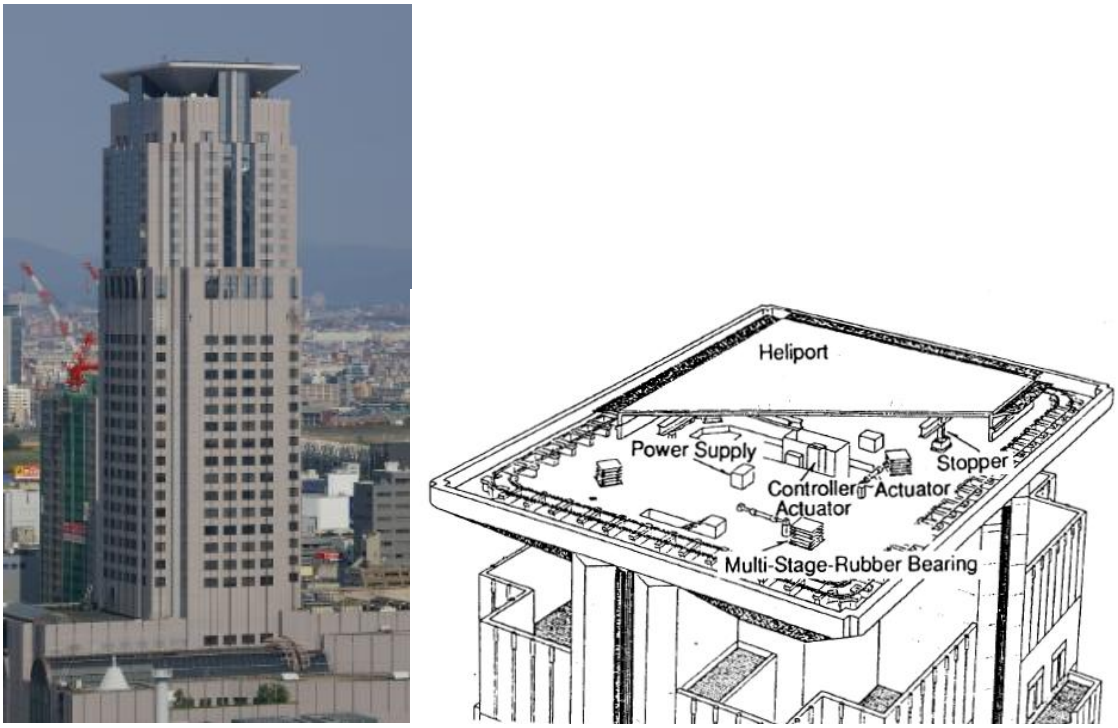

Figure 18. The Hankyu Chayamachi Building which utilises the heliport as the damper mass.

2.2.3 Semi-Active Vibration Control with Applications

The third broad category of vibration control is semi-active control. This type of control lies between passive and active on the control spectrum. In a semi-active system, the control device acts to remove the building from a state of resonance. The control action is produced by the movement of the structure but this is regulated by an external source of energy. The energy is used to change the mechanical properties of the device, such as the stiffness or damping coefficient rather than to provide the actual control force as in active systems. It was therefore developed in order to employ the best characteristics of both passive and active control devices. It uses less power than an active system and the required power is not dependant on the magnitude of the seismic excitation. A very significant advantage is that it also has a much lower chance of destabilising the structure than active control. It is also more reliable and less susceptible to detuning than a passive system. Lynch (1998) says that

the research of semi-active systems seems to be getting the most funding and looks to be the most promising type of vibration control going forward.
A number of different types of semi-active dampers have been researched and include: variable-orifice fluid dampers, variable stiffness devices, controllable friction devices, controllable tuned liquid dampers, controllable-fluid dampers and controllable impact dampers (Spencer and Sain, 1997).

The active variable stiffness (AVS) system has received significant attention and is shown in Figure 19. It can actively change the structural stiffness of a building during seismic excitation and in this way, it attempts to create a 'non-resonant' situation. Large V-shaped braces which are connected to variable stiffness devices are installed on each storey and are locked or unlocked by a controller. The devices are activated when a valve is opened, and the system is 'locked' in place when the valve is closed. The controller 'analyses' the seismic ground motions and in this way, chooses an appropriate stiffness which will alter the frequencies of the building so as to make sure that excessive motion of the building does not take place (Sakamoto & Kabori, 1996).

This system was successfully applied to a full-scale three storey steel structure which was built on a shaking table at the Kajima Technical Research Institute in Japan in 1990. Sensors placed at the base of the structure were used to study the seismic motion of the ground floor, and the information gathered by these sensors was sent to the AVS controller. If the ground floor accelerations exceed 10cm/s^2, the valve is opened and the brace system is engaged. The braces manipulate the structure's stiffness so as to create an optimum stiffness which relates to the lowest possible motion response from the structure. The system only requires about 20W per control device which means that an emergency generator would be capable of keeping the system going in the case of a power failure (Lynch, 1998).

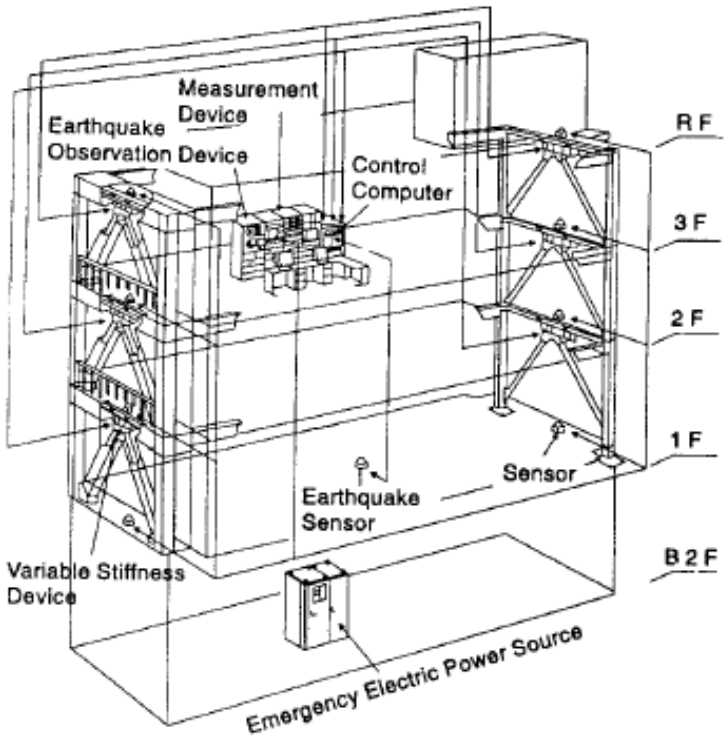

Figure 19. The AVS system proposed by Kobori and Sakamoto (1996).

A semi-active variable stiffness tuned mass damper (SAIVS-TMD) proposed by Nagarajaiah and Varadarajan (2004), is a variable stiffness damper which aims to counteract detuning by adjusting the stiffness automatically, as needed. The continuous retuning (in real time) is done using a semi-active control algorithm which tracks the excitation frequency (also in real time) by short term Fourier transform. The damper's frequency can either be tuned to the dominant excitation frequency or the structure's natural frequency – both give positive results.

The SAIVS is made up of four spring elements which are arranged in a rhombus shape and have pivot joints at the vertices as shown in Figure 20. The aspect ratio of the rhombus is altered by an actuator as needed, which varies the stiffness of the system between minimum and maximum stiffness. Nagarajaiah and Varadarajan (2004) analytically evaluated the performance of a 76-storey building with no damper; a TMD and a SAIVS. It was found that the SAIVS produced higher damping than the other two cases and was robust to changes in the building's stiffness.

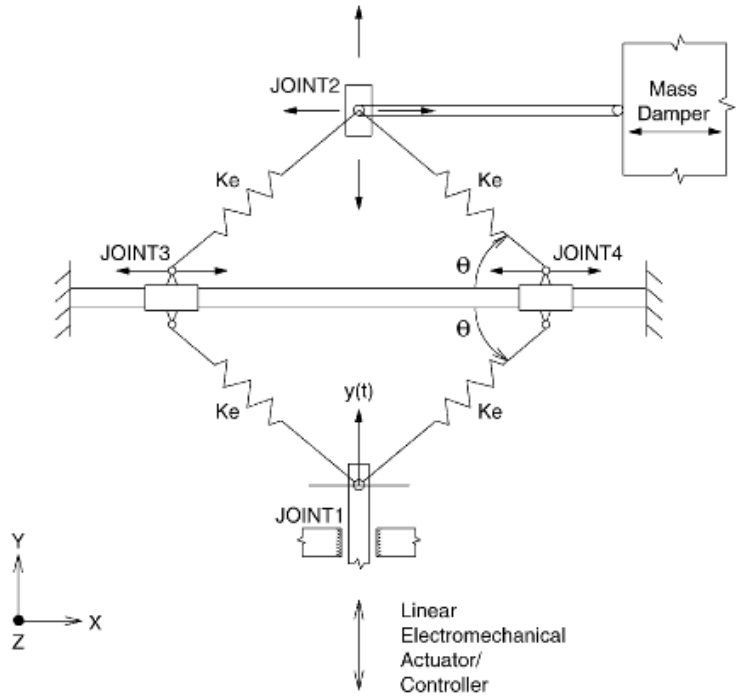

Figure 20. The SAIVS-TMD device proposed by Nagarajaiah and Varadarajan (2004).

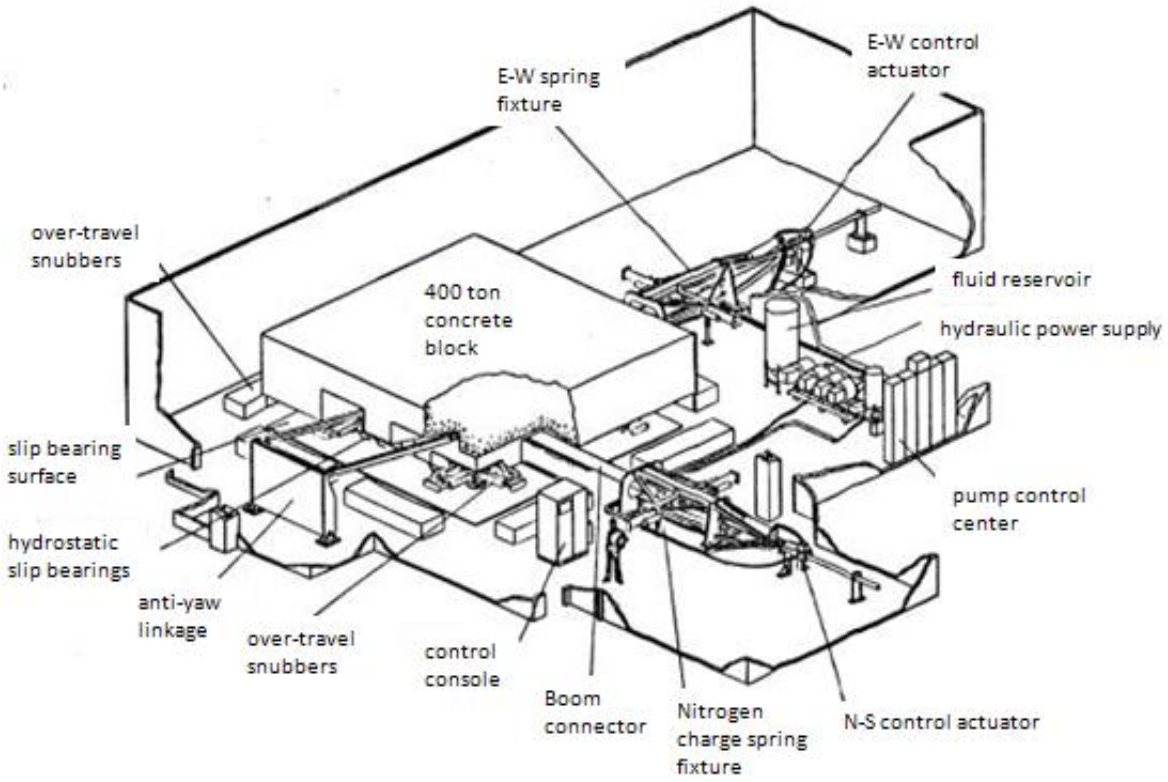

Figure 21. The SMTD in use in the Citicorp Center.

The Citicorp building in New York contains a semi-active TMD. The concrete mass is supported on low friction hydraulic bearings and connects to nitrogen springs. These springs provide the primary restoring force, however, the mass is also connected to two hydraulic actuators (one in the East-West direction and one in the North-South direction) which are used to 'fine tune' the stiffness of the TMD. Furthermore, they also help the mass to overcome the friction in the bearings (Nagarajaiah, 2009).

2.3 Dampers and Torsional Vibration

Although the research and application of the control of translational vibrations in structures has become more common, the control of torsional vibrations is significantly more challenging. Clearly as in translational motion control, increasing the stiffness of the structure will reduce the structure's torsional vibration response. A concept called the Vierendeel bandage has been implemented in the Capella Tower, formally known as First Bank Place in Minneapolis. The support of the structure is provided by a cruciform spine and steel columns whilst four massive composite supercolumns extend the full height of the building. The structure however lacked torsional stiffness and 3-storey Vierendeel bandages were implemented at three locations which tripled the buildings torsional stiffness whilst increasing the lateral stiffness by 36% (Kareem, Kijewski and Tamura, 1999).

In most of the studies described in the preceding text, the structure to be controlled was considered to be a SDOF system and the control devices were therefore designed only to deal with the first mode of vibration. However, in real life cases, the building always possesses multiple degrees of freedom (MDOF). Even if the plan is nominally symmetric, it will usually have some asymmetric features and will therefore undergo lateral as well as torsional vibrations simultaneously under purely translational excitation (Lin, Ueng and Haung, 1999). Therefore, simplifying a system to a SDOF system and thereby only considering the first mode of vibration could potentially overestimate the effectiveness of the damper as lateral-torsional coupling of the structure is ignored.



Figure 22. The Capella Tower.

Research has been done into reducing the torsionally coupled response of irregular structures by using auxiliary devices (Lin, Ueng and Haung (1999), Yoshida and Dyke (2005)). The control devices which have been studied for torsional control are mainly semi-active or active, and often multiple dampers are required in order for it to be effective against torsional vibrations. Lin, Ueng and Haung (1999) came up with the optimum design of two passive tuned mass dampers to control torsional vibrations of an irregular building. They state that it is not only the modal parameters of the primary structure that need to be considered, but also the location of the installed damper(s) and they present their research into its optimal placement. The TMDs installed into the John Hancock building were used to attenuate torsional as well as translational vibration. The two TMDs were installed at opposite ends of the 58th floor and help to control the movement when the building twists under wind loading.

As mentioned earlier, the Kyobashi Seiwa Building in Tokyo was the first application of an active damper. The building is 11 storeys high and consists of rigid steel frames. Again, two

dampers were used in order to control the first two modes of the structure (Datta, 2003). The first dominant mode of vibration is in the transverse direction, with a natural frequency of 0.88Hz. The second mode of vibration is in the torsional direction and has a natural frequency of 1.03Hz. The first AMD weighs 4 tons and is located in the center of the building, as close to the building's center of mass as possible; whilst the second, smaller AMD weighs 1 ton and is placed an eccentric distance from the center of mass in order to counteract torsion (Lynch, 1998). The sensors are placed in the basement, on the 6th floor and on the 11th floor and the computer is situated on the top floor. A hydraulic pump is used to actuate the masses and can respond to movement in one hundredth of a second. The AMDs weigh about 1.5% of the primary structure's mass and can reduce the torsional and translational response by up to one half or two thirds.

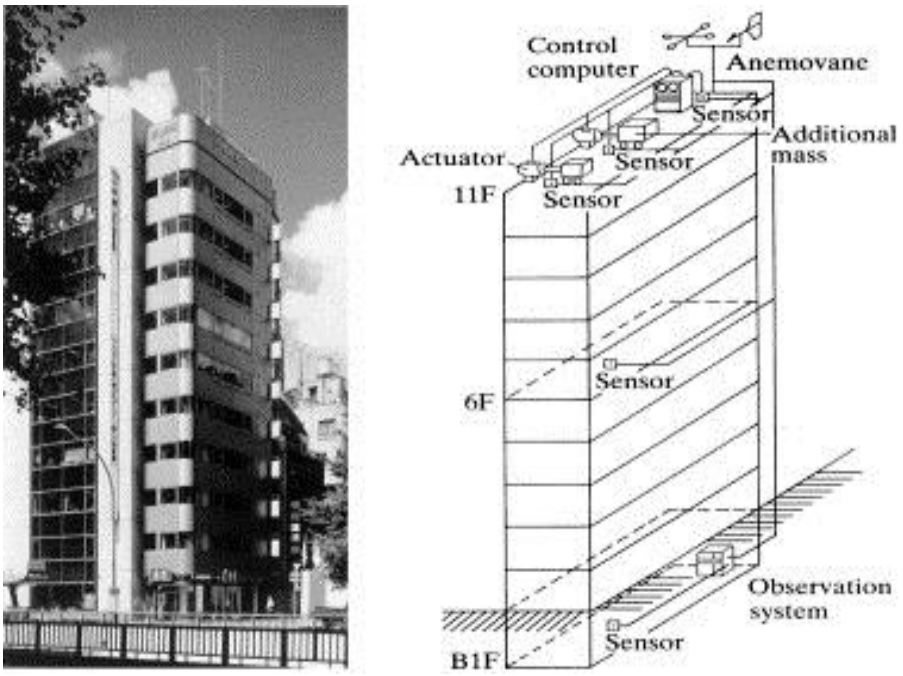

Figure 23. The Kyobashi Seiwa Building in Tokyo (Soong and Spencer, 2002).

Chapter 3

EXPERIMENTAL METHOD

3.1 Introduction

Two distinct types of tests were carried out during the experimental investigations. The first set of tests, the PATMD efficiency tests, aimed at evaluating the PATMD's effectiveness at controlling vibration and attenuating the response of the test structure. Its efficiency in controlling torsional and coupled vibration was particularly under review. Once the PATMD proved to be effective, a parameter test was carried out in order to evaluate its robustness against detuning. It was therefore tested under different conditions without 'tuning' the PATMD in any way. The natural frequencies of the primary (undamped) test model were altered by changing the stiffness or the mass of the test structure. Next, the natural frequencies of the PATMD were changed by altering its mass ratio and its connection to the test structure.

3.2 Experimental Structure and Set-up

3.2.1 PATMD Efficiency Tests

The PATMD efficiency tests evaluated the effectiveness of the proposed PATMD as a vibration control device. Experimental tests were carried out on a tall, flexible test model. The primary model is illustrated in Figure 24a, whilst the model containing the PATMD is

shown in Figure 24b and 24c. The primary model consists of four 1.3m high, 12mm threaded rod columns and a 300mm x 600mm x 10mm thick S355J mild steel plate. The plate is secured at a height of 1m using nuts. There are two more threaded rods which are connected to the plate and are used for the purpose of connecting the PATMD to the model. The columns are bolted rigidly to the base such that the ends are rotationally fixed, and the base is fixed to a unidirectional shaking table. Prokon was used to simulate the behavior of the primary model, and to determine its first three natural frequencies and associated mode shapes. It was ensured that the values of the dynamic properties obtained during the Prokon simulation closely matched those which would be expected for a real-life tall, flexible structure. A number of model dimensions were entered and simulated until suitable frequency values were obtained, and therefore suitable model dimensions were decided. The simulated model's first three natural frequencies, corresponding to the first three mode shapes are f_{n1} = 2.48Hz, f_{n2} = 2.55Hz and f_{n3} = 4.29Hz as shown in Figure 25. The Prokon simulations can be found in Appendix A. The aspect ratio of the model is perhaps not very similar to that of a real life structure, however the aspect ratio is not a critical property at this stage as the principle of the PATMD is under investigation in this report.

The PATMD, shown attached to the primary model in Figure 24b and 24c, is in the form of a 15cm square metal plate with a thickness of 10mm. It has a mass of 0.75kg which is about 5% of the primary model's mass of 14.13kg. It is tied, with inelastic ropes, to the six threaded rods at a height of 20cm above the plate and the damper mass sits 5cm above the plate. The rope was used in the experiments due to its inelastic and flexible nature.

The test setup is shown in a photograph in Figure 26 and in a schematic diagram in Figure 27. An accelerometer is attached to the primary model in order to measure the accelerations after excitation. The accelerometer is connected to a data logger which records the acceleration readings over time. The data logger is connected to a computer so that the data acquired during the test can be viewed, analysed and processed using the programs TCE Build and Matlab.

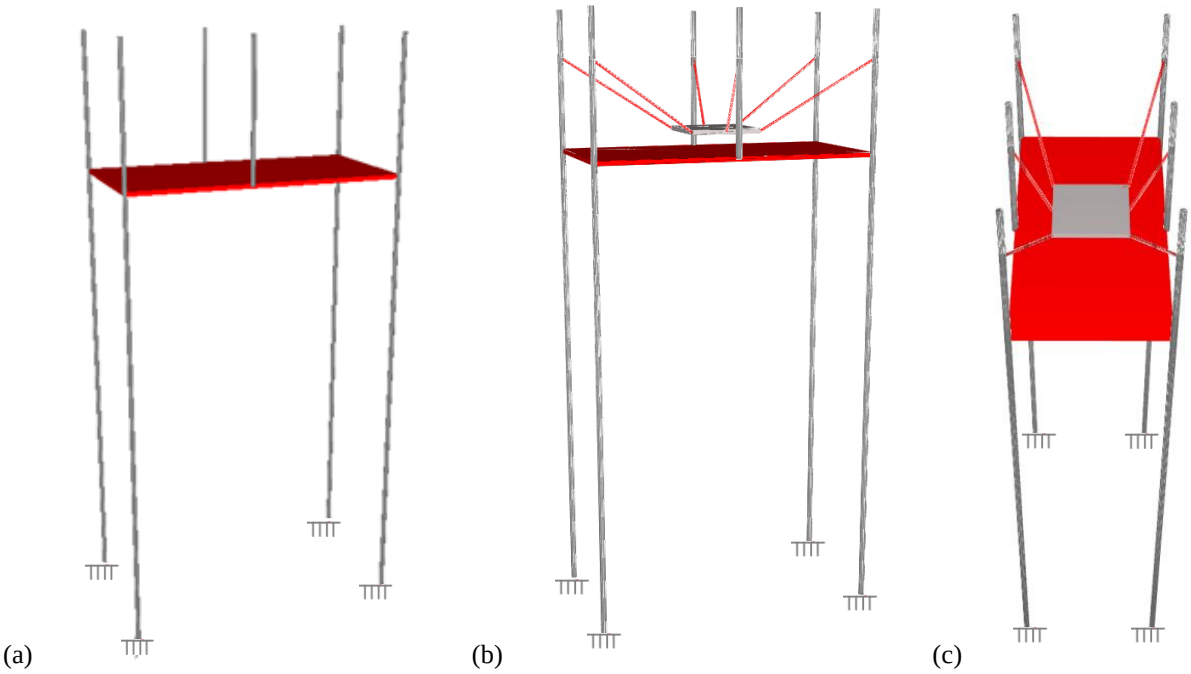

Figure 24. (a) The primary test model (b) The test model containing the PATMD (c) A view from above.

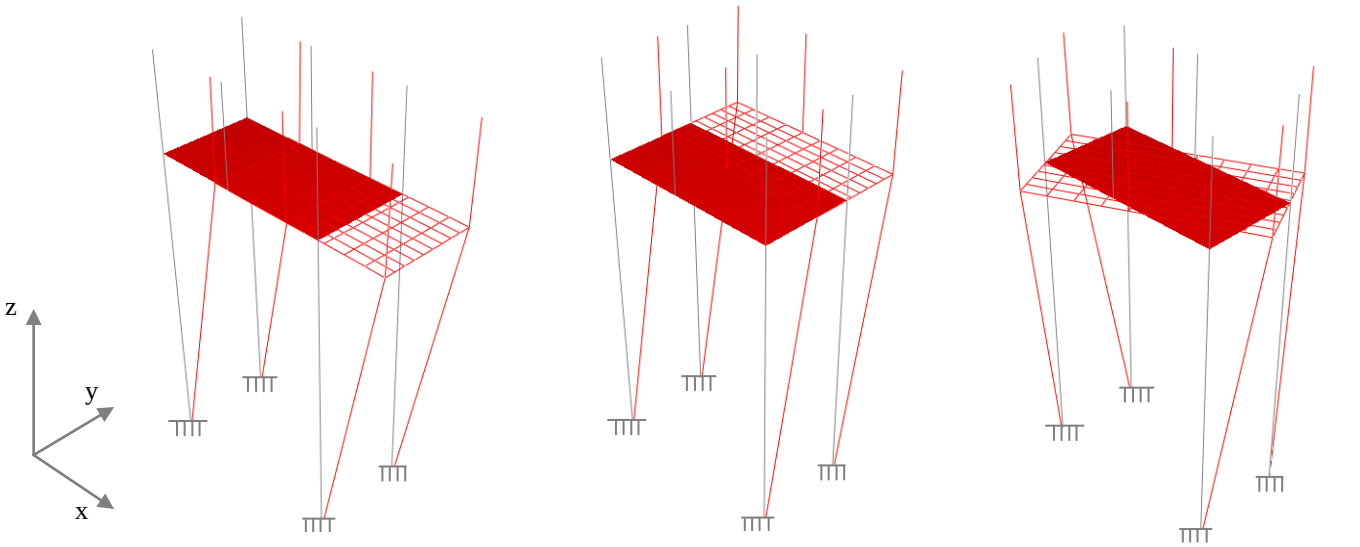

Mode 1 – Translation in the X-direction
Natural Frequency = 2.48Hz

Mode 2 – Translation in the Y-direction
Natural Frequency = 2.55Hz

Mode 3 - Torsion
Natural Frequency = 4.29Hz

Figure 25. The primary model's first three natural frequencies and corresponding mode shapes.

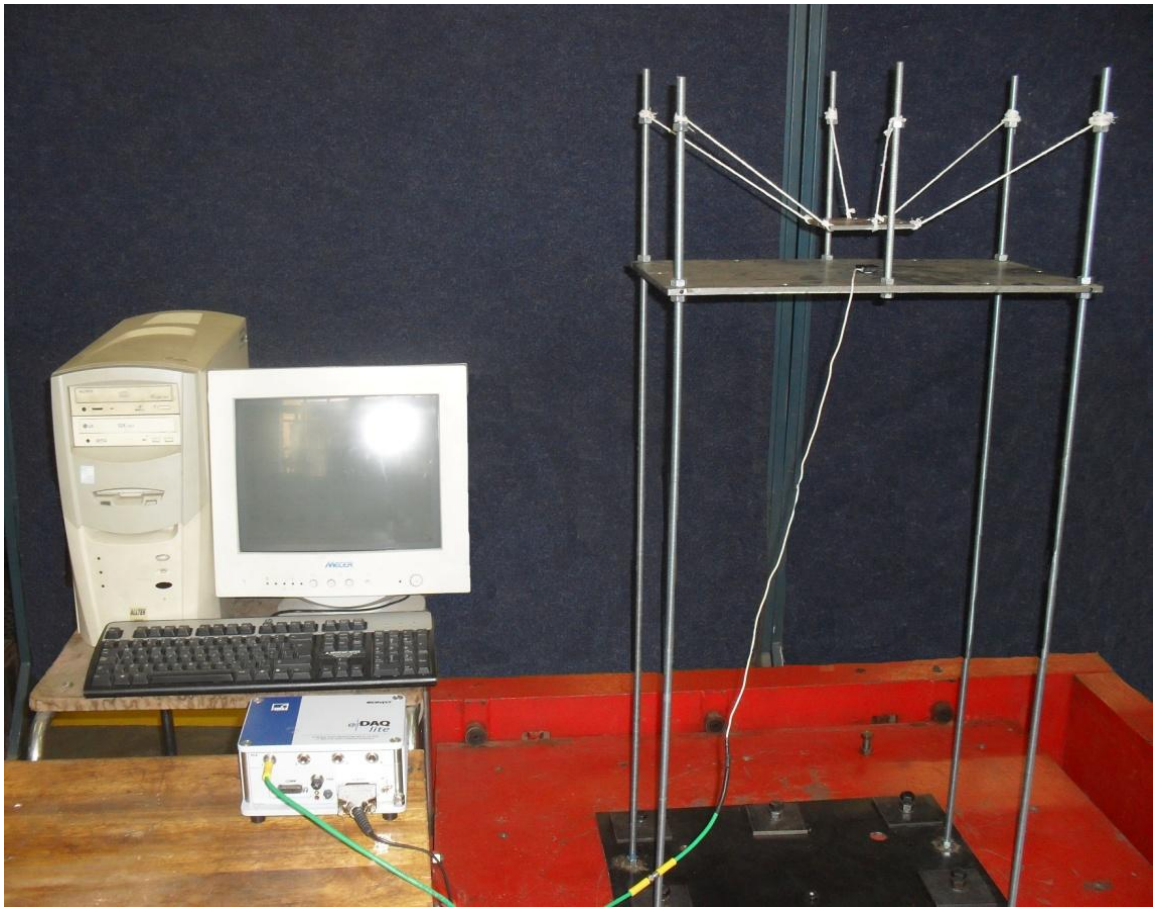

Figure 26. The experimental setup showing the test model, accelerometer, data logger and computer.

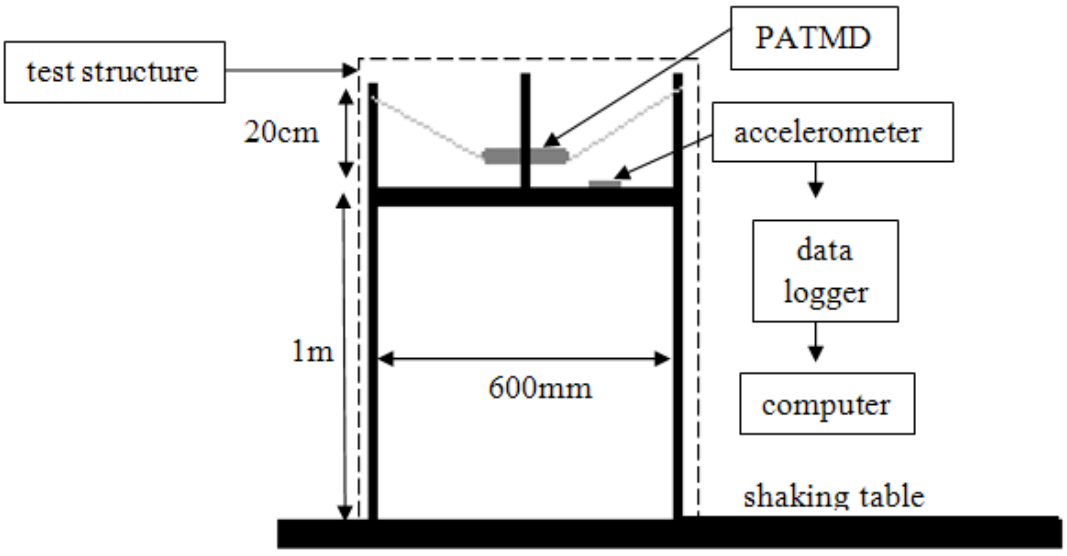

Figure 27. A schematic diagram of the experimental setup.

3.2.2 Changing the Model's Stiffness

The stiffness of the test model was changed by altering its height. The steel plate was moved up and down as needed and was secured to the threaded rod columns at various heights using nuts. The model was set to heights of 0.5m, 0.75m and 1m for the tests. The PATMD was not adjusted at all during these tests, the mass ratio was kept constant at 5% and the connection to the test model remained unchanged during the tests.

Again, a Prokon simulation was carried out in order to check the natural frequencies which could be expected in the experimental tests, prior to carrying them out. These analyses can be found in Appendix A. Figure 28 shows the three different Prokon models used in the simulations, whilst photos of the test structure at various heights are shown in Figure 29.

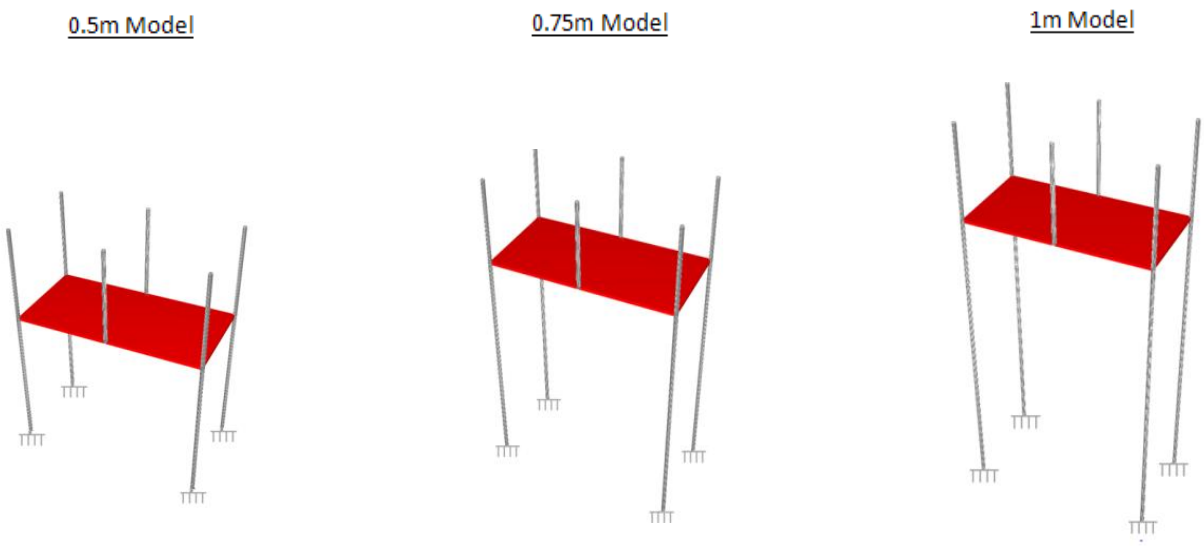

Mode 1 – Translation in the X-direction
Natural Frequency = 6.65Hz

Mode 2 – Translation in the Y-direction
Natural Frequency = 6.72Hz

Mode 3 – Torsion
Natural Frequency = 12.44Hz

Mode 1 – Translation in the X-direction
Natural Frequency = 3.77Hz

Mode 2 – Translation in the Y-direction
Natural Frequency = 3.79Hz

Mode 3 – Torsion
Natural Frequency = 5.83Hz

Mode 1 – Translation in the X-direction
Natural Frequency = 2.48Hz

Mode 2 – Translation in the Y-direction
Natural Frequency = 2.55Hz

Mode 3 – Torsion
Natural Frequency = 4.29Hz

Figure 28. A Prokon illustration of the three heights at which the model was tested in order to vary the model's stiffness- 0.5m, 0.75m and 1m respectively.

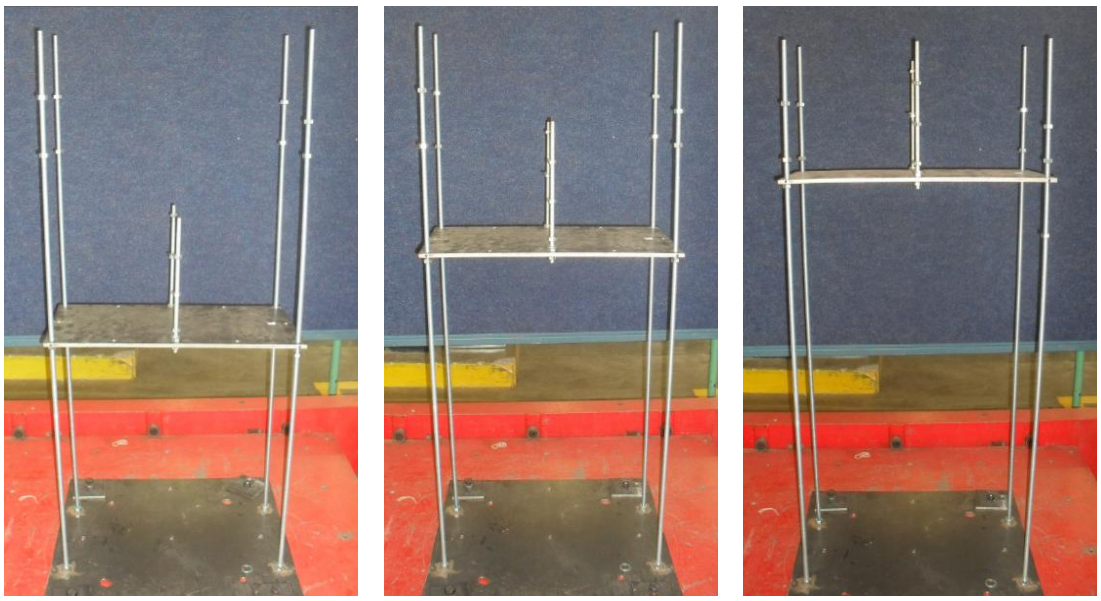

Figure 29. Photographs of the three heights at which the model was tested in order to vary the model's stiffness- 0.5m, 0.75m and 1m respectively.

3.2.3 Changing the Model's Mass

Next, the mass of the test model was varied whilst its height was kept constant at 1m. The PATMD was not adjusted during the tests; its mass was kept constant at 0.7kg and its connection to the test structure was left unchanged. The primary test structure's mass was 14kg, and extra weights were secured to the primary steel plate so that the required masses of 20kg and 32kg were achieved. These three model masses, shown in Figure 30 were considered for testing.

Again, a Prokon simulation was carried out in order to check the natural frequencies which could be expected in the experimental tests, prior to carrying them out. In Prokon, a thicker steel plate was considered in order to reach the required model masses. Figure 31 shows the three Prokon models considered in the simulations, which are presented in Appendix A.

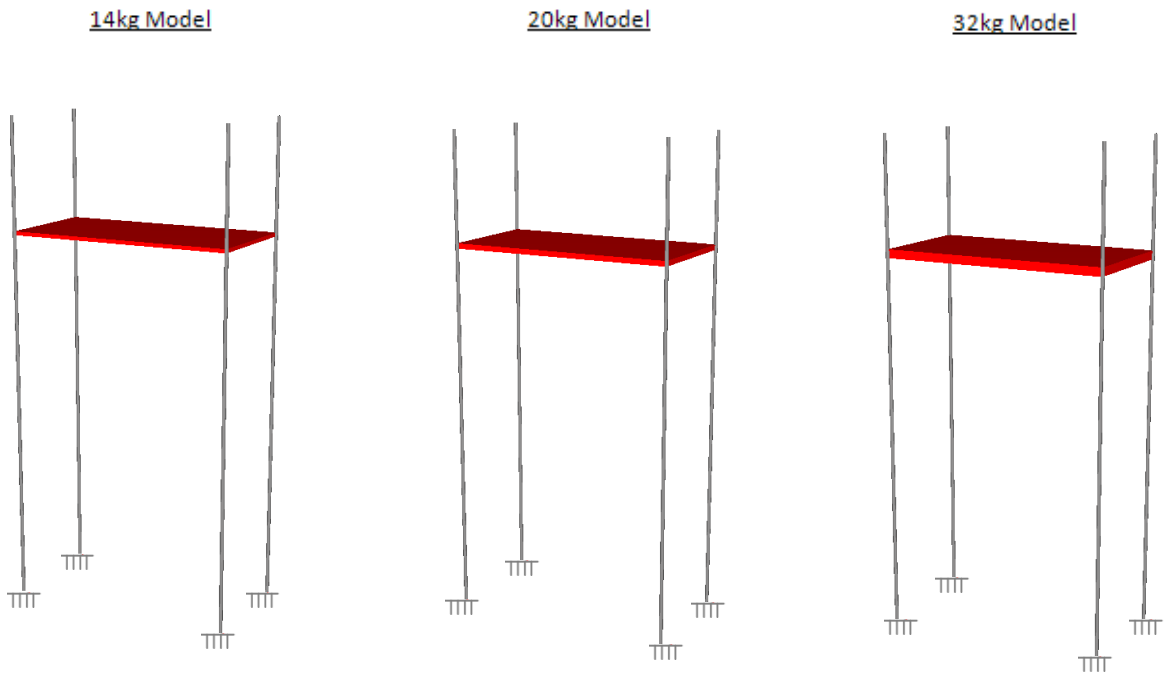

Mode 1 – Translation in the X-direction
Natural Frequency = 2.48Hz

Mode 2 – Translation in the Y-direction
Natural Frequency = 2.55Hz

Mode 3 – Torsion
Natural Frequency = 4.29Hz

Mode 1 – Translation in the X-direction
Natural Frequency = 2.04Hz

Mode 2 – Translation in the Y-direction
Natural Frequency = 2.13Hz

Mode 3 – Torsion
Natural Frequency = 4.47Hz

Mode 1 – Translation in the X-direction
Natural Frequency = 1.78Hz

Mode 2 – Translation in the Y-direction
Natural Frequency = 1.88Hz

Mode 3 – Torsion
Natural Frequency = 3.41Hz

Figure 30. A Prokon illustration of the three masses at which the model was tested – 14kg, 20kg and 32kg respectively.

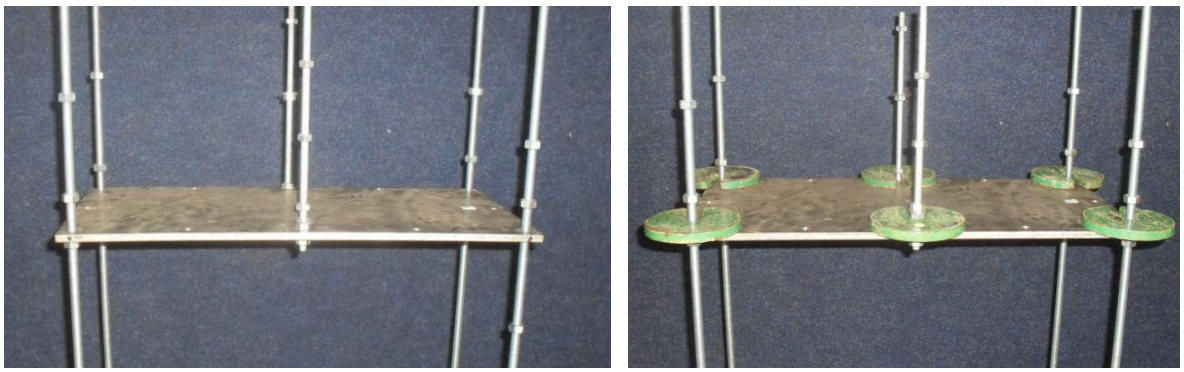

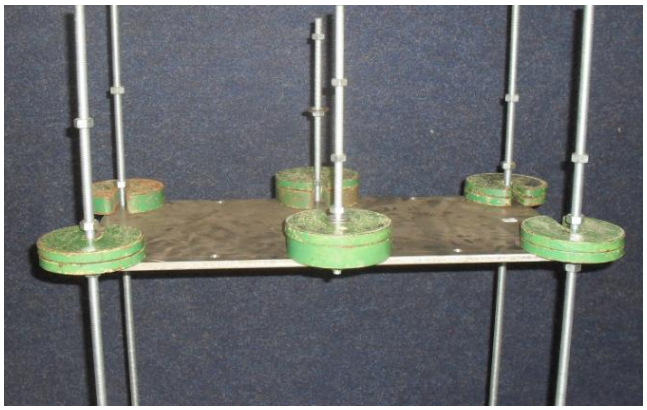

Figure 31. Photographs of the three masses at which the model was tested – 14kg, 20kg and 32kg respectively.

3.2.4 Changing the PATMD's Mass Ratio

A 2.5% mass ratio (0.35kg), a 5% mass ratio (0.7kg) and a 7.5% mass ratio (1.05kg) were considered in the tests, as shown from left to right in Figure 32 below.

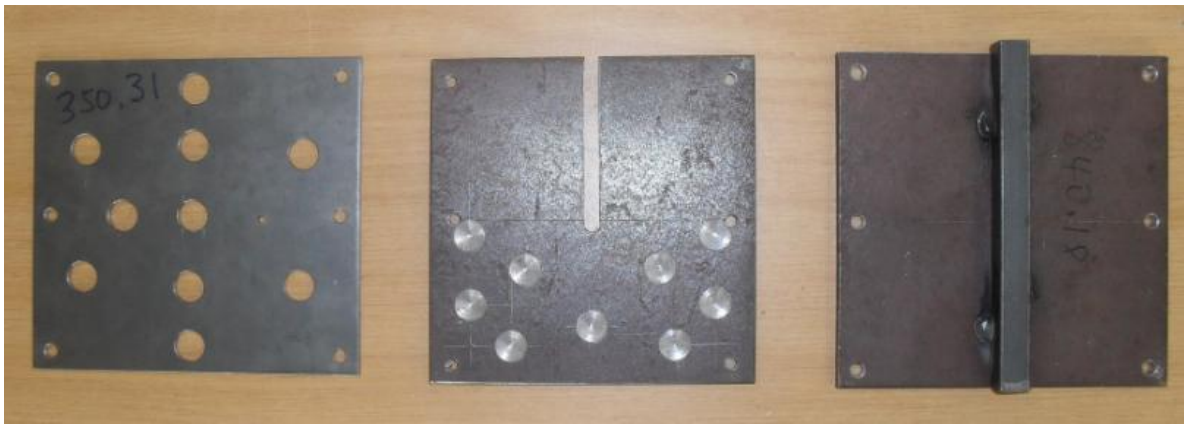

Figure 32. A photograph of the three different damper masses used to create different mass ratios– 2.5%, 5% and 7.5% respectively.

3.2.5 Changing the PATMD's Connection to the Test Model

The PATMD was connected to the test structure in eight different ways in order to determine its efficiency under different connecting conditions. The different connections are described below and are shown in Prokon models in Figure 33.

Configuration 1 – The corner ropes and the side ropes are all connected at the same height i.e. 20cm above the plate. This was the connection configuration used in the PATMD efficiency tests and all of the other parameter tests described above.

Configuration 2 – Only the four corner ropes are connected; the side ropes are not connected.

Configuration 3 – The four corners ropes are connected at a height of 20cm above the plate whilst the side ropes are pulled tighter and are connected 10cm above the plate.

Configuration 4 – Only the two side ropes are connected, not the corner ropes.

Configuration 5 – All the ropes are connected tightly, at 15cm above the plate.

Configuration 6, 7 and 8 – All six ropes were randomly connected at different heights in each case.

Configuration 1 Configuration 2 Configuration 3 Configuration 4

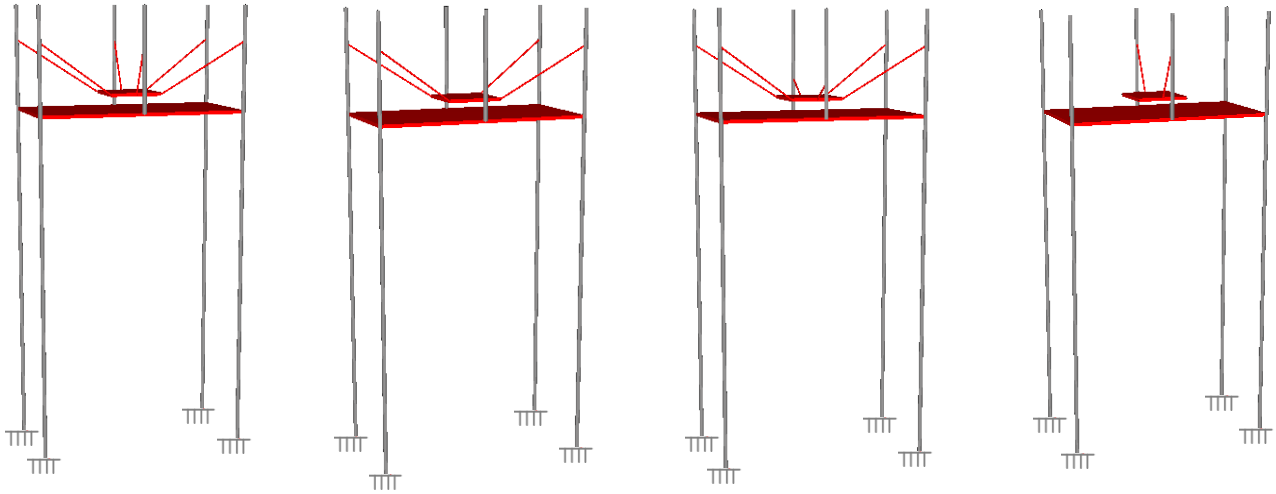

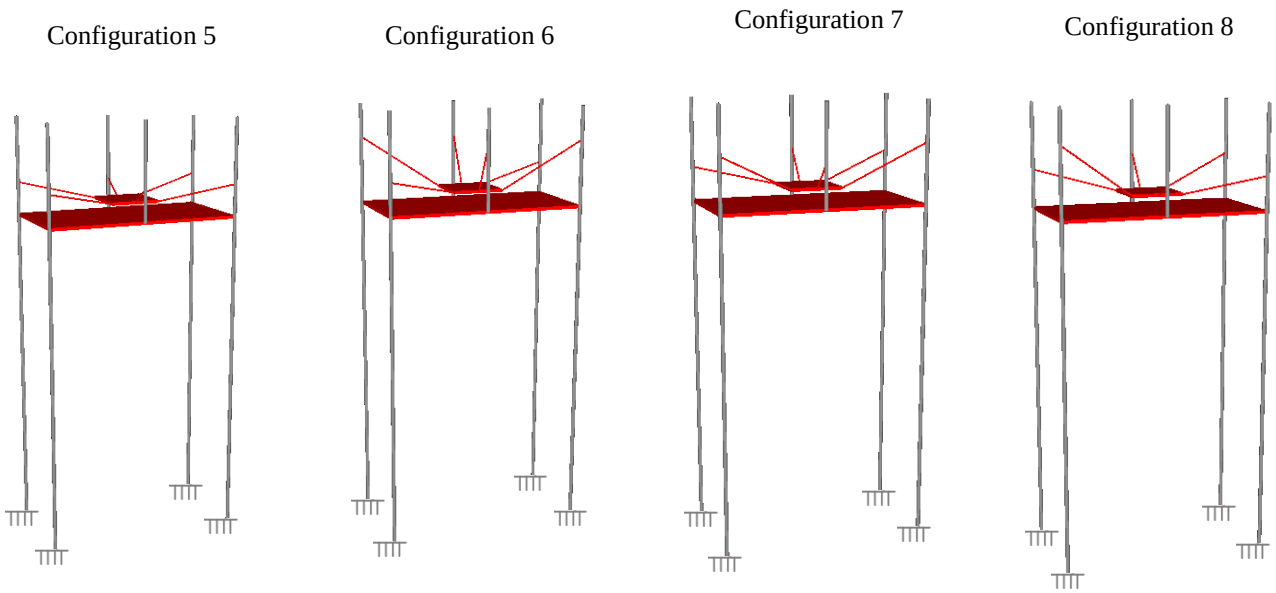

Figure 33. An illustration of the different PATMD connection configurations that were tested.

3.3 Experimental Procedure

3.3.1 Free Vibration Tests

The following testing procedure was carried out in the PATMD efficiency tests and parameter tests. Free vibration tests were performed on the primary undamped test model. The model was excited by giving it an initial displacement of 30mm, which was measured using a dial gauge, and then releasing it. The tests were done for five different excitations of the test model - it was excited in two translational directions; torsion; and lastly it was given two coupled excitations. The two translational directions were the orthogonal X and Y-directions, depicted by mode shapes 1 and 2 respectively in Figure 25 above. It was excited torsionally, as shown by mode 3 in Figure 25, by applying an initial twist to the model and then releasing it. Lastly, the model was subjected to two coupled excitations which were achieved by giving it initial torsional as well as translational displacements simultaneously.

The PATMD was then added to the primary structure and the tests described above were repeated. The sampling frequency chosen for these experiments was 250Hz, meaning that 250 acceleration readings were collected by the data logger per second. The accelerometer is capable of recording the acceleration readings in two directions and therefore did not have to

be reorientated during the testing procedure. PSD (power spectral density) graphs and time-history of acceleration graphs are used to show the PATMD's damping effects.

3.3.2 Forced Vibration Tests

Forced vibration tests were also carried out on the damped and undamped test structure. The test model was secured to a unidirectional shaking table which produced a sinusoidal base excitation. The stroke of the table was set to 30mm and the sampling frequency was 250Hz. The forced tests were carried out in two directions; the translational X-direction and Y-direction. No forced torsional vibration tests were carried out due to the fact that a forced torsional excitation could not be produced. The frequency was swept from 0.2Hz to 16Hz in 120 seconds for all of the tests. PSD graphs are used to show the damping effects of the PATMD.

Chapter 4

PATMD EFFICIENCY TESTS

4.1 Free Vibration

4.1.1 Translational Vibration in the X-Direction

An initial displacement of 30mm was given to the primary test model in the X-direction before releasing it. The PATMD was then connected and this procedure was repeated. Figure 34 below shows a high peak at 2.36Hz which is the model's natural frequency for translation in the X-direction, with a smaller peak at half of this value, 1.18Hz. It is observed that the natural frequencies obtained by simulation (2.48Hz) and by experimentation (2.36Hz) do not match up exactly, however they are very close in value. This is to be expected as the simulation results represent those of an 'ideal' test. Figure 34 shows that the PATMD provides a high level of attenuation to both of the peaks. The peak under consideration, at 2.36Hz is reduced by 99.5%. The time history of acceleration response shows that near the beginning of the test, as the PATMD starts moving, the acceleration peaks generated in the damped model are very high, exceeding those generated in the undamped model. These high accelerations subside and the accelerations rapidly become less than those found in the undamped model; however these initial high accelerations are undesirable. It was discovered that by altering the connection slightly, by making the inelastic ropes tighter i.e. reducing the height at which they are tied onto the threaded columns from 20cm to 15cm, the high accelerations decrease in value, becoming equal to or

less than the undamped peaks. However, regardless of this small modification, the positive damping effects of the PATMD evident in Figures 34 and 35 are still significant.

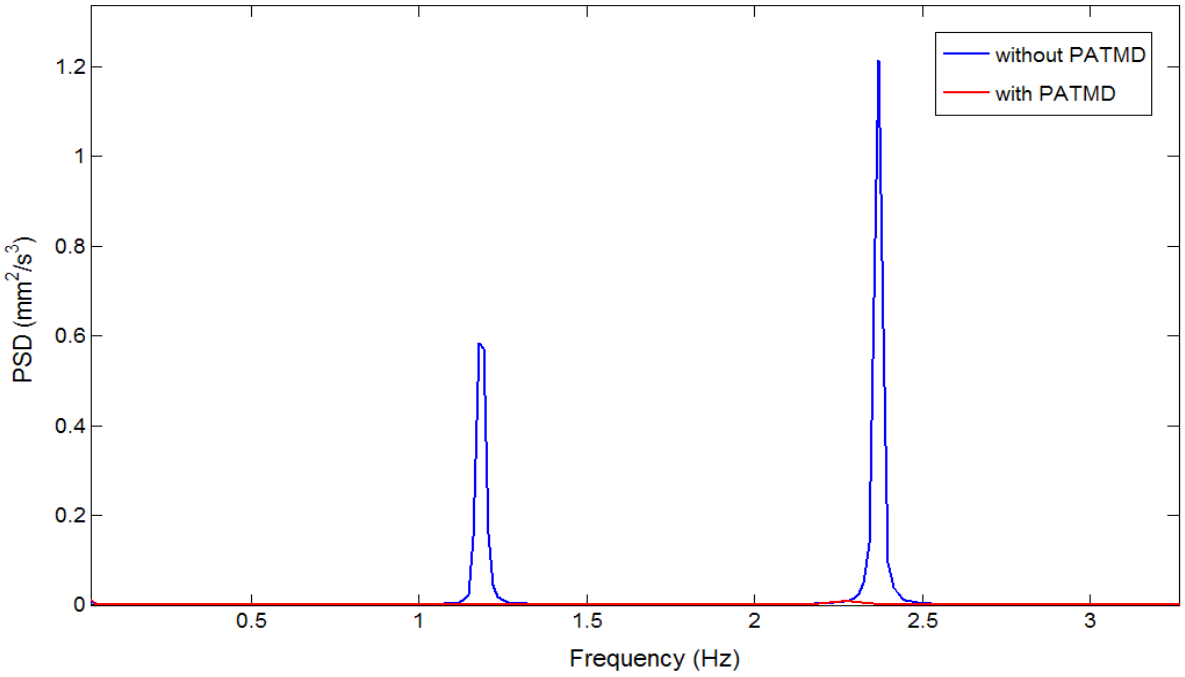

Figure 34. Power spectral density (PSD) of the acceleration response for free translational vibration in the X-direction.

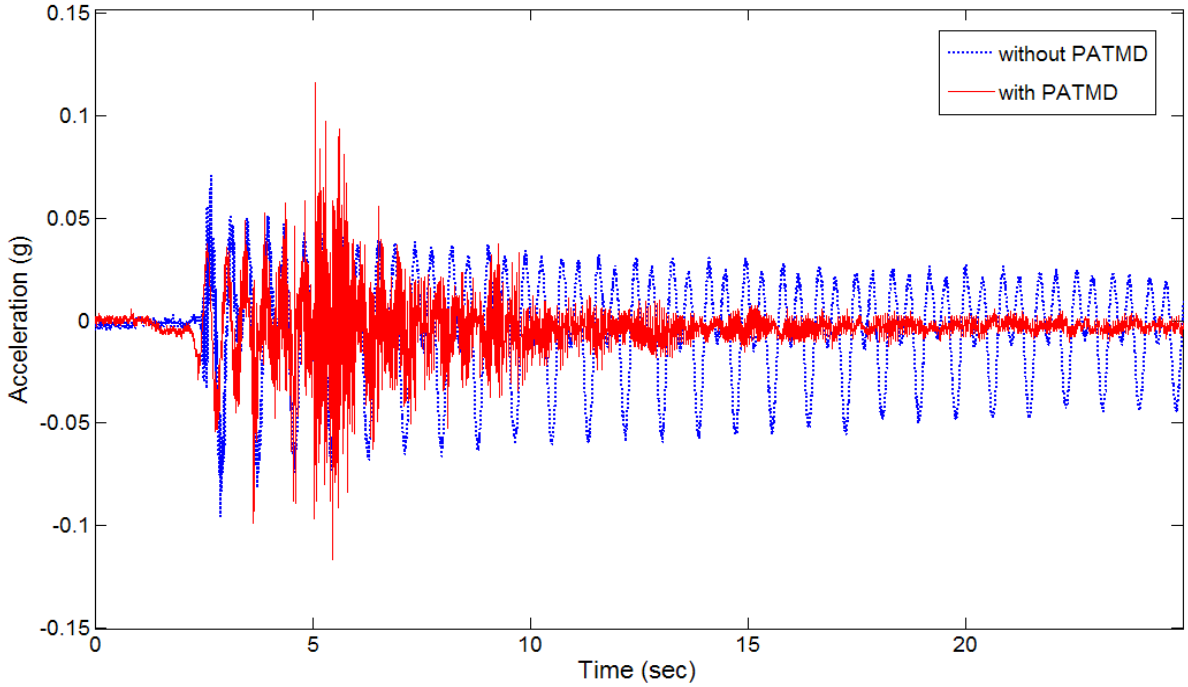

Figure 35. Time history of acceleration response for free translational vibration in the X-direction.

4.1.2 Translational Vibration in the Y-Direction

Next, an initial displacement of 30mm was given to the primary test model in the Y-direction before releasing it. The PATMD was then connected and this procedure was repeated. The PSD graph shows a high peak at 2.4Hz, which is the model's natural frequency in the Y-direction. Again, this is very similar to the simulated result of 2.55Hz. A smaller peak can be seen at half of this value, 1.2Hz. Both of these peaks are reduced significantly as the structure is controlled by the addition of the PATMD. The peak at the natural frequency for translation in the Y-direction, 2.4Hz, is reduced by 97.5%. The time history of acceleration response, shown in Figure 37, also contains high acceleration peaks for the damped model initially as the PATMD starts moving, with these peaks rapidly decreasing to well below those of the undamped model. Again, these initial high accelerations can be controlled by the slight tightening of the inelastic ropes of the PATMD, which does not affect the positive damping results.

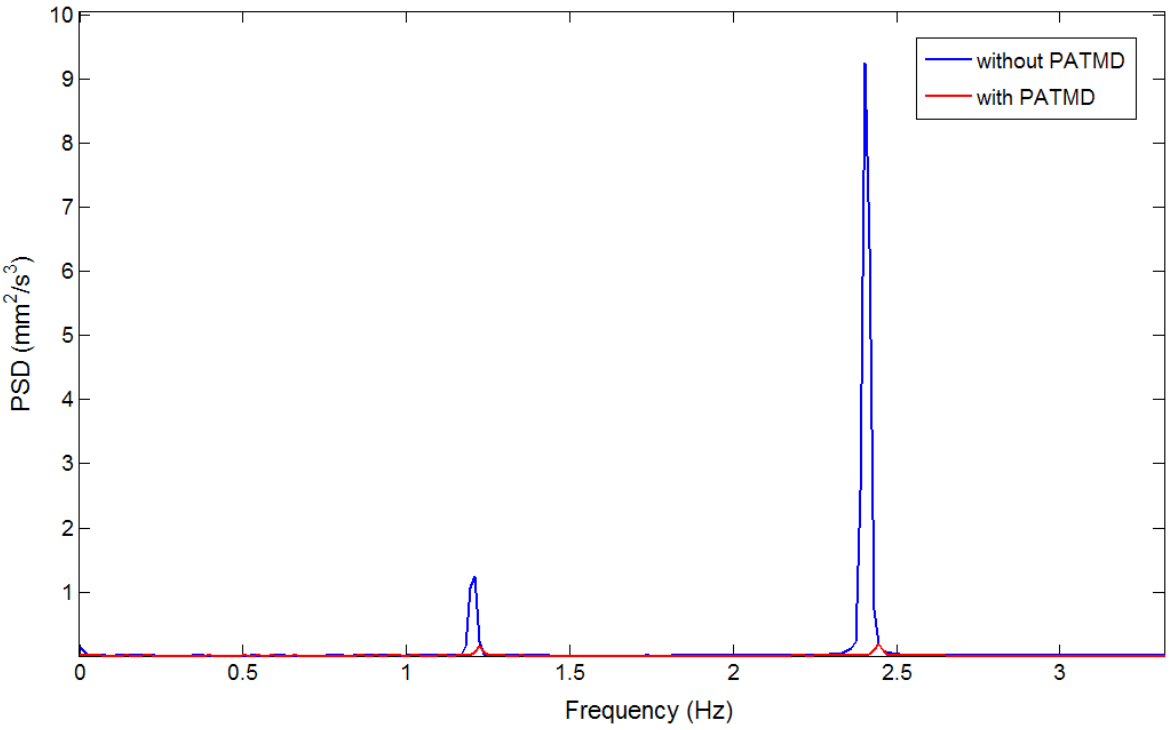

Figure 36. Power spectral density (PSD) of the acceleration response for free translational vibration in the Y-direction.

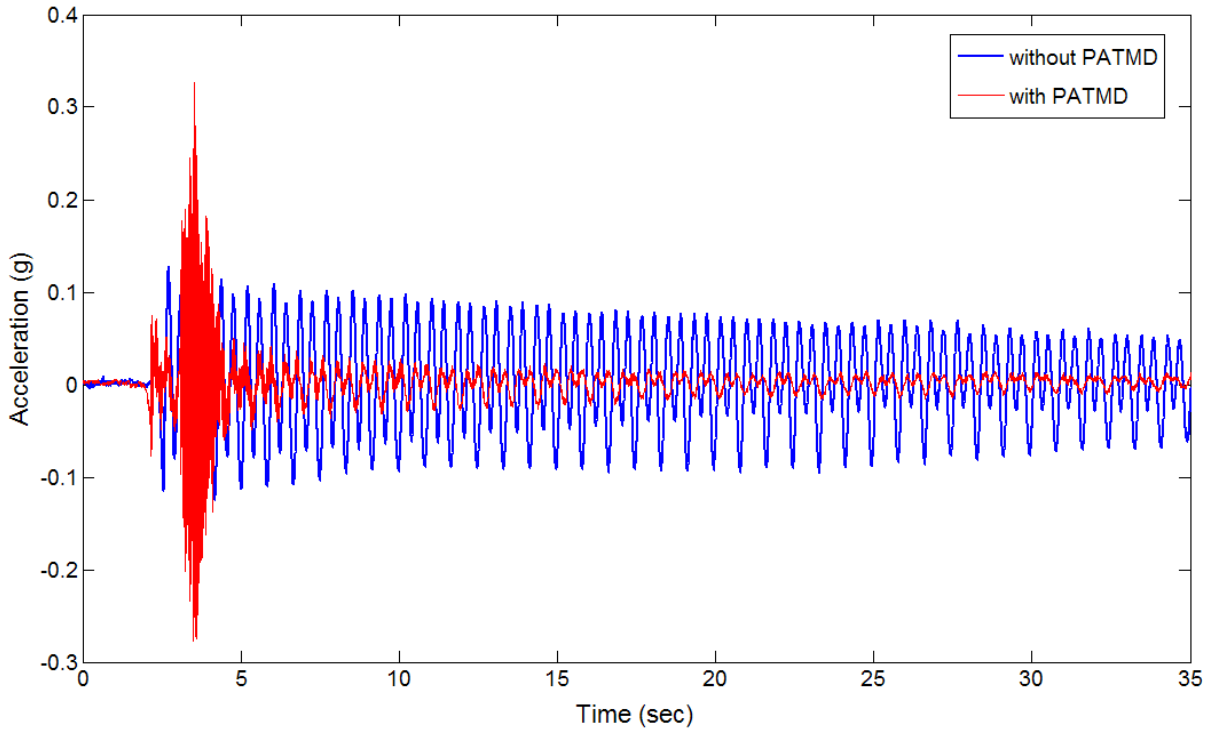

Figure 37. Time history of acceleration response for free translational vibration in the Y-direction.

4.1.3 Torsional Vibration

Next, the primary model was displaced torsionally by 30mm before releasing it. The PATMD was then connected and this procedure was repeated. The PSD graph below shows a high peak at 4.75Hz, the torsional frequency of the model, as well as smaller peaks at 1.2Hz, 2.4Hz and 3.6Hz. The torsional frequency obtained during simulation was 4.29Hz, which is relatively close to the experimental value. The fact that there is a peak at 2.4Hz means that although the model was excited in torsion, it had some movement in the Y-direction as well. Once again, all of the peaks are reduced by the addition of the PATMD, with the peak at the natural frequency for torsional vibration, 4.75Hz, being reduced by 77%. The time history of acceleration response for the model containing the PATMD shows a more gradual decrease in accelerations as opposed to the translational time history graphs. However, the effect of the PATMD is still obvious as time passes.

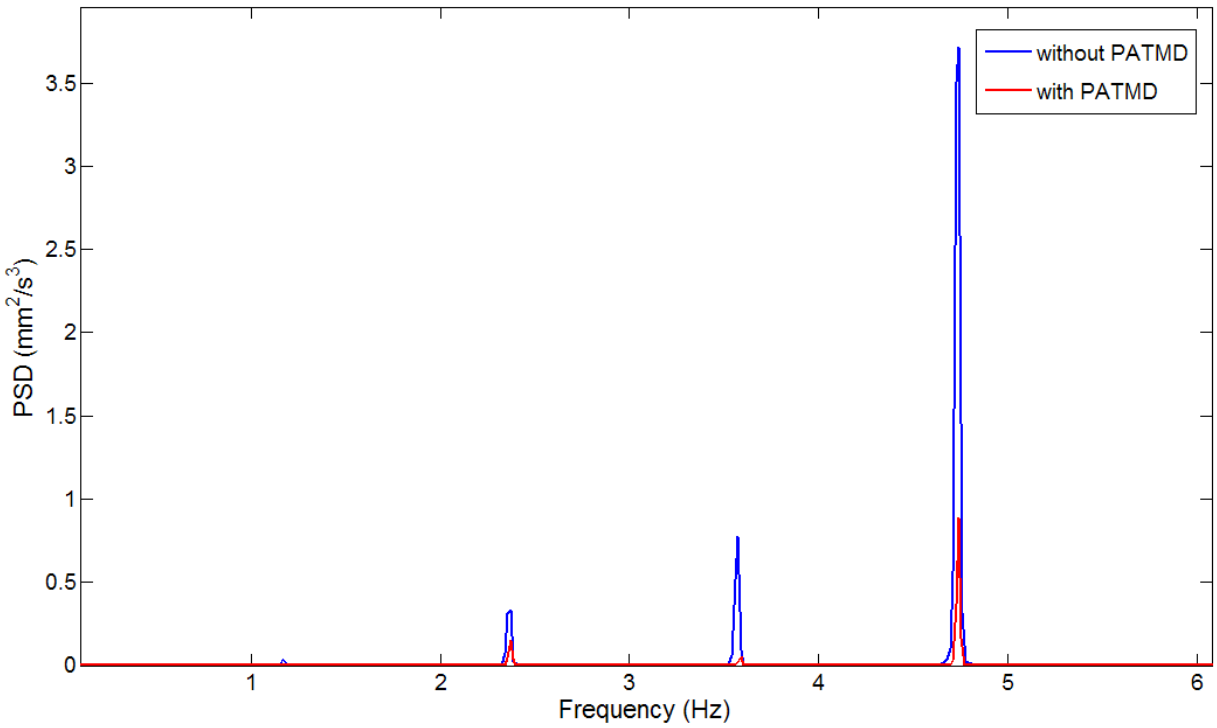

Figure 38. Power spectral density (PSD) of the acceleration response for free torsional vibration.

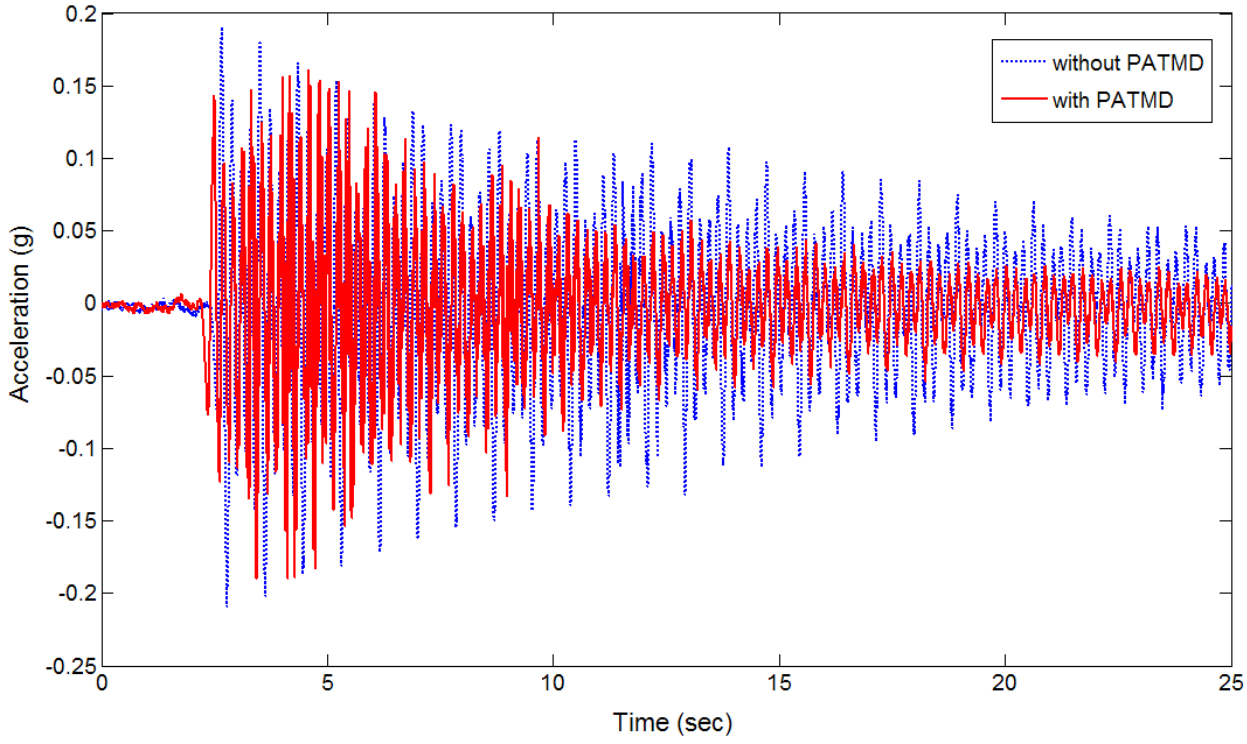

Figure 39. Time history of acceleration response for free torsional vibration.

4.1.4 Coupled Vibration (Translation in X-Direction and Torsion)

Next, the model was subjected to a coupled excitation - it was given initial translational and torsional displacements at the same time. In Figures 40 and 41, the model was displaced in the X-direction as well as twisted. As can be seen, there are peaks at the natural frequency of translation in the X-direction, 2.36Hz and at the torsional natural frequency, 4.75Hz, as well as smaller peaks at 1.2Hz and 3.6Hz. All of these peaks are decreased by at least 90% by the addition of the PATMD, indicating its control effect. This control is also obvious in the time history of acceleration response where the acceleration peaks generated in the model containing the PATMD decrease much more rapidly than those generated in the model without the PATMD.

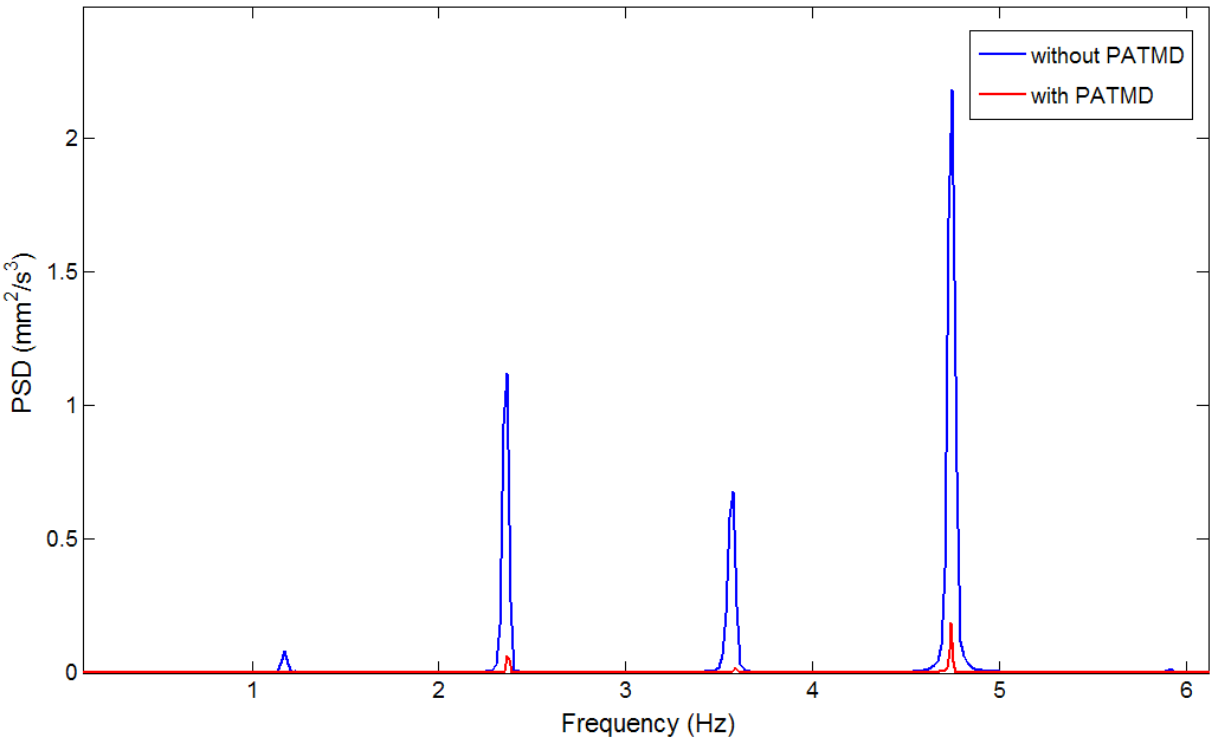

Figure 40. Power spectral density (PSD) of the acceleration response for free coupled vibration (translation in the X-direction and torsion).

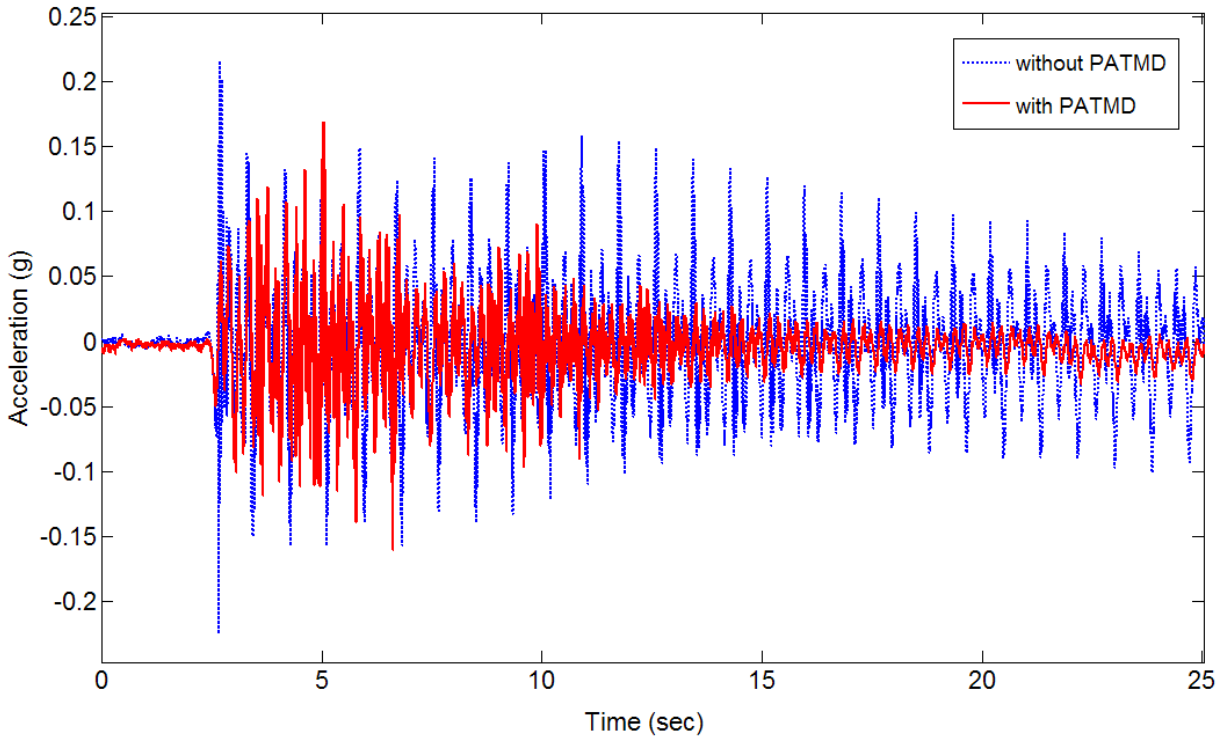

Figure 41. Time history of acceleration response for free coupled excitation (translation in the X-direction and torsion).

4.1.5 Coupled Vibration (Translation in Y-Direction and Torsion)

Lastly, the model was subjected to a second coupled excitation. It was given a translational displacement in the Y-direction and a torsional displacement simultaneously. The PSD shows peaks at the natural frequency for the translation in the Y-direction, 2.4Hz, the natural frequency for torsion, 4.75Hz as well as a peak at 3.6Hz. The control effect of the PATMD is obvious for all of the peaks in the PSD graph, as they are all reduced by at least 94%. The time-history of acceleration graph also demonstrates the significant damping effects.

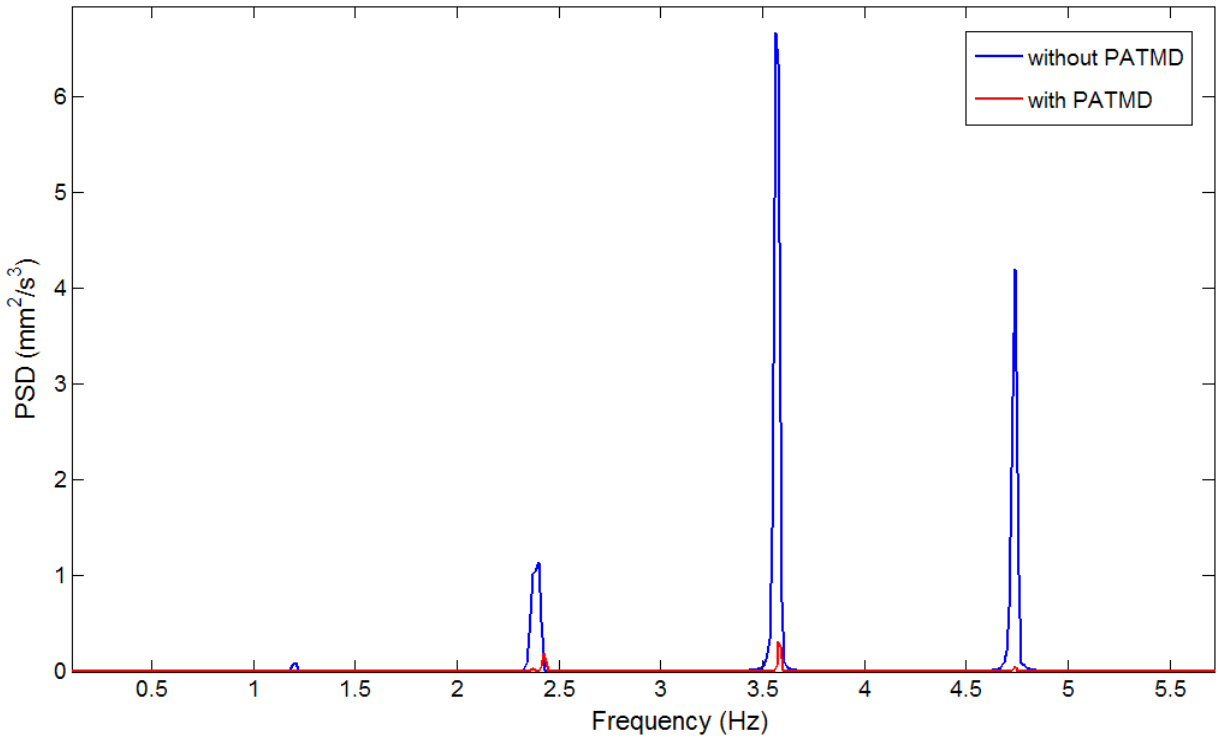

Figure 42. Power spectral density (PSD) of the acceleration response for free coupled excitation (translation in the Y-direction and torsion).

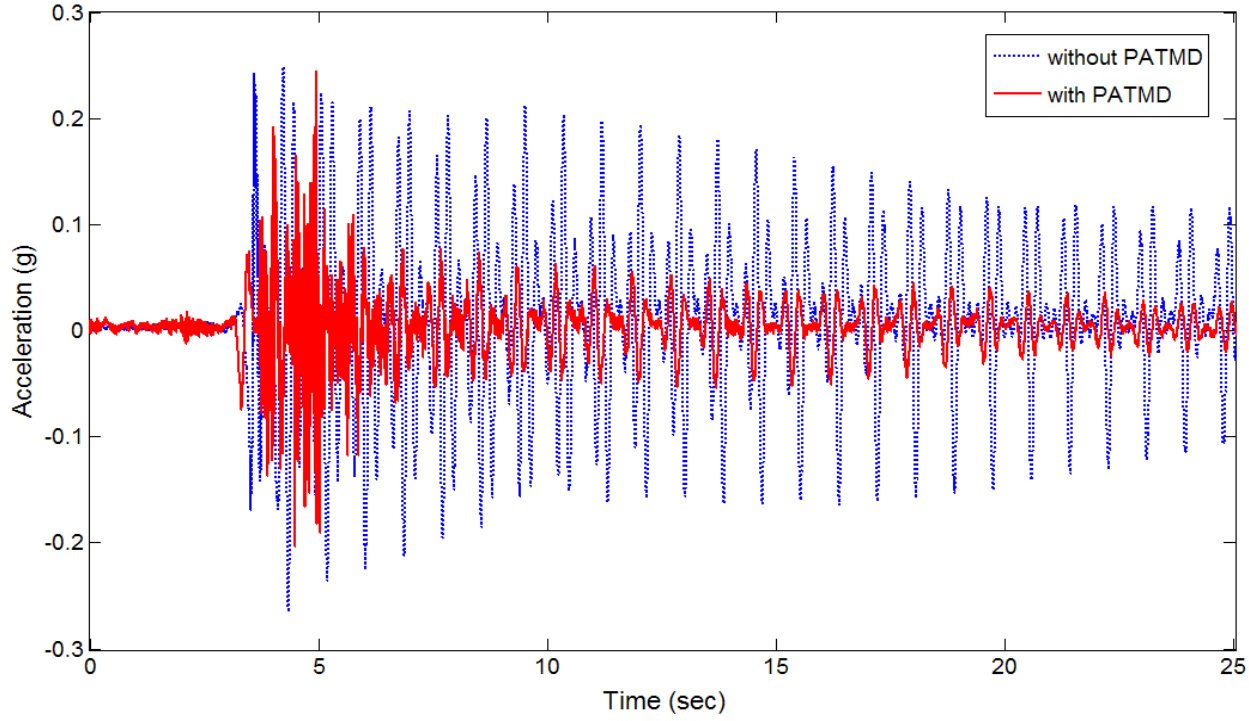

Figure 43. Time history of acceleration response for free coupled excitation (translation in the Y-direction and torsion).

4.2 Forced Vibration

4.2.1 Translational Vibration in the X-Direction

First, the test model was orientated on the shaking table so as to generate forced vibrations in the X-direction on the model. A frequency sweep was performed and PSD peaks are seen at 2.36Hz and 1.18Hz, as in the free vibration tests above. The control provided by the PATMD during the forced vibration tests is obvious from the PSD graph in Figure 44, where the peak occurring at the natural frequency for translational vibration in the X-direction is reduced by 92%.

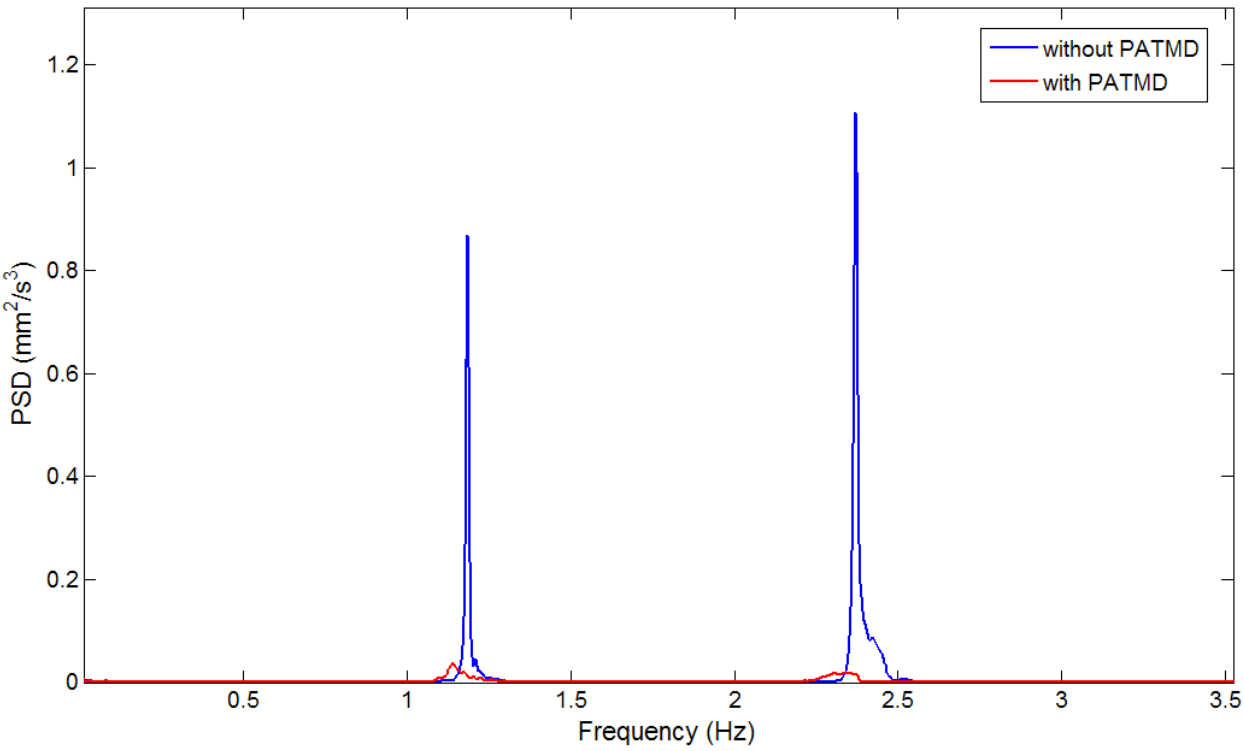

Figure 44. Power spectral density (PSD) of the acceleration response of the model under forced excitation in the X-direction.

4.2.2 Translational Vibration in the Y-Direction

The test model was then turned 90° on the shaking table so as to experience forced vibrations in the Y-direction. A frequency sweep was performed and PSD peaks can be seen at 2.4Hz and 1.2Hz as in the free vibration tests. Again the PSD graph which resulted illustrates the

control effect of the PATMD, with the peak at the natural frequency for translational vibration in the Y-direction being reduced by 98%.

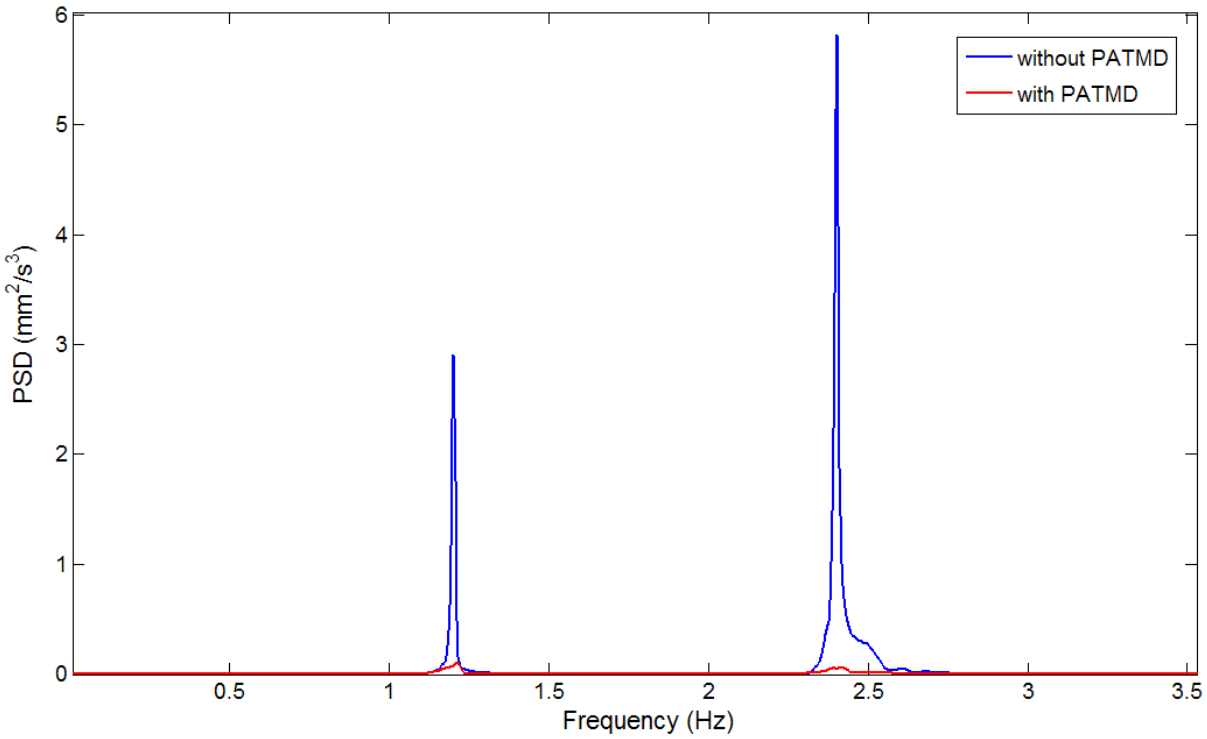

Figure 45. Power spectral density (PSD) of the acceleration response of the model under forced excitation in the Y-direction.

4.3 Summary and Conclusions

The experimental test results above reveal that the PATMD can successfully attenuate translational, torsional and coupled vibration when subjected to free or forced excitations. The PSD peak was reduced by at least 92% for translational vibrations, 77% for torsional vibrations and 90% for coupled vibrations which demonstrates its ability to effectively control all three types of excitation. This is a vast advantage over TMDs which can, in general, only control a single frequency. Furthermore, torsional vibration, which has been more difficult to control, was significantly attenuated. The two translational time-history of acceleration graphs reveal high accelerations in the damped model soon after excitation, however it was found that these could be reduced by the slight tightening of the inelastic ropes, without adversely affecting the positive vibration control.

Chapter 5

EFFECTS OF CHANGING MODEL'S STIFFNESS

In order to demonstrate the auto-tuning properties of the proposed PATMD, the dynamic properties, such as the natural frequencies of the test structure (the structure to be controlled) are modified by changing its stiffness whilst no tuning or adjustment of the PATMD takes place. This is achieved by changing the length of the columns.

5.1 Free Vibration

5.1.1 Translational Vibration in the X-Direction

The PSD and time-history of acceleration graphs for models of different stiffness, subjected to translational vibration in the X-direction, are shown below. The mass ratio was kept constant at 5% during the tests that follow. The stiffness of the model decreases significantly with increased model height, therefore, the natural frequencies also change considerably. As is to be expected, the 0.5m model has the greatest stiffness, whilst the 1m model is the least stiff for vibration in all directions. The experimental value for natural frequency obtained from the tests for the 0.5m model is 6.38Hz, for the 0.75m model is 3.64Hz and for the 1m model is 2.36Hz, which are similar to the simulated results shown earlier. In all cases, the model containing the PATMD has a much smaller peak PSD reading than the model without the PATMD. The PSD peaks were reduced by between 85%-97% by the addition of the

PATMD. Again, the time-history of acceleration graphs show that near the beginning of the test, as the PATMD starts moving, the acceleration peaks generated in the damped model are very high, exceeding those generated in the undamped model. As stated earlier, these high accelerations could be removed by altering the PATMD connection to the test structure slightly. However, regardless of this small modification, the positive damping effects of the PATMD are still significant. These graphs demonstrate that even though the natural frequencies of the test structure were changed significantly, the PATMD, without any tuning or adjustment, produced effective control on the X-direction translational vibration for each case.

0.5m Model

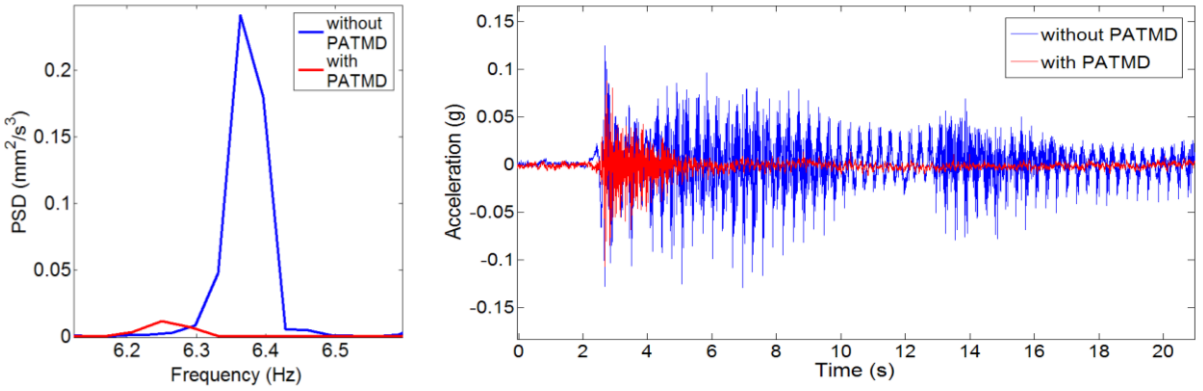

0.75m Model

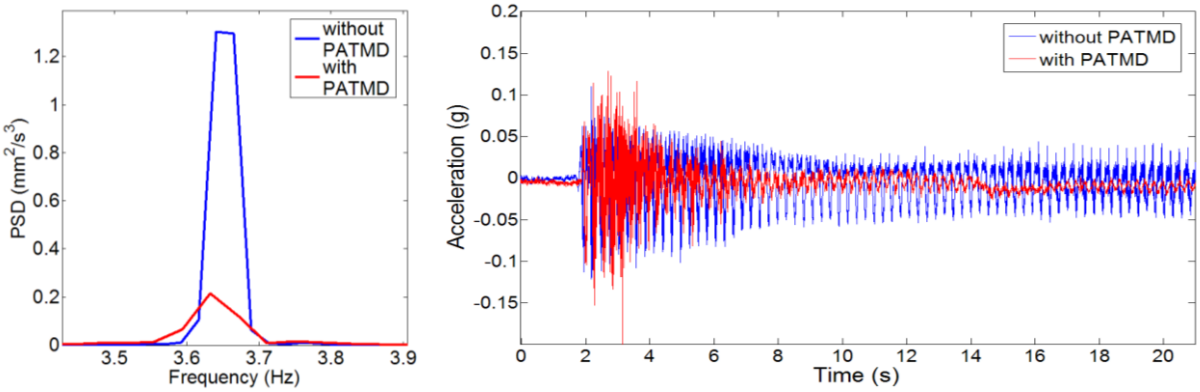

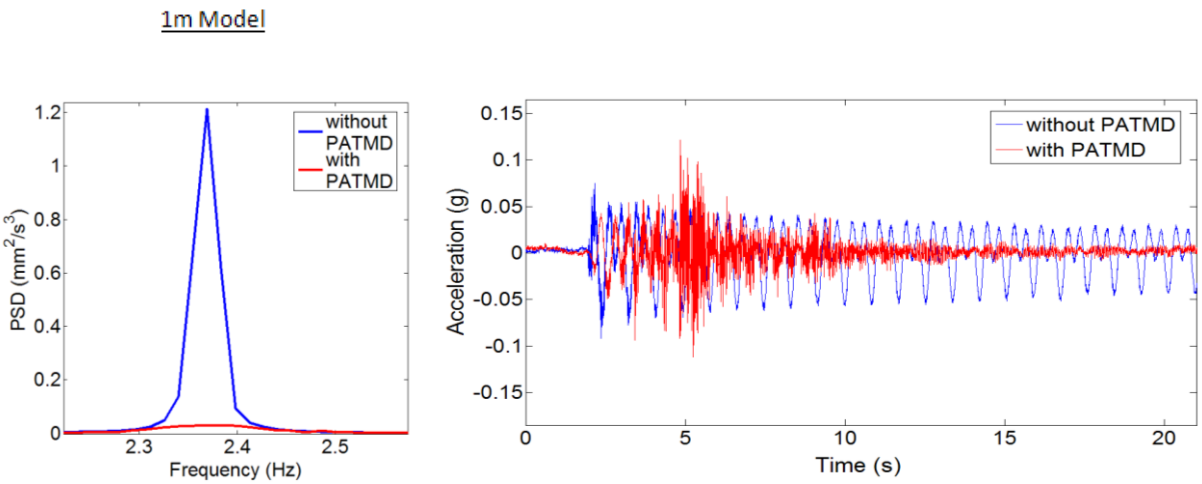

Figure 46. The PSD and time-history of acceleration graphs for free translational vibration in the X-direction for model heights of 0.5m, 0.75m and 1m respectively.

5.1.2 Translational Vibration in the Y-Direction

The PSD and time-history of acceleration graphs for models of different stiffness, subjected to translational vibration in the Y-direction, are shown below. The natural frequencies change significantly as the model stiffness is altered. The natural frequency for the 0.5m model is 6.63Hz, for the 0.75m model is 3.76Hz and for the 1m model is 2.4Hz, in close agreement with the simulated natural frequencies obtained earlier. These frequencies are slightly higher than the frequencies for X-direction translational vibration due to the model's marginally increased stiffness in this direction as a result of the model's dimensions.

In all cases, the model with the PATMD, has a smaller peak PSD reading. The PSD peaks are reduced by between 85% and 95% by the addition of the PATMD. This demonstrates that the PATMD, without any tuning or adjustment, can produce effective control on the Y-direction translational vibration even when the natural frequencies of the test structure are changed significantly. The time-history of acceleration graphs also show the positive damping effects as time passes.

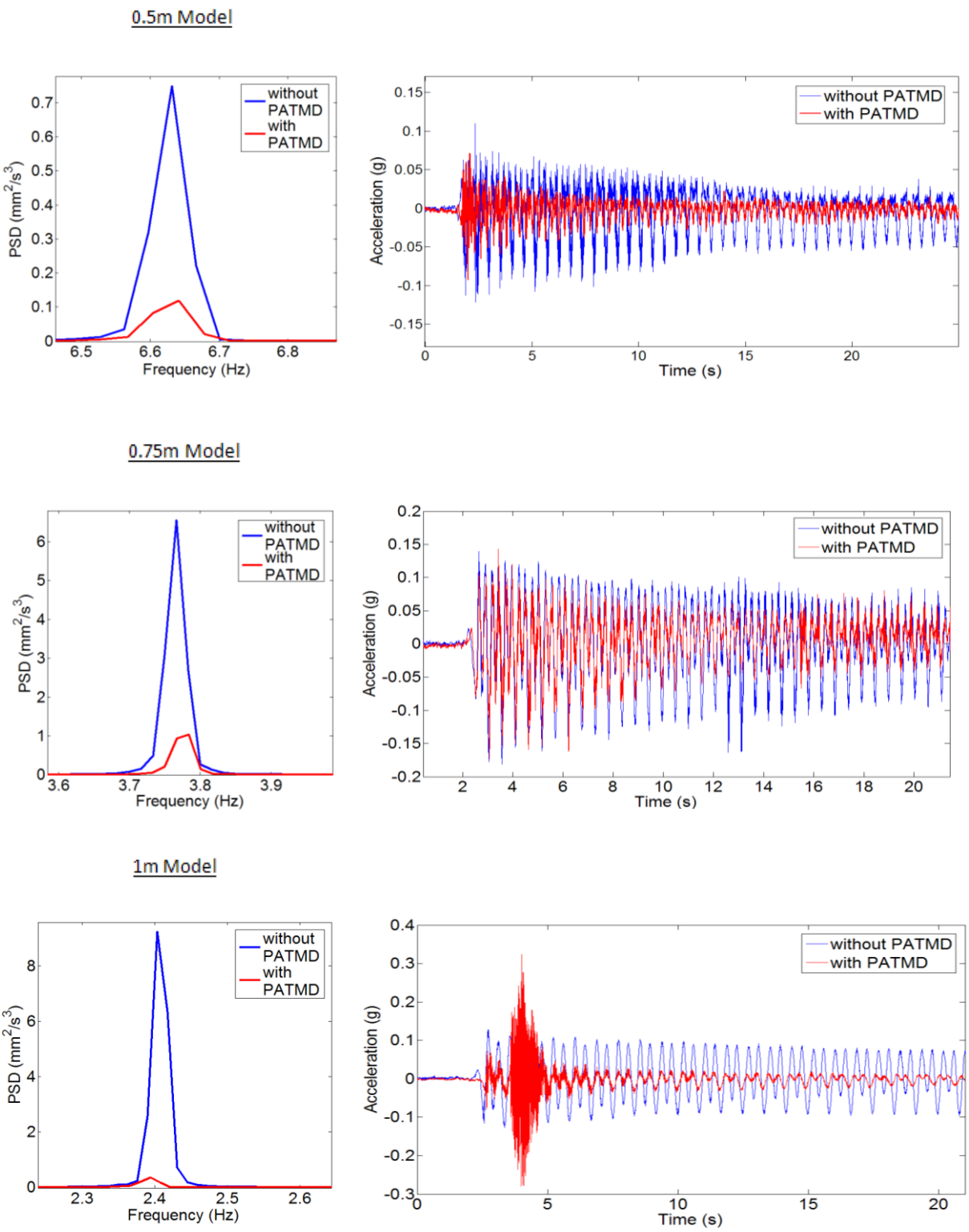

Figure 47. The PSD and time-history of acceleration graphs for free translational vibration in the Y-direction for model heights of 0.5m, 0.75m and 1m respectively.

5.1.3 Torsional Vibration

The PSD and time-history of acceleration graphs for models of different stiffness, subjected to torsional vibration are shown below. As can be seen in Figure 48 below, the natural frequencies for torsion also change significantly with changing model stiffness. The natural frequency for the 0.5m model is 13.59Hz, for the 0.75m model is 6.44Hz and for the 1m model is 4.75Hz, which are similar to the simulated results. As expected, these frequencies are higher than the frequencies for translational vibration due to the model's increased stiffness in torsion. In all cases, the PATMD, reduces the peak PSD reading by about 76% – 86% which is not quite as significant as for the translational vibration cases above but still demonstrates that the PATMD, without any tuning or adjustment, can produce highly effective control on torsional vibration over a wide range of frequencies. The damping effects are less obvious in the time-history of acceleration graphs however a reduction, due to the addition of the PATMD, can still be seen.

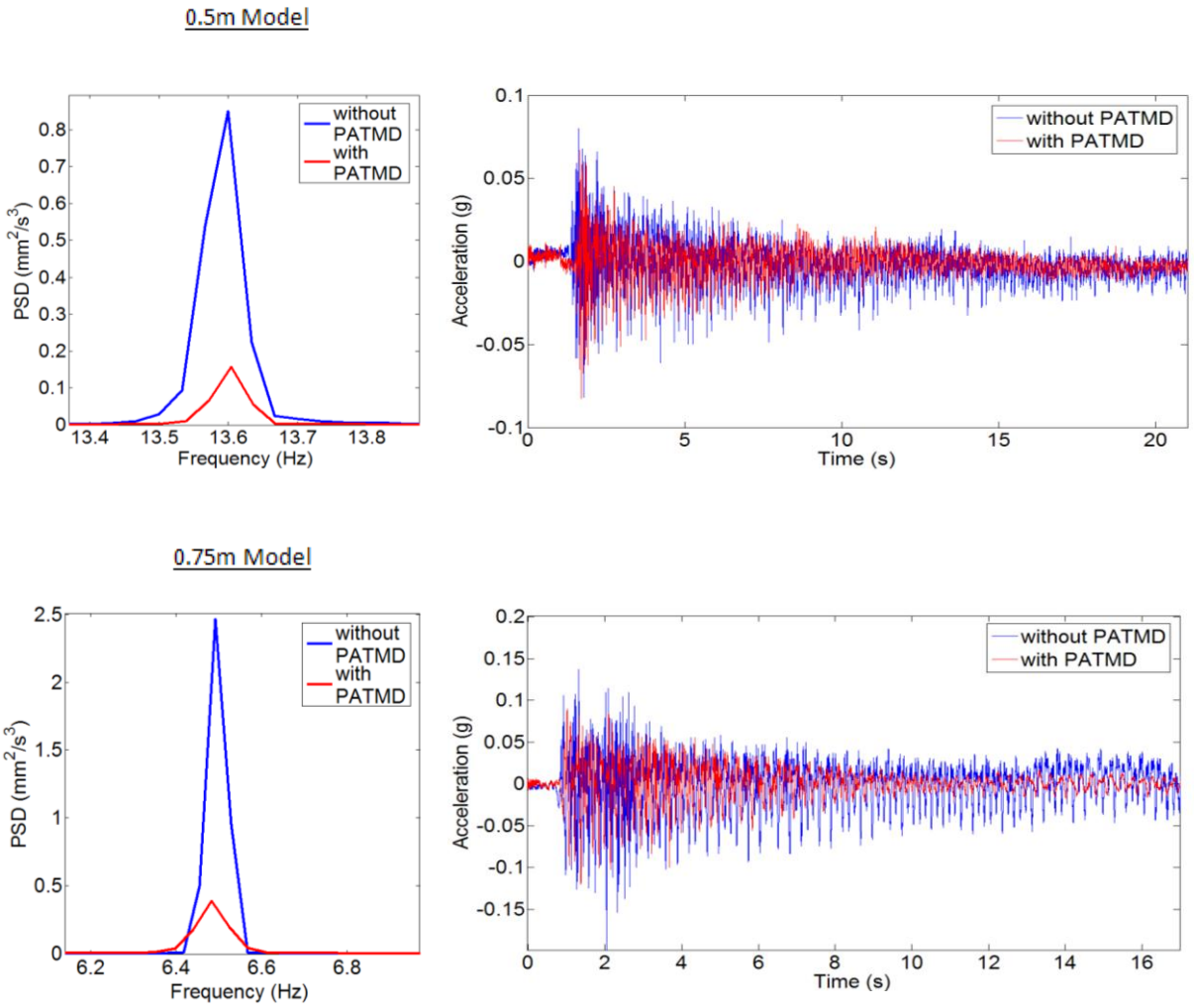

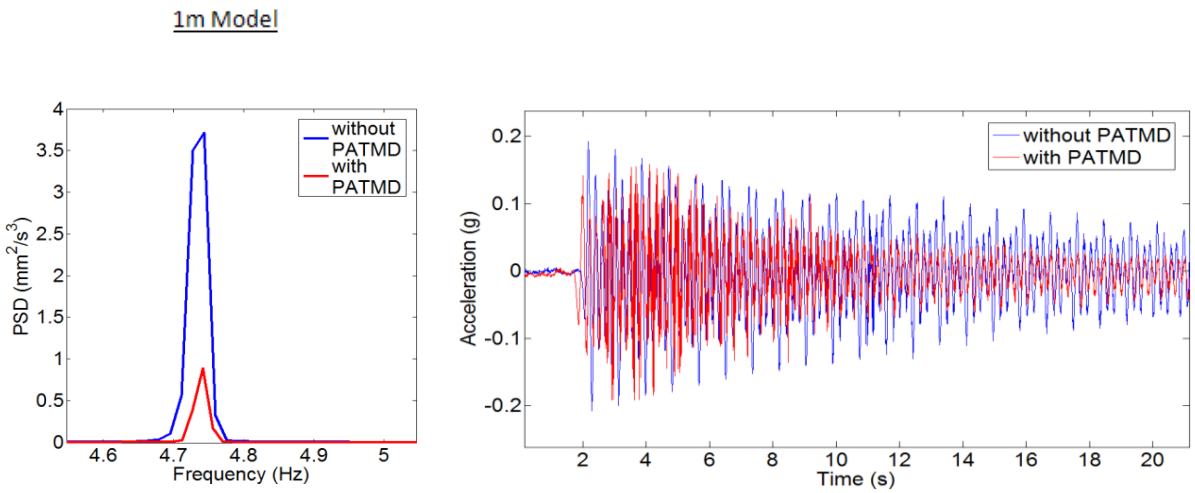

Figure 48. The PSD and time-history of acceleration graphs for free torsional vibration for model heights of 0.5m, 0.75m and 1m.

5.1.4 Coupled Vibration (Translation in the X-Direction and Torsion)

The graphs below show PSD and time-history of acceleration readings for the 0.5m model, 0.75m model and 1m model for coupled vibration (X-direction translation and torsion). There are peaks at the natural frequency for translation in the X-direction as well as the natural frequency for torsion in each case. For the 0.5m model, the X-direction translational peak is at 6.38Hz and the torsional peak is at 13.59Hz. For the 0.75m model, the X-direction translational peak is at 3.64Hz and the torsional peak is at 6.44Hz. For the 1m model, the X-direction translational peak is at 2.36Hz and the torsional peak is at 4.75 Hz. All of the peaks are reduced by the addition of the PATMD (except for one peak, at 5.2Hz for the 0.75m model which stays the same – fortunately, this peak is the smallest) demonstrating the PATMD's capability of controlling coupled vibration over a relatively wide range of frequencies without any tuning or adjustment taking place. The damping effects are less obvious in the time-history of acceleration graphs however a reduction, due to the addition of the PATMD, can still be seen.

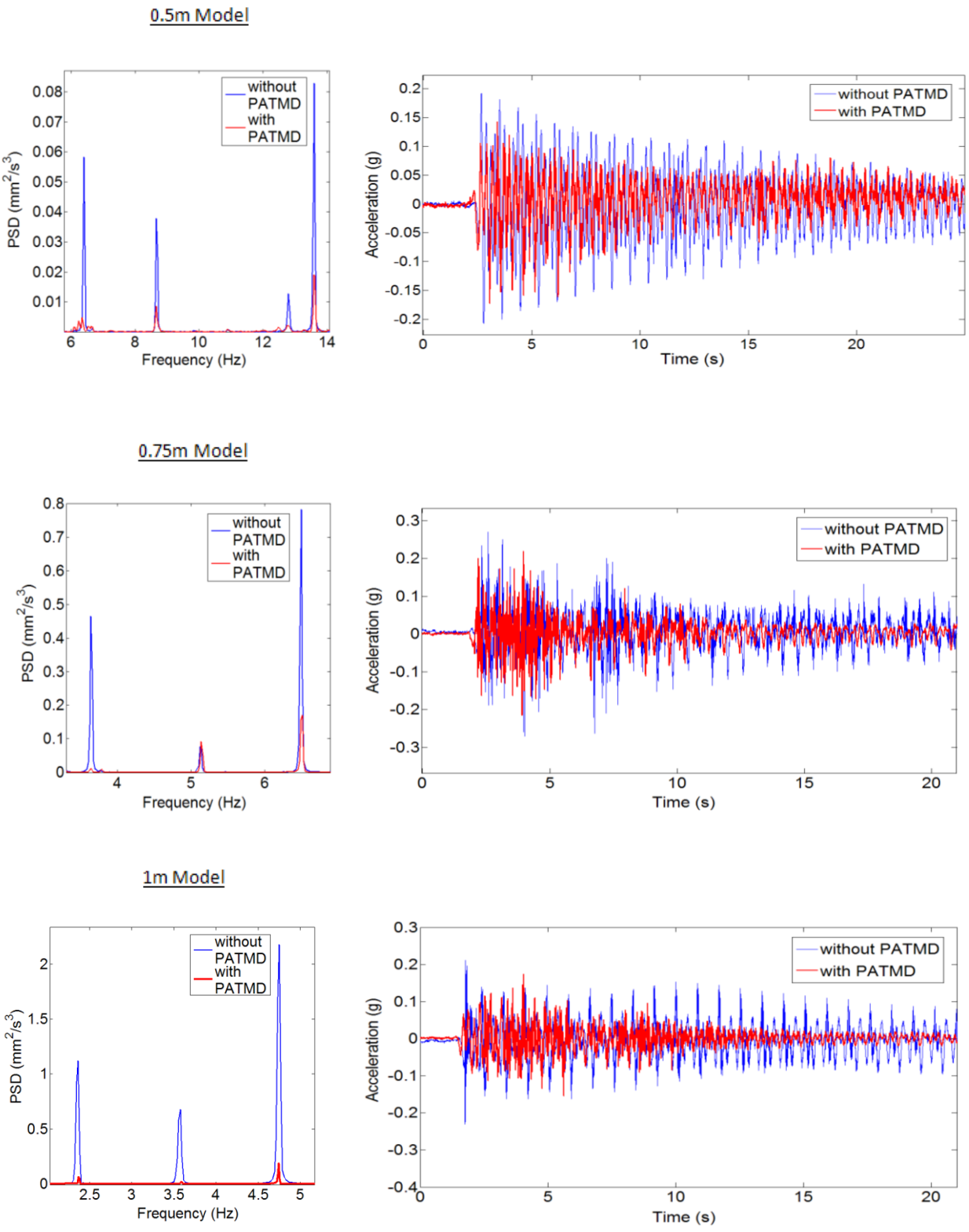

Figure 49. The PSD and time-history of acceleration graphs for free coupled vibration (translation in the X-direction and torsion) for model heights of 0.5m, 0.75m and 1m.

5.1.5 Coupled Vibration (Translation in the Y-Direction and Torsion)

The PSD and time-history of acceleration graphs for models of different stiffness, subjected to coupled vibration (Y-direction and torsion) are shown below. There are peaks at the natural frequency for translation in the Y-direction as well as the natural frequency for torsion in each case. For the 0.5m model, the Y-direction translational peak is at 6.63Hz and the torsional peak is at 13.59Hz. For the 0.75m model, the Y-direction translational peak is at 3.76Hz and the torsional peak is at 6.44Hz. For the 1m model, the Y-direction translational peak is at 2.4Hz and the torsional peak is at 4.75 Hz. Both of these peaks are reduced by the PATMD in every case, as well as any other peaks that occur, demonstrating its ability to control coupled vibration without any tuning or adjustment. Again in some cases, the damping effects are less obvious in the time-history of acceleration graphs however a reduction, due to the addition of the PATMD, can still be seen.

0.5m Model

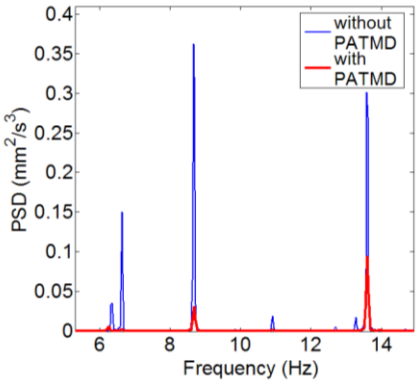

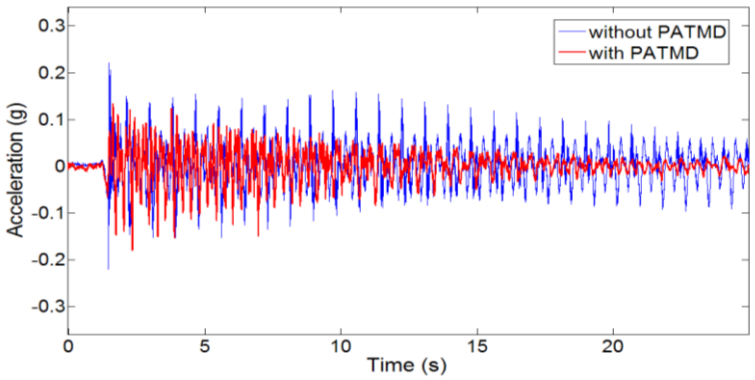

0.75m Model

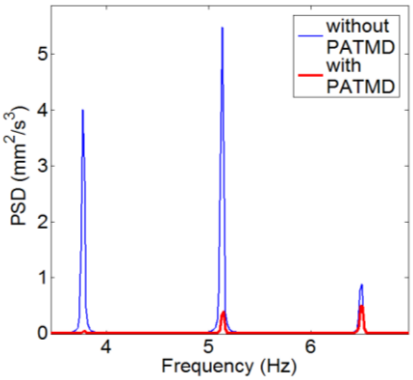

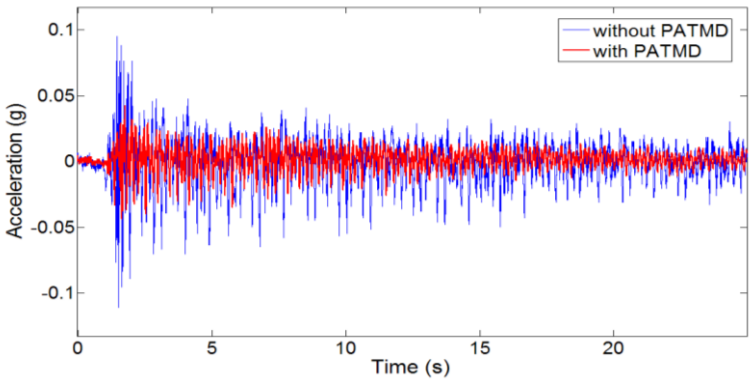

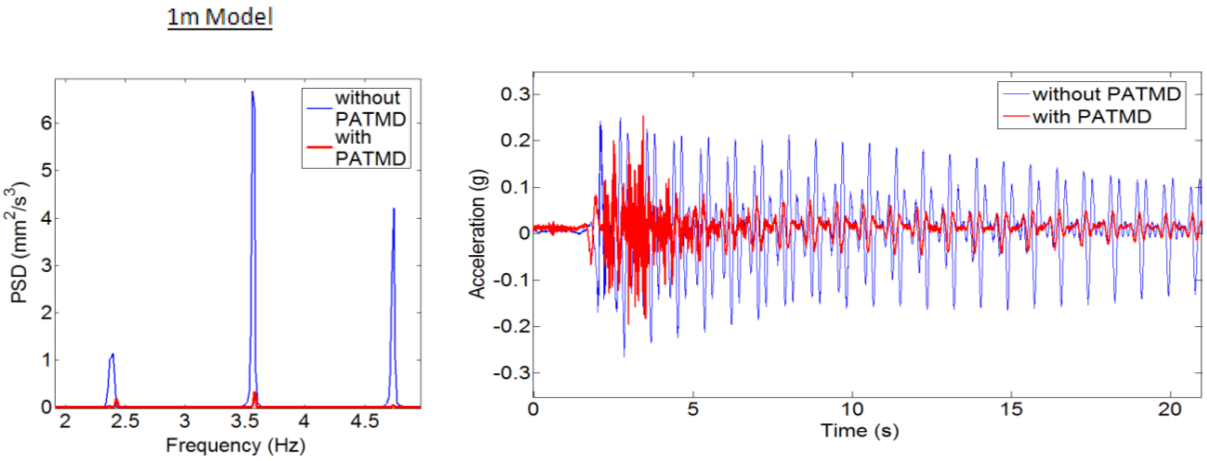

Figure 50. The PSD and time-history of acceleration graphs for free coupled vibration (translation in the Y-direction and torsion) for model heights of 0.5m, 0.75m and 1m respectively.

5.2 Forced Vibration

5.2.1 Translational Vibration in the X-Direction

The same positive results that were observed in the free vibration tests were achieved in the forced vibration tests. As can be seen in Figure 51 below, the PSD peaks are reduced by around 95% - 98% by the addition of the PATMD.

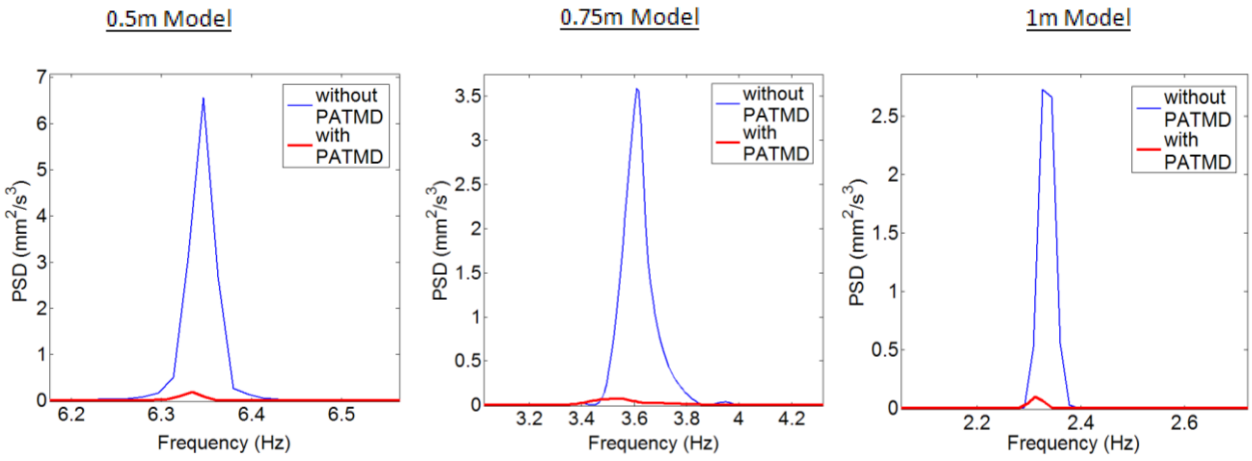

Figure 51. The PSD graphs for forced vibration in the translational X-direction for model heights of 0.5m, 0.75m and 1m respectively.

5.2.2 Translational Vibration in the Y-Direction

Again, the positive results that were achieved in the free vibration tests were observed in the forced vibration tests for translational vibration in the Y-direction. The PSD peaks are reduced by about 93% - 97% in the damped case by the addition of the PATMD.

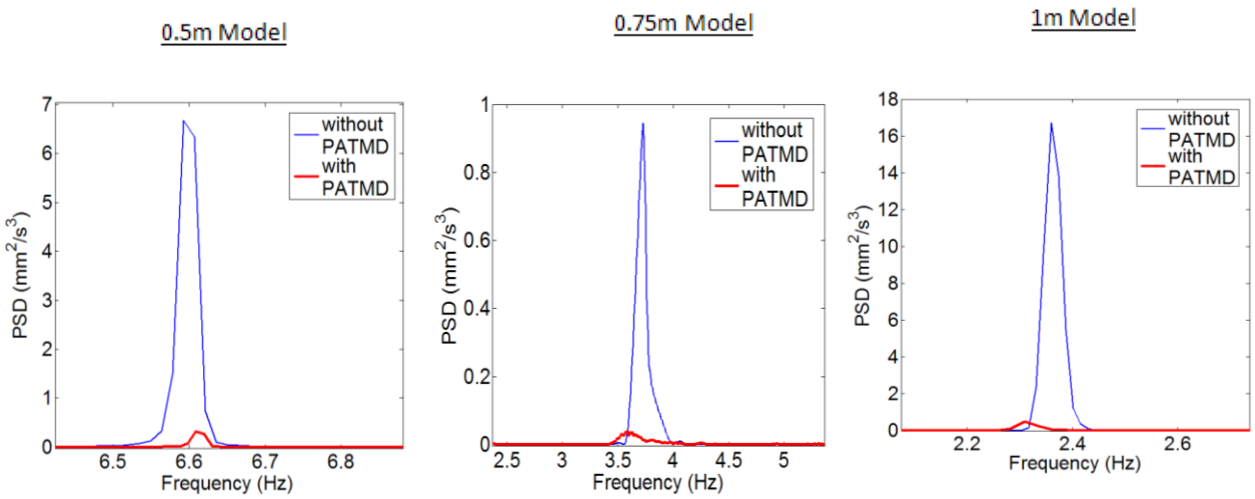

Figure 52. The PSD graphs for forced vibration in the translational Y-direction for model heights of 0.5m, 0.75m and 1m respectively.

5.3 Summary and Conclusions

By changing the height of the test model, its stiffness was altered and the natural frequencies were changed significantly. The test results reveal that the PATMD reduced the model's vibration response considerably in every case, meaning that it worked effectively over a relatively wide frequency range without any tuning or specific adjustment. The PSD peaks for translational vibration were reduced by at least 85% in every case, whilst the PSD peaks for torsional vibration were reduced by at least 76% in every case. Again high accelerations were seen in the models containing the PATMD soon after excitation in some instances; however these could be reduced by the slight tightening of the inelastic ropes. In general, the test models subjected to forced excitation attained higher levels of attenuation than those subjected to free excitation, as shown in the PSD graphs above.

Chapter 6

EFFECTS OF CHANGING THE MODEL'S MASS

As mentioned previously, in order to demonstrate the auto-tuning properties of the proposed PATMD, the dynamic properties, such as the natural frequencies of the test structure (the structure to be controlled) are modified. Its mass is altered whilst no tuning or adjustment of the PATMD takes place. This is achieved by adding 1kg or 2kg masses to the test structure.

6.1 Free Vibration

6.1.1 Translational Vibration in the X-Direction

The graphs below show the PSD and time-history of acceleration readings for the 14kg model, 20kg model and 32kg model respectively, for translational vibration in the X-direction. As can be seen, the natural frequency decreases with increasing model mass. The natural frequency for the 14kg model is 2.36Hz, for the 20kg model is 2Hz and for the 32kg model is 1.6Hz which is in agreement with the simulated results shown earlier. In all cases, the model containing the PATMD, has a much smaller peak PSD reading which again demonstrates the PATMD's effectiveness in controlling translational vibration over a relatively wide range of frequencies, without any tuning having taken place. The PSD peak values were reduced by between 77% and 96% by the addition of the PATMD. The time-

history of acceleration graphs also demonstrate the PATMD's control effect, but not as obviously as the PSD graphs.

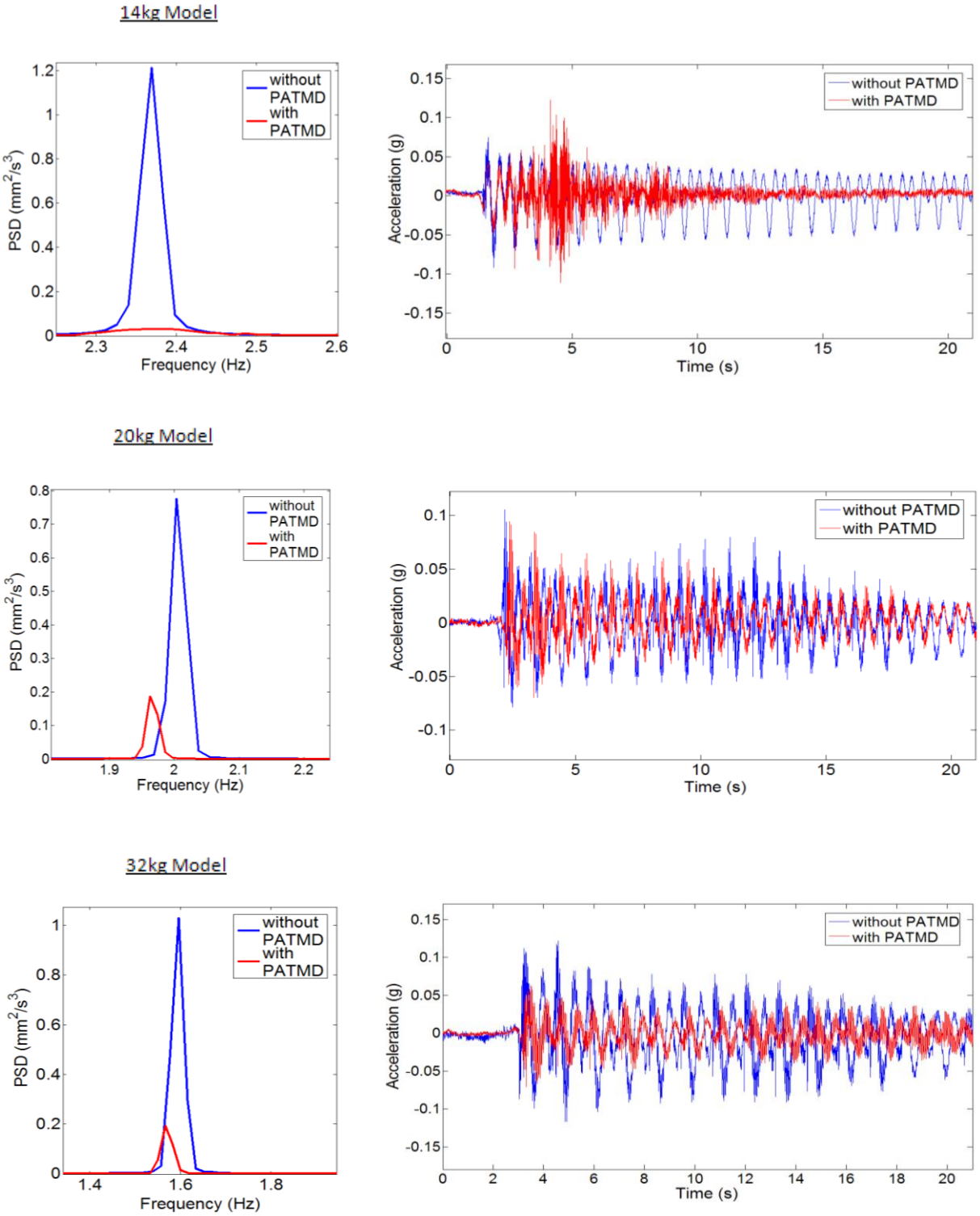

Figure 53. The PSD and time-history of acceleration graphs for free translation in the X-direction for model masses of 14kg, 20kg and 32kg respectively.

6.1.2 Translational Vibration in the Y-Direction

The graphs below show the PSD and time-history of acceleration readings for translational vibration in the Y-direction for each of the three model masses. Again, the natural frequencies are slightly higher than the X-direction values due to the slight increase in stiffness in this direction. The natural frequency for the 14kg model is 2.4Hz, for the 20kg model is 2.09Hz and for the 32kg model is 1.62Hz which is in agreement with the simulated results shown earlier. In all cases, the model containing the PATMD, has a much smaller peak PSD reading which demonstrates the PATMD's effectiveness in controlling translational vibration over a relatively wide range of frequencies, without any tuning taking place. The PSD peak values were reduced by between 85% and 96% by the addition of the PATMD. The time-history of acceleration graphs also demonstrate the PATMD's positive damping effects.

14kg Model

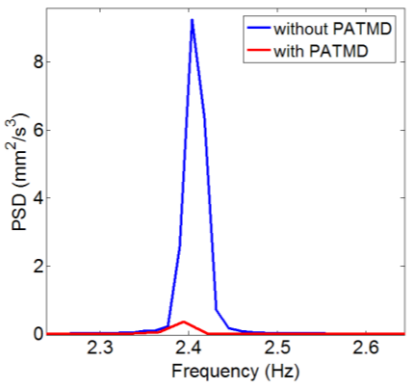

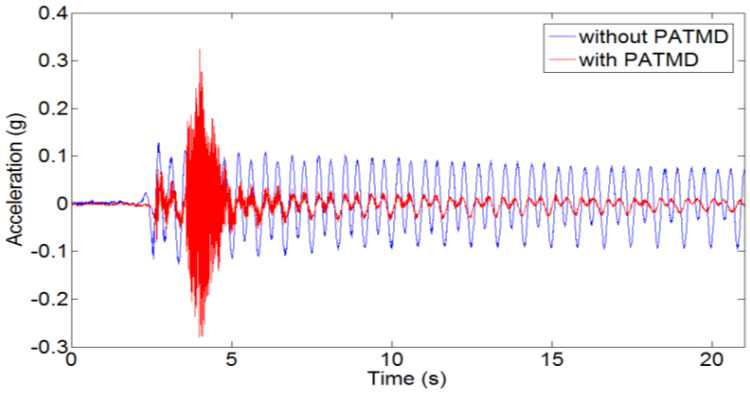

20kg Model

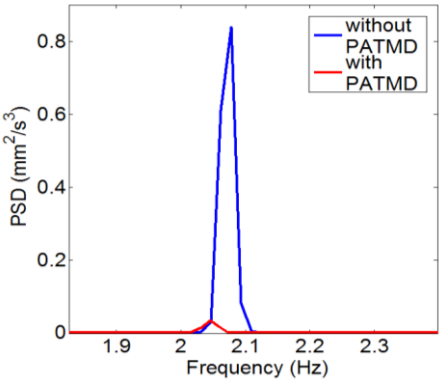

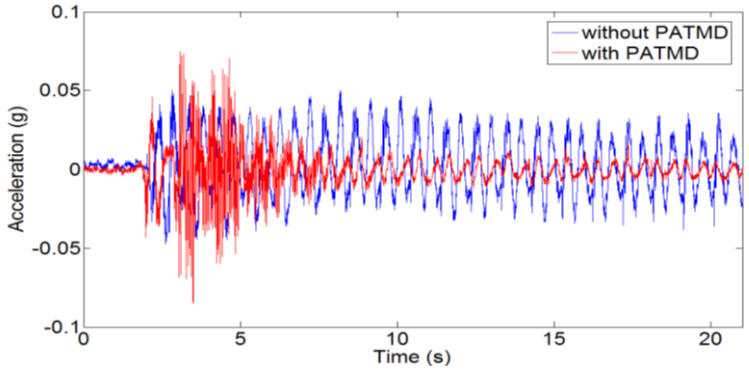

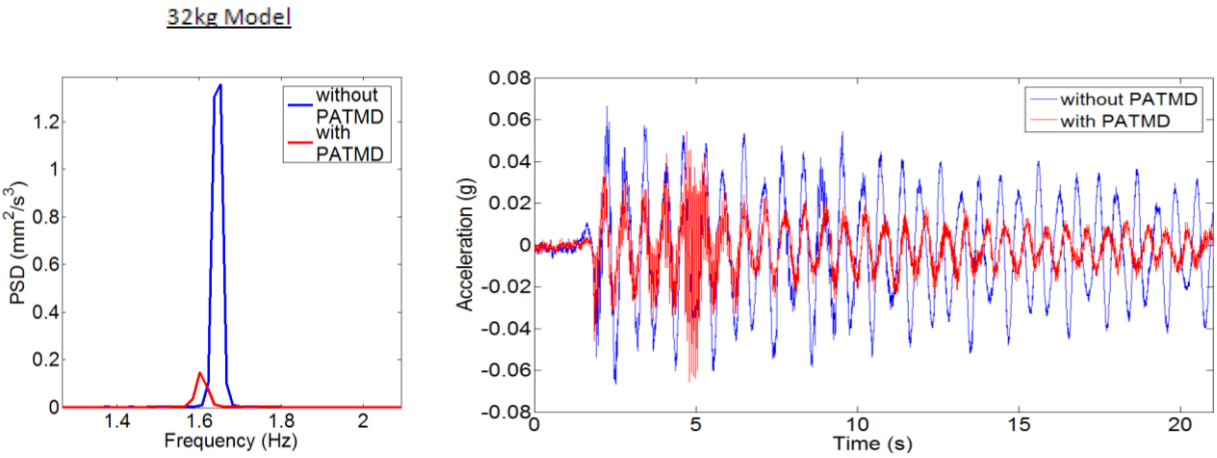

Figure 54. The PSD and time-history of acceleration graphs for free translation in the Y-direction for model masses of 14kg, 20kg and 32kg respectively.

6.1.3 Torsional Vibration

The graphs below show the PSD and time-history of acceleration readings for torsional vibration for each of the three model masses. As can be seen, the natural frequency for torsion decreases with increasing model mass. The natural frequency for the 14kg model is 4.75Hz, for the 20kg model is 4.21Hz and for the 32kg model is 3.61Hz which are similar to the simulated results. In all cases, the PATMD, reduced the PSD reading by between 71% and 80%, demonstrating the control effect of the PATMD on torsional vibration, without any tuning or adjustment.

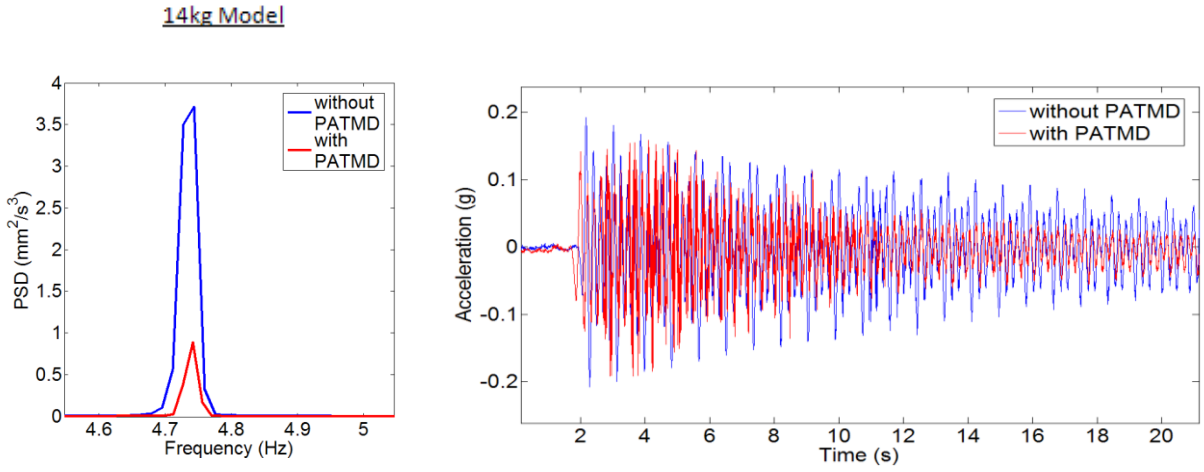

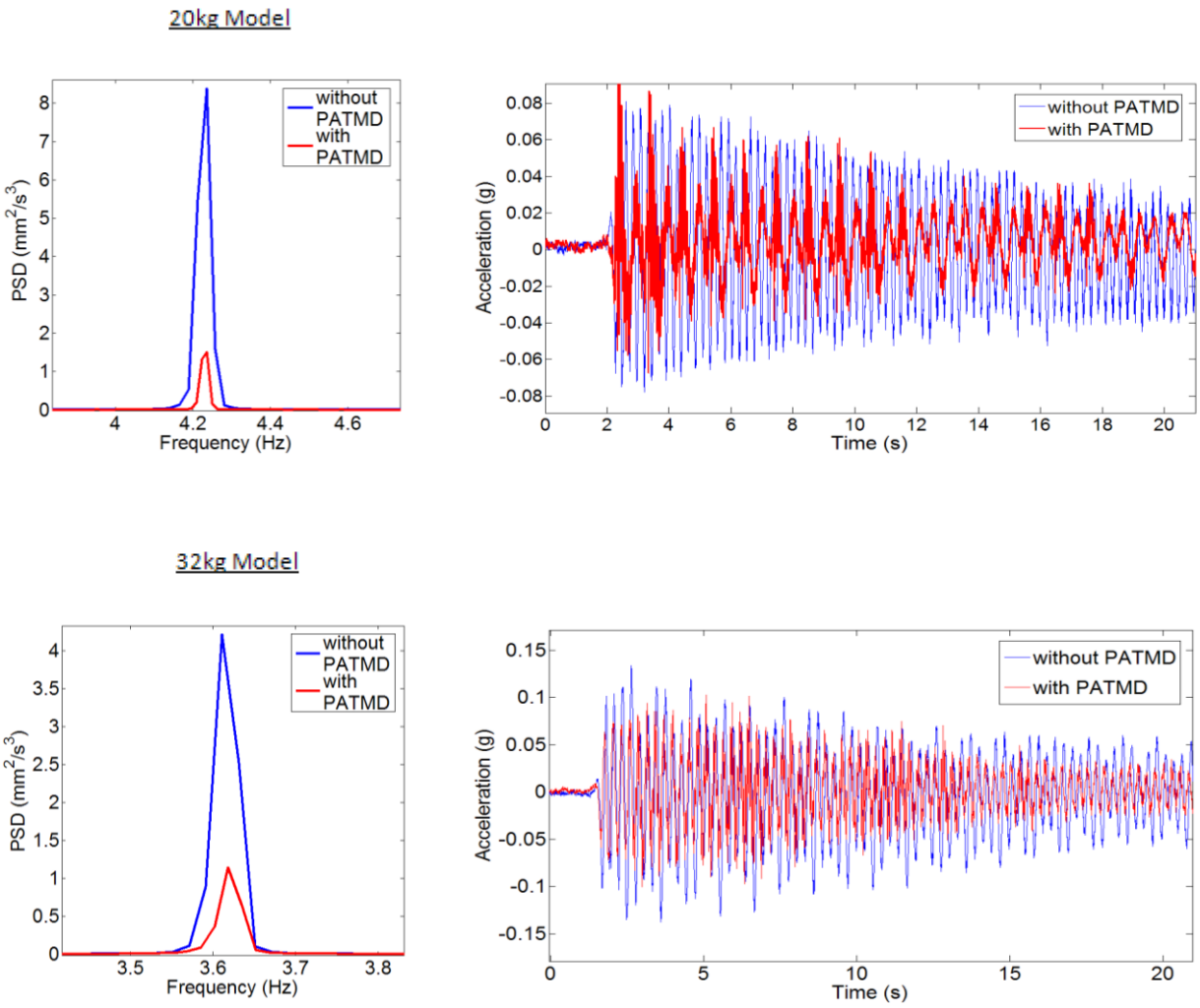

Figure 55. The PSD and time-history of acceleration graphs for free torsional vibration for model masses of 14kg, 20kg and 32kg respectively.

6.1.4 Coupled Vibration (Translation in the X-Direction and Torsion)

The graphs below show the PSD and time-history of acceleration readings for the 14kg model, 20kg model and 32kg model respectively for coupled vibration (translation in the X-direction and torsion). As can be seen, there are peaks at the translational natural frequency as well as the torsional natural frequency. For the 14kg model, the X-direction translational peak is at 2.36Hz and the torsional peak is at 4.75Hz. For the 20kg model, the X-direction translational peak is at 2Hz and the torsional peak is at 4.21Hz. For the 32kg model, the X-direction translational peak is at 1.6Hz and the torsional peak is at 3.61 Hz.

In all cases, the model containing the PATMD, has a much smaller peak PSD reading which demonstrates its effectiveness in controlling coupled vibration without having been tuned.

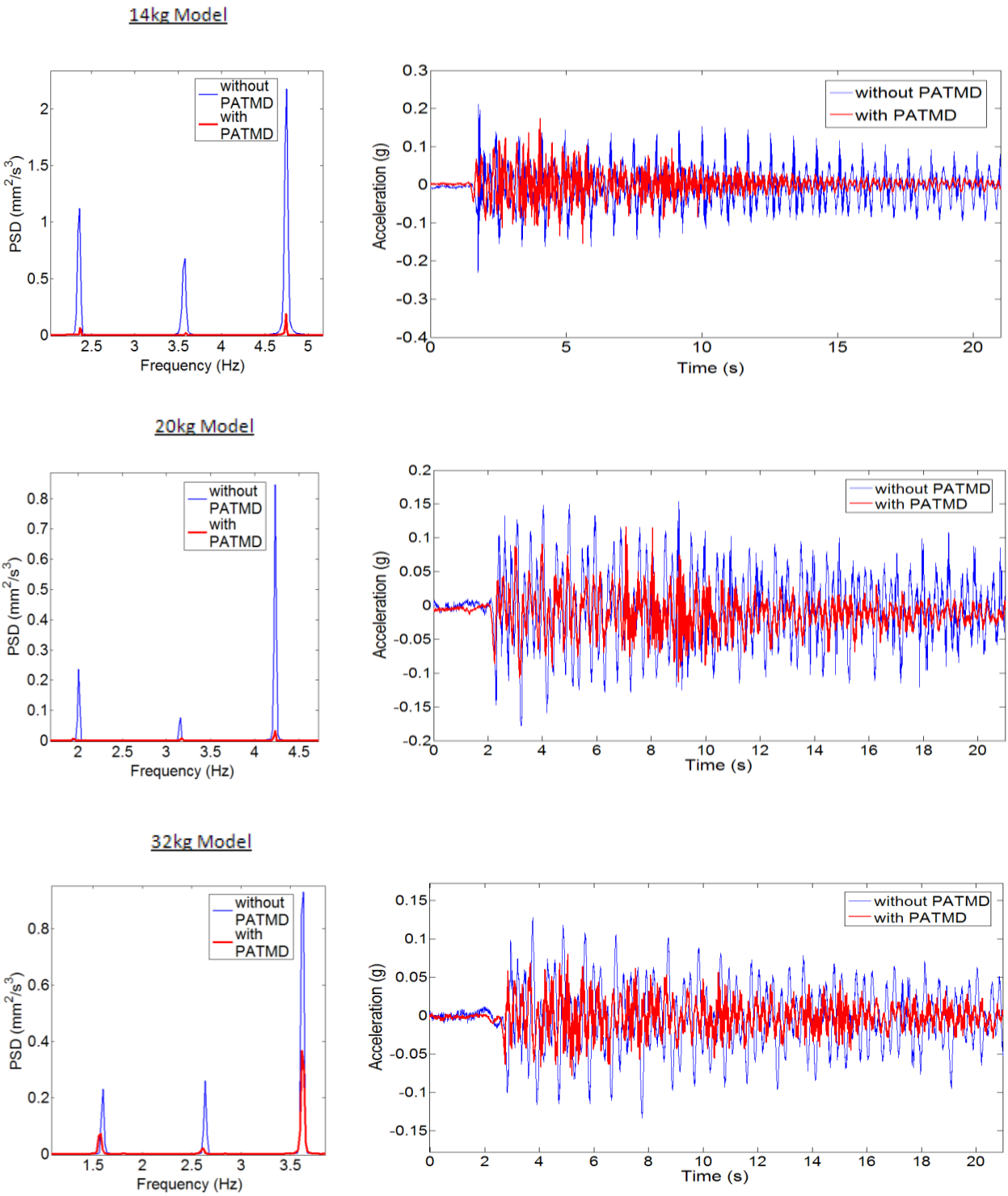

Figure 56. The PSD and time-history of acceleration graphs for free coupled vibration (translation in the Y-direction and torsion) for model masses of 14kg, 20kg and 32kg respectively.

6.1.5 Coupled Vibration (Translation in the Y-Direction and Torsion)

The graphs below show the PSD and time-history of acceleration readings for the 14kg model, 20kg model and 32kg model for coupled vibration (Y-direction translation and torsion). There are peaks at the natural frequency for translation in the Y-direction as well as the natural frequency for torsion in each case. For the 14kg model, the Y-direction translational peak is at 2.4Hz and the torsional peak is at 4.75Hz. For the 20kg model, the Y-direction translational peak is at 2.09Hz and the torsional peak is at 4.21Hz. For the 32kg model, the Y-direction translational peak is at 1.62Hz and the torsional peak is at 3.61Hz. Both of these peaks are reduced by the PATMD in every case, as well as any other peaks that occur, demonstrating its control effect without any tuning or adjustment. The time-history of acceleration graphs also demonstrate the PATMDs positive damping effects.

14kg Model

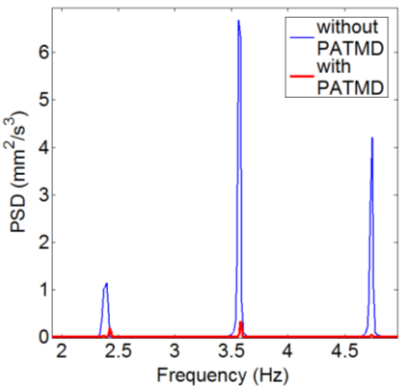

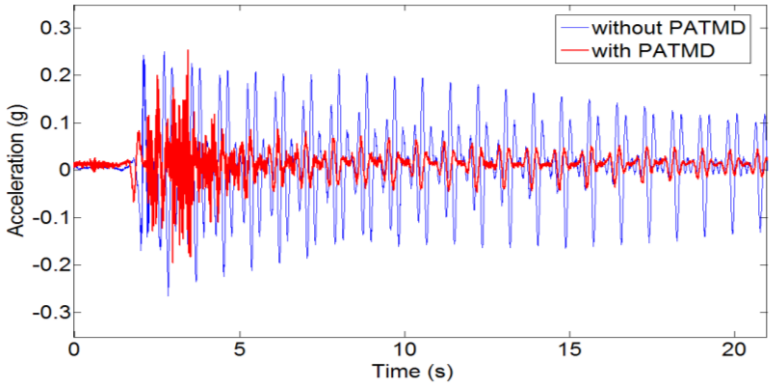

20kg Model

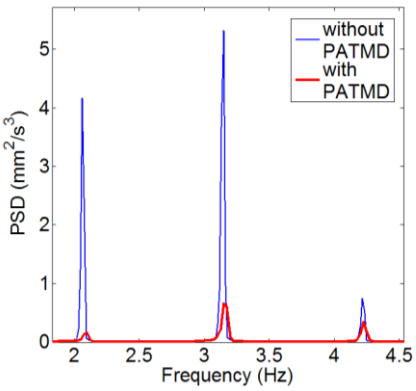

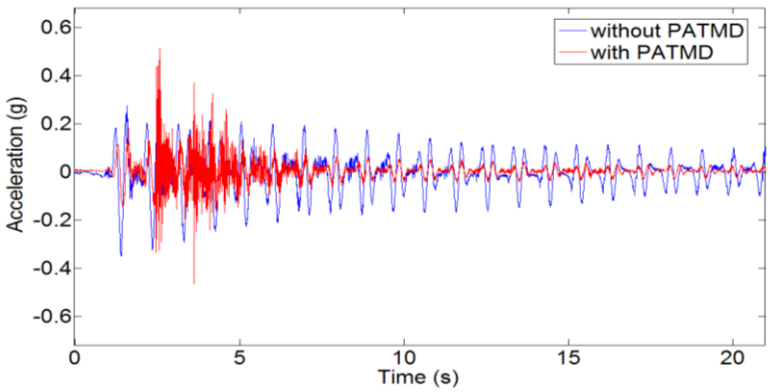

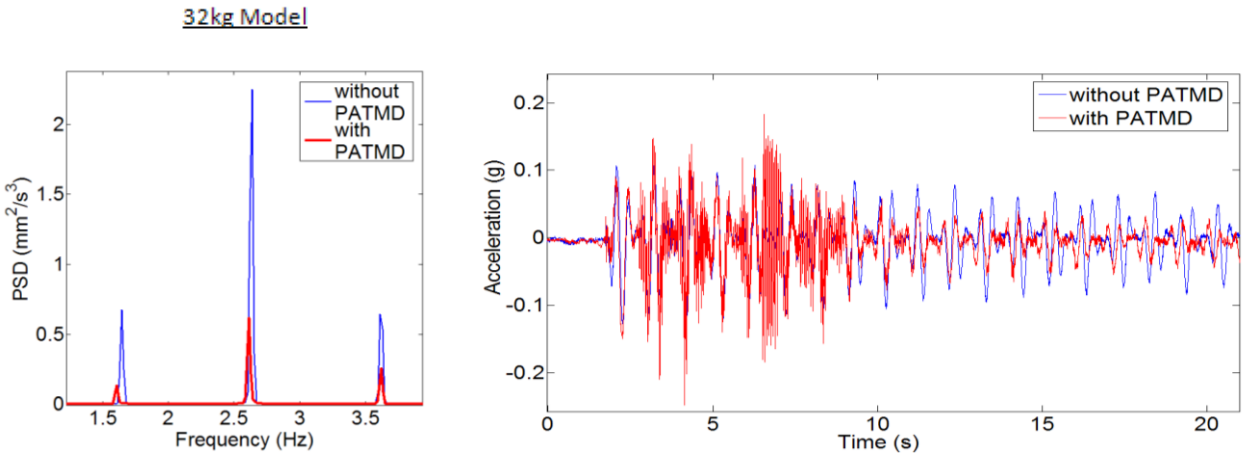

Figure 57. The PSD and time-history of acceleration graphs for coupled vibration (translation in the X-direction and torsion) for model masses of 14kg, 20kg and 32kg respectively.

6.2 Forced Vibration

6.2.1 Translational Vibration in the X-Direction

The same positive results that were observed in the free vibration tests were achieved in the forced vibration tests. The PSD peaks are significantly reduced by the addition of the PATMD in each case. The peak PSD values are reduced by 75%-96%.

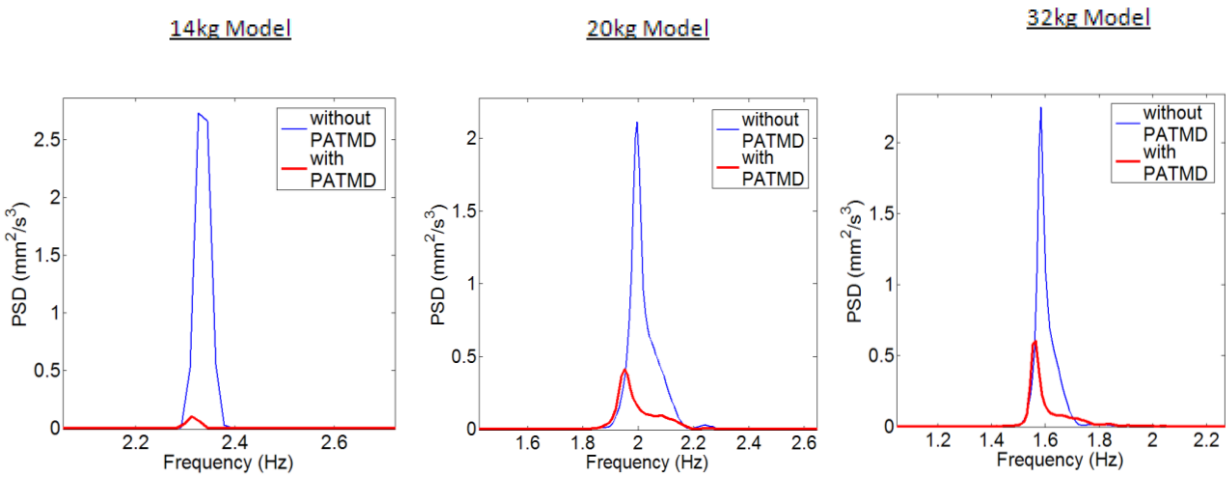

Figure 58. The PSD graphs for forced translational vibration in the X-direction for model masses of 14kg, 20kg and 32kg respectively.

6.2.2 Translational Vibration in the Y-Direction

As with the X-direction translational vibration, the tests for the Y-direction also produced the same positive results that were observed in the free vibration tests. The PSD peaks are reduced by 85%-97% by the addition of the PATMD.

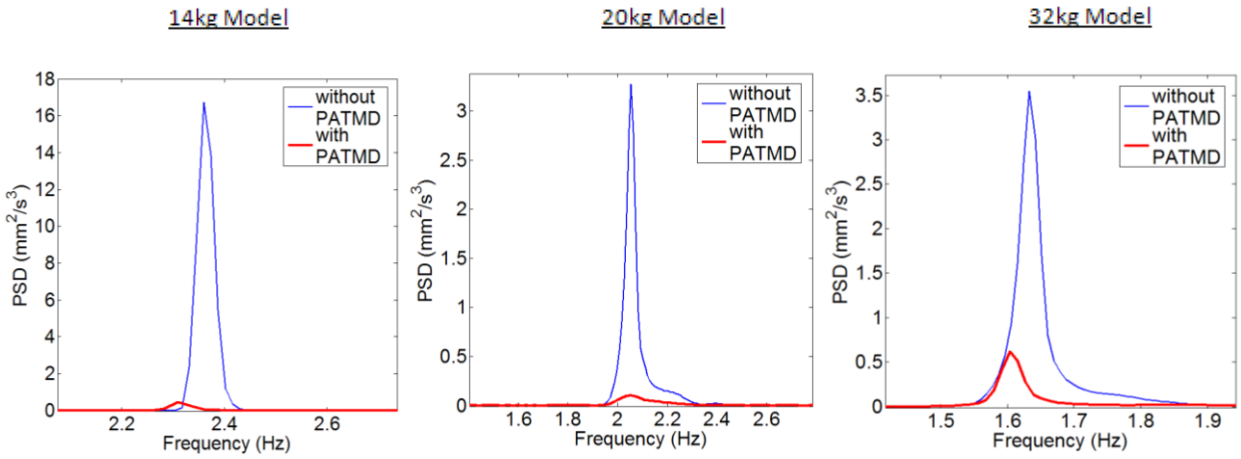

Figure 59. The PSD graphs for forced translational vibration in the Y-direction for model masses of 14kg, 20kg and 32kg respectively.

6.3 Summary and Conclusions

By changing the mass of the test model, the natural frequencies were altered. The test results reveal that the PATMD reduced the model's vibration response significantly in every case, meaning that it worked effectively over a relatively wide frequency range without any tuning or specific adjustment. The PSD peak for translational vibration was reduced by greater than 75% in every case, whilst the PSD peak for torsional vibration was reduced by greater than 71% in every case. The positive damping results were often not as obvious from the time-history of acceleration graphs. Again high accelerations were seen in the damped case soon after excitation in some instances; however these could be reduced by the slight tightening of the inelastic ropes.

Chapter 7

EFFECTS OF CHANGING THE MASS RATIO

7.1 Free Vibration

7.1.1 Translational Vibration in the X-Direction

The tests were then carried out using three different damper mass ratios, a 2.5% (0.35kg) mass, a 5% (0.7kg) mass and a 7.5% (1.05kg) mass. All other parameters remained constant during these tests, with the model having a mass of 14kg and a height of 1m. One-by-one the PATMD's were connected to the model, and the model was given an initial displacement in the X-direction, placing it into free vibration. The damping effect of each of the PATMD masses can be seen in the graph below. All three of the masses of the PATMD produced significant damping of the model's vibrations, reducing the PSD peaks by at least 90%.

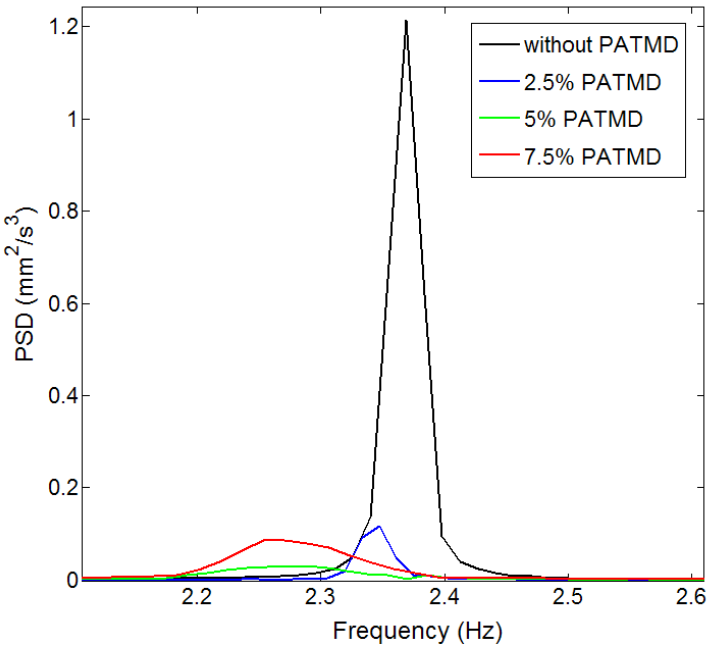

Figure 60. The PSD graphs for free translational vibration in the X-direction for mass ratios of 2.5%, 5% and 7.5%.

7.1.2 Translational Vibration in the Y-Direction

The tests were then repeated for translational vibration in the Y-direction. Again all three of the PATMD masses reduced the peak PSD value considerably - by around 95%.

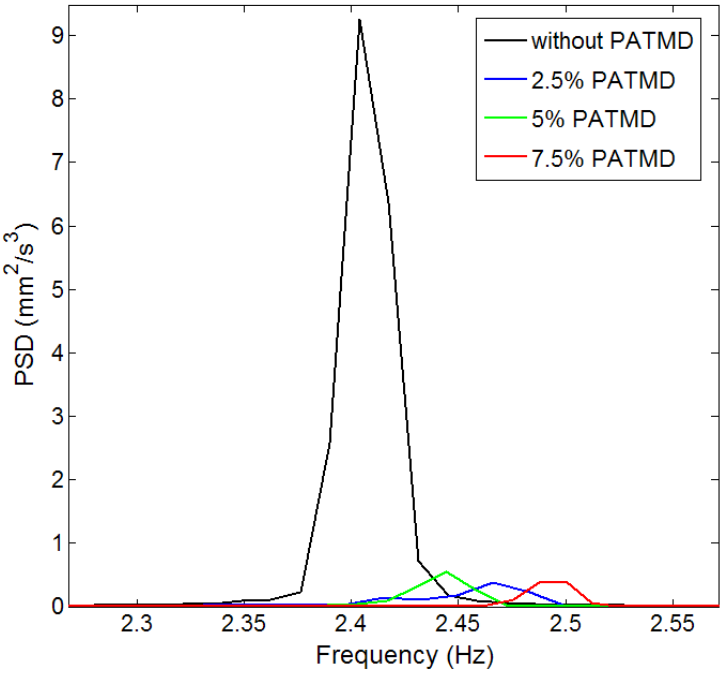

Figure 61. The PSD graphs for free translational vibration in the Y-direction for mass ratios of 2.5%, 5% and 7.5%.

7.1.3 Torsional Vibration

Next, each of the three PATMD's was connected separately and the model was then subjected to torsional vibration. The damping effect of the PATMD is obvious; however it is not as significant as in the case of translational vibration. All of the damped peak PSD values were reduced by about 65%-70% by the addition of the PATMD.

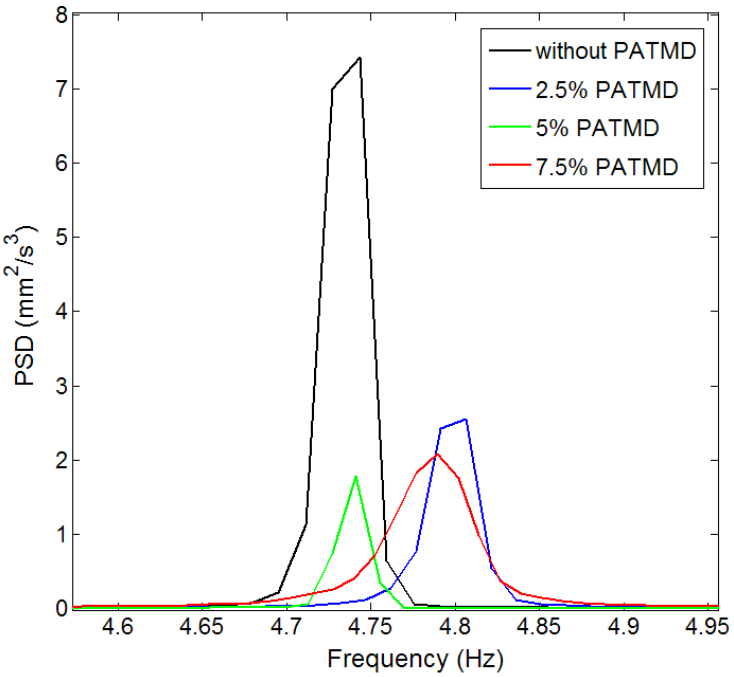

Figure 62. The PSD graphs for free torsional vibration for mass ratios of 2.5%, 5% and 7.5%.

7.1.4 Coupled Vibration (Translation in the X-Direction and Torsion)

The different PATMD masses were then connected one-by-one as the model was given initial torsional and translational displacements simultaneously. There are peaks at the natural frequency for translational vibration in the X-direction, 2.36Hz and at the natural frequency for torsional vibration, 4.75Hz. All of the peaks were damped by the addition of the PATMD.

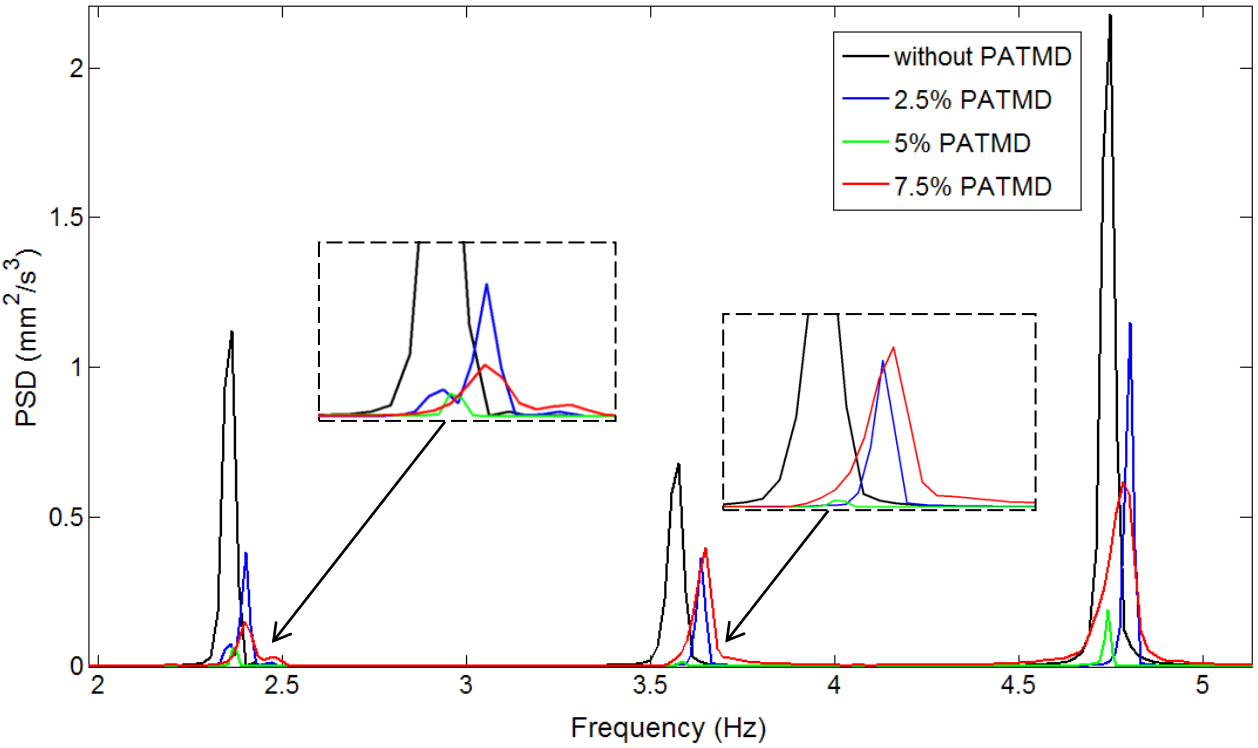

Figure 63. The PSD graphs for free coupled vibration (translation in the X-direction and torsion) for mass ratios of 2.5%, 5% and 7.5%.

7.1.5 Coupled Vibration (Translation in the Y-Direction and Torsion)

Next, the model was given initial torsional and translational displacements in the Y-direction simultaneously whilst the different PATMD masses were connected one-by-one. There are peaks at the natural frequency for translational vibration in the Y-direction, 2.55Hz and at the natural frequency for torsional vibration, 4.75Hz. All of the peaks were damped by the addition of the PATMD.

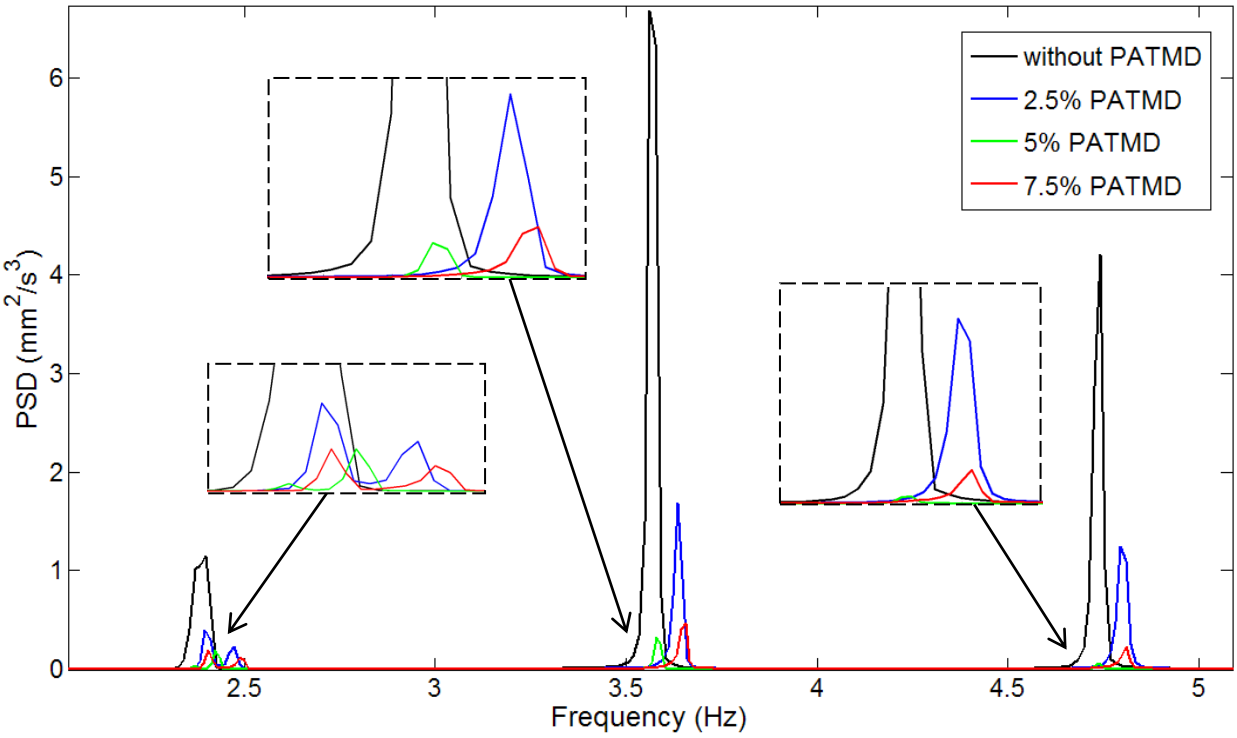

Figure 64. The PSD graphs for free coupled vibration (translation in the Y-direction and torsion) for mass ratios of 2.5%, 5% and 7.5%.

7.2 Forced Vibration

7.2.1 Translational Vibration in the X-Direction

The model was then placed on the shaking table in order to carry out the forced vibration tests. Again the PATMD's were connected one-by-one and the damping effect of each was recorded in the graph below. All three PATMD masses produced significant damping of the model's vibrations, reducing the peak PSD values by at least 93%.

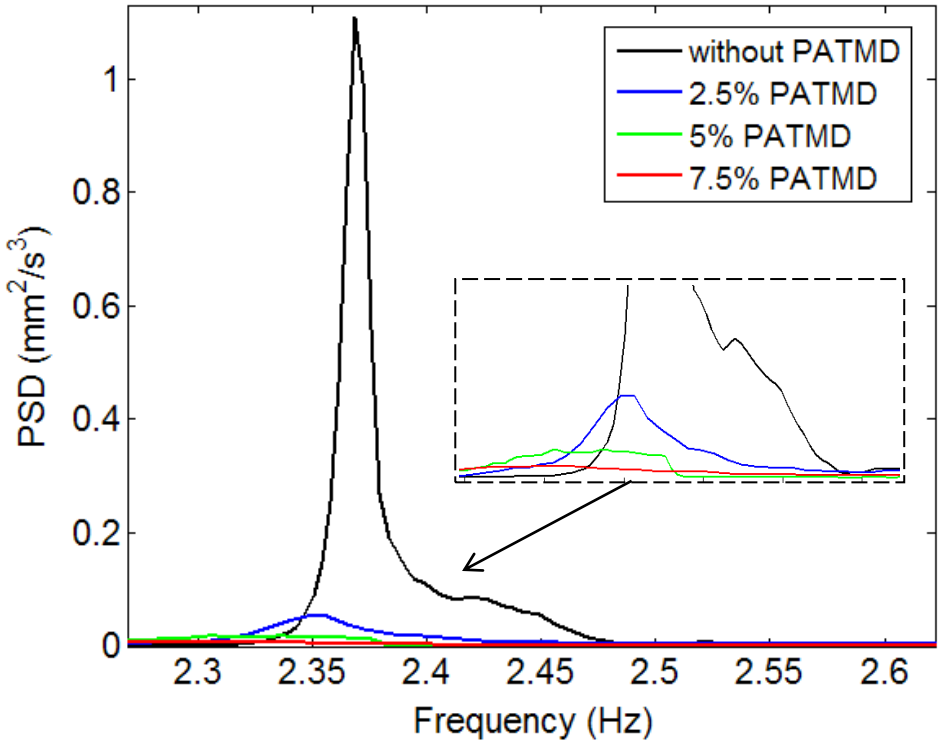

Figure 65. The PSD graphs for forced translational vibrations in the X-direction for mass ratios of 2.5%, 5% and 7.5%.

7.2.2 Translational Vibration in the Y-Direction

The model was then subjected to forced translational vibration in the Y-direction. Again all three of the PATMD masses reduced the peak PSD value considerably. The PSD readings were reduced by at least 96% by the addition of the PATMD.

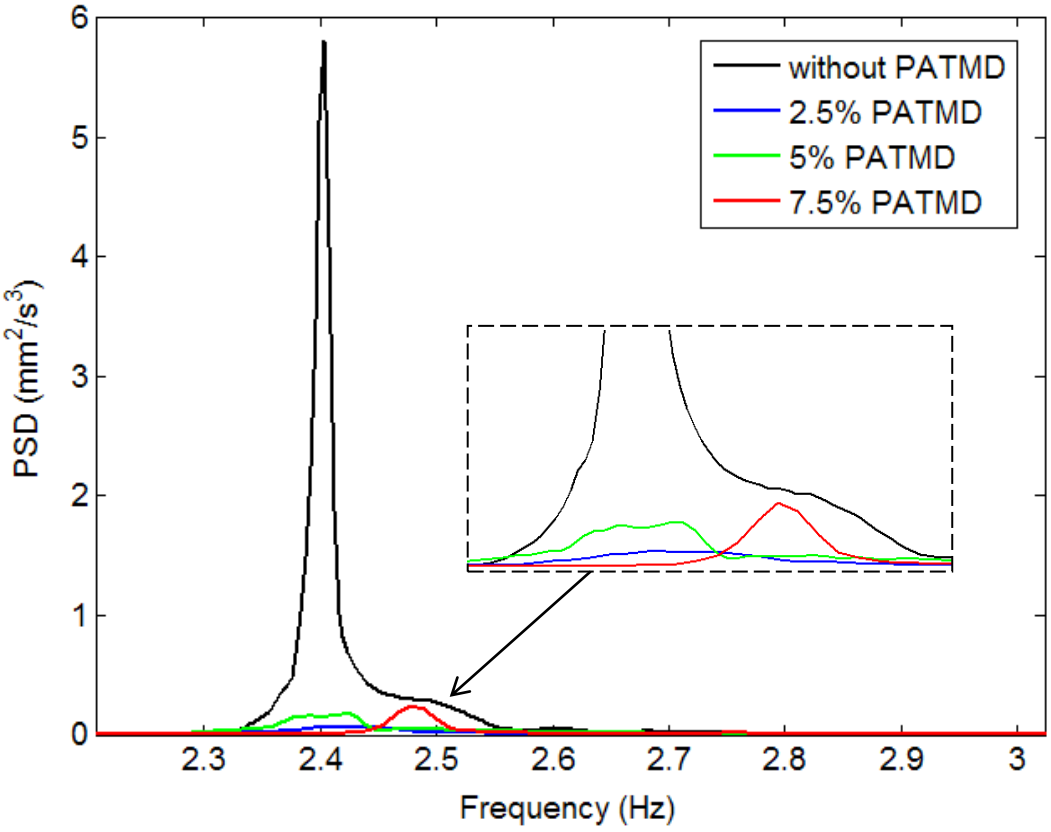

Figure 66. The PSD graphs for forced translational vibrations in the Y-direction for mass ratios of 2.5%, 5% and 7.5%.

7.3 Summary and Conclusions

All three of the PATMD mass ratios successfully reduced the vibration for translational, torsional and coupled vibration. The attenuation of translational vibration was the most significant, with the PSD peaks being reduced by greater than 90% in each test. The peak PSD reductions for torsional and coupled vibration were not as high; however the attenuation was still significant with the PSD peak being reduced by greater than 65% for torsion. The PATMD of 5% mass ratio produced the highest attenuation in most cases, whilst the 2.5% produced the lowest attenuation.

Chapter 8

EFFECTS OF CHANGING THE PATMD CONNECTION

8.1 Free Vibration

8.1.1 Translational Vibration in the X-Direction

The PATMD was connected to the primary structure in eight different ways in order to determine the effect of this connection on the damping of the structure. During these tests, no adjustment of the PATMD's mass ratio took place; and the mass and stiffness of the primary structure were left constant at 14kg and 1m high respectively. The eight different configurations have been described in Section 3.2.5, and are shown in photographs in Appendix B.

In this first test, the model was given an initial displacement in the X-direction and released. The PSD graph below demonstrates that the PATMD provides a postive damping effect for all the connection configurations considered. Most of the connecting configurations reduced the PSD peak by more than 97%. Three of the configurations however, 4,5 and 7 provided less attenuation, reducing the PSD peak by 50%-40%. The attenuation provided by the PATMD in all of the cases again demonstrates the PATMD's capability of providing vibration control under very different conditions and without having been specifically tuned.

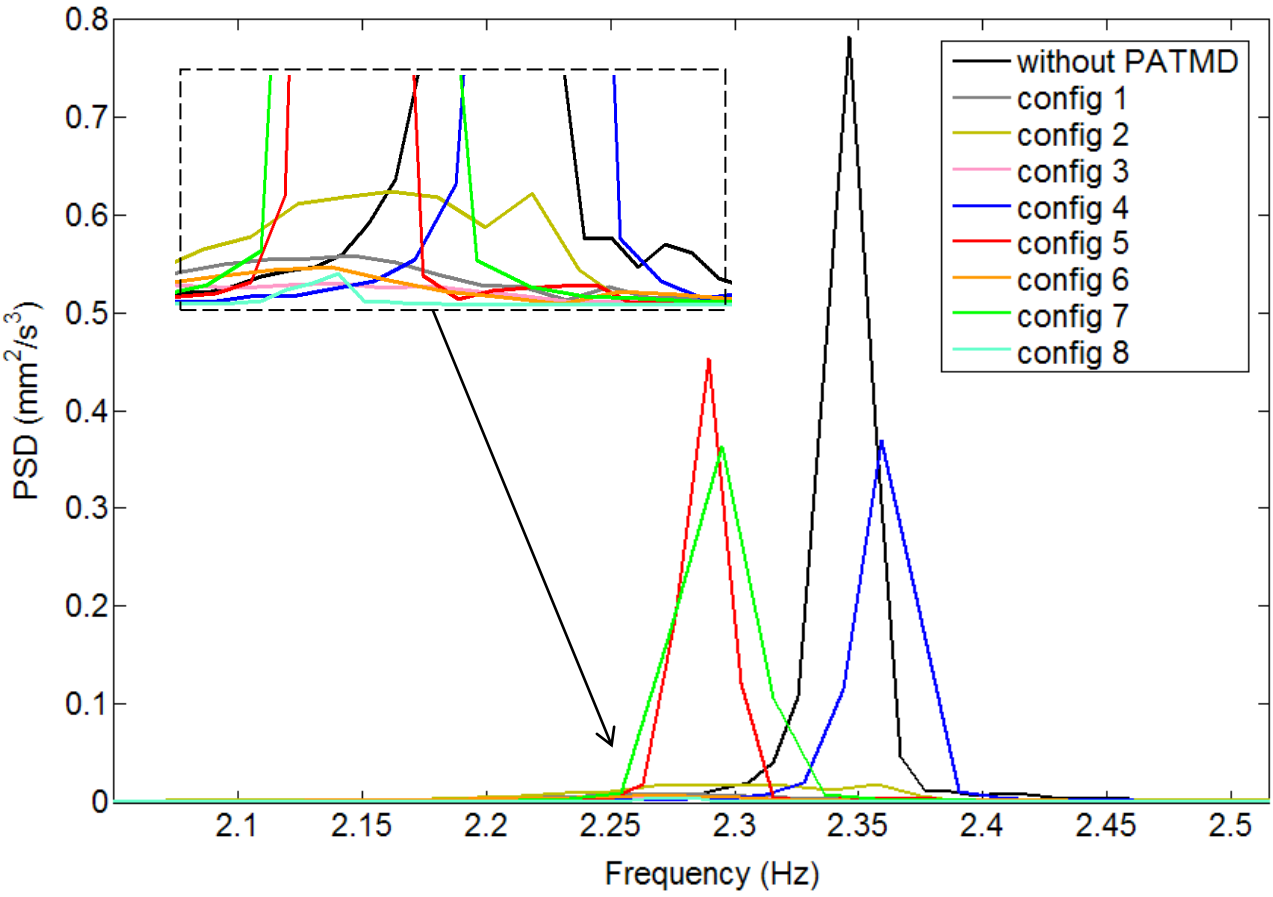

Figure 67. The PSD graphs for free translational vibration in the X-direction for the different connecting configurations of the PATMD.

8.1.2 Translational Vibration in the Y-Direction

The model was then given an initial displacement in the Y-direction and released. The PSD graph below demonstrates that the PATMD provides a postive damping effect for all of the connection configurations considered, reducing the damped peak PSD by greater than 86% in all cases, again demonstrating it's efficiency without having been tuned.

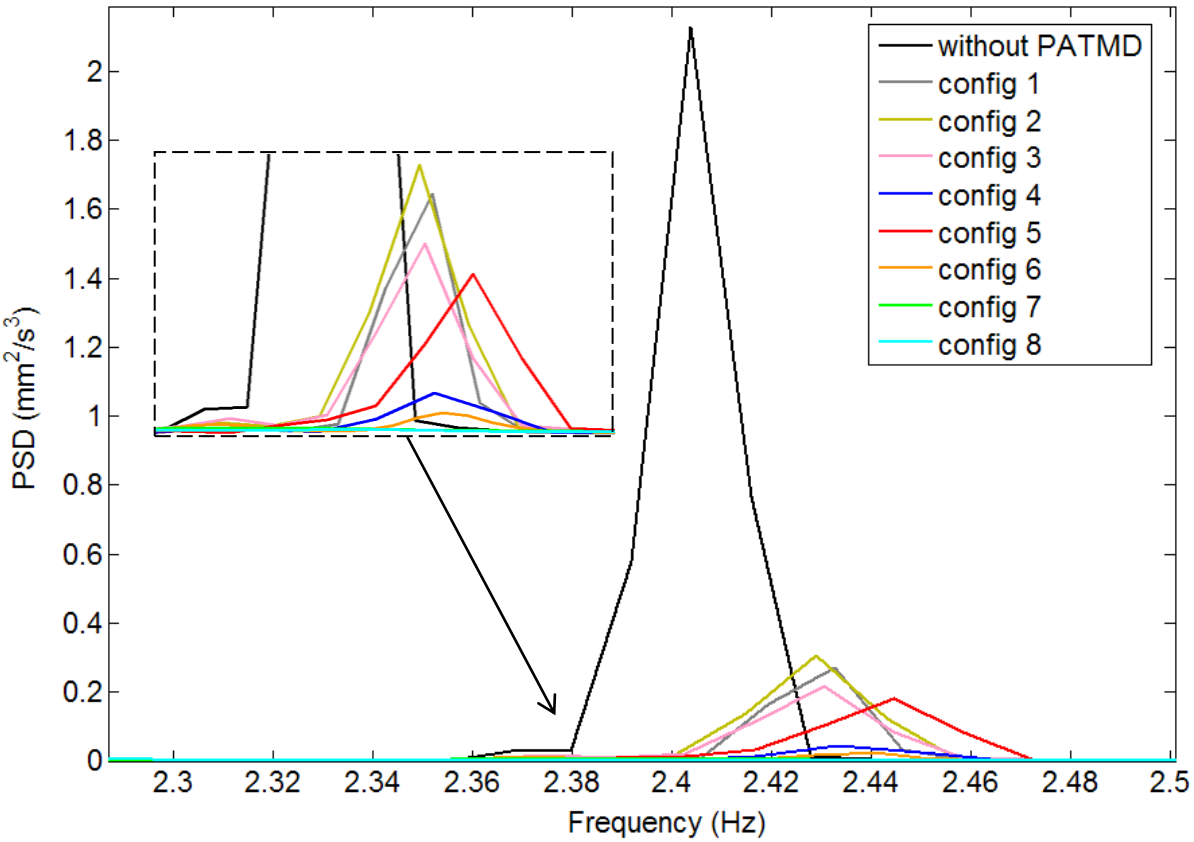

Figure 68. The PSD graphs for free translational vibration in the Y-direction for the different connecting configurations of the PATMD.

8.1.3 Torsional Vibration

The model was then given an initial torsional displacement. The PSD graph below shows that the amount of attenuation provided by the PATMD for torsional vibration, is not as significant as for translation vibration. The PSD peaks for the different configurations were reduced by between 40%-93% by the addition of the PATMD. This demonstrates that the connecting configuration can have a large impact on the level of attenuation achieved, however all of the configurations provided control, without any tuning of the PATMD. Again configurations 4,5 and 7 provided the least control.

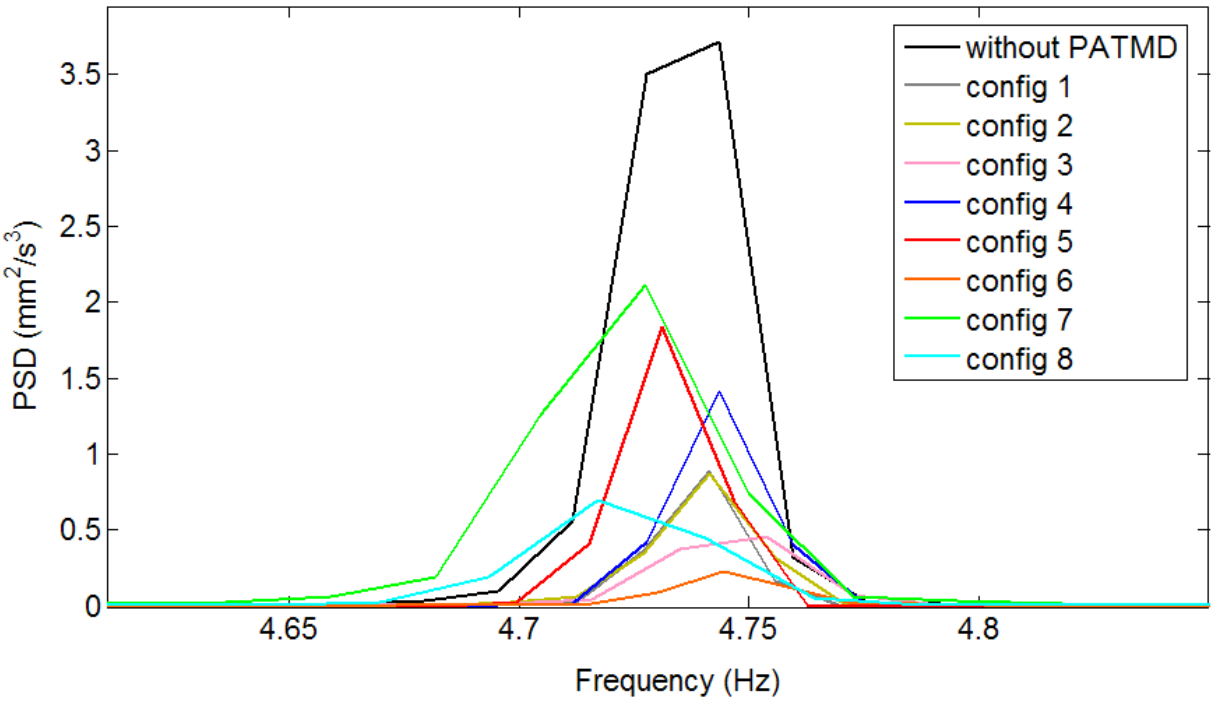

Figure 69. The PSD graphs for free torsional vibration for the different connecting configurations of the PATMD.

8.1.4 Coupled Vibration (Translation in the X-Direction and Torsion)

The model was then subjected to an initial coupled displacement (X-direction and torsion). The PSD graph below shows the translational peak at 2.36Hz and a torsional peak at 4.75Hz. Configurations 4 and 5 provided the least control again, with configuration 4, in fact exacerbating the situation at the translational peak of 2.36Hz. Once more this demonstrates that the connecting configuration can have a large impact on the level of attenuation achieved, however the PATMD provided relatively significant attenuation for all but two of the configurations considered, without any tuning having taken place.

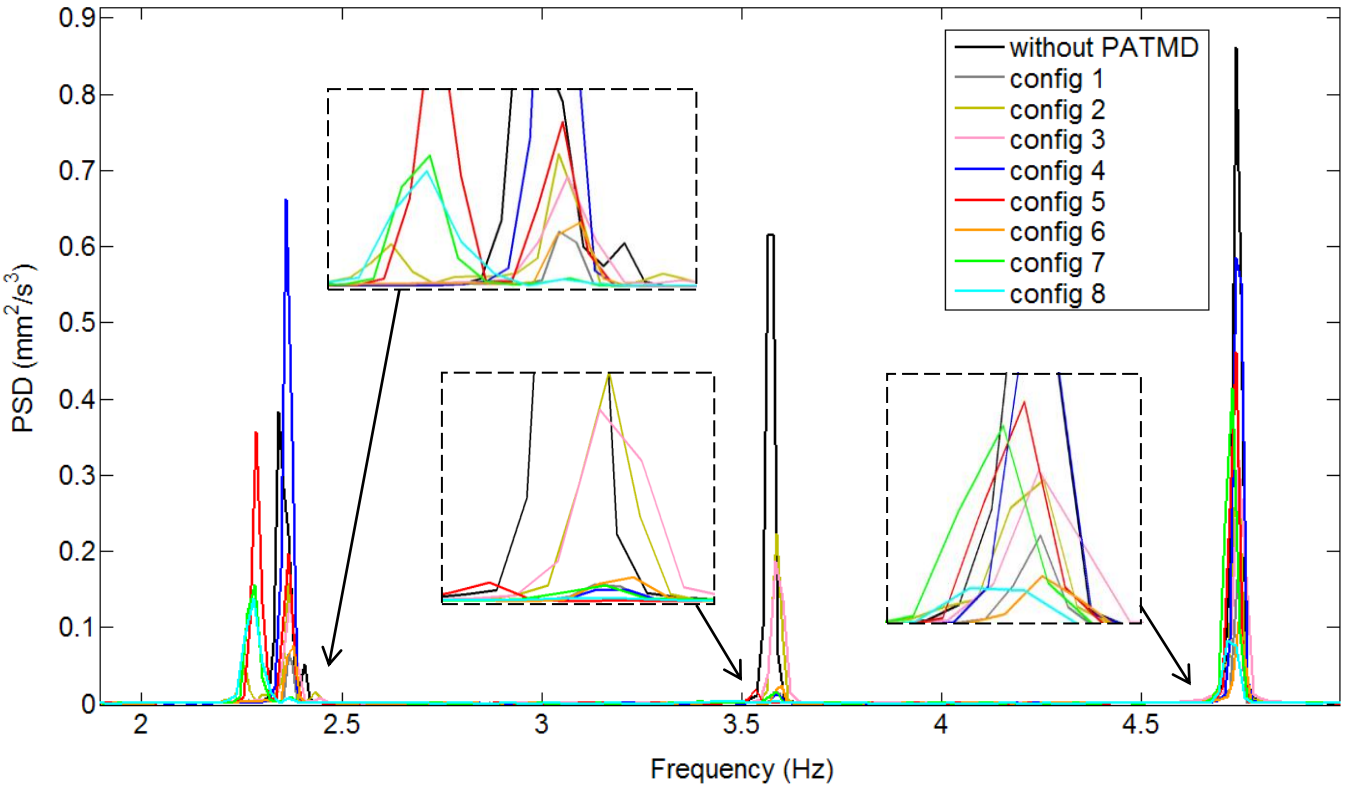

Figure 70. The PSD graphs for free coupled vibration (translation in the X-direction and torsion) for the different connecting configurations of the PATMD.

8.1.5 Coupled Vibration (Translation in the Y-direction and Torsion)

The model was then subjected to another initial coupled displacement (Y-direction and torsion). The PSD graph below shows the translational peak at 2.4Hz and a torsional peak at 4.75Hz. Again configuration 5 provided the least control, worsening the the situation at the translational peak of 2.4Hz. Configuration 8 also did not provide much control for the torsional peak at 4.75Hz, however all of the other six configurations provided significant attenuation.

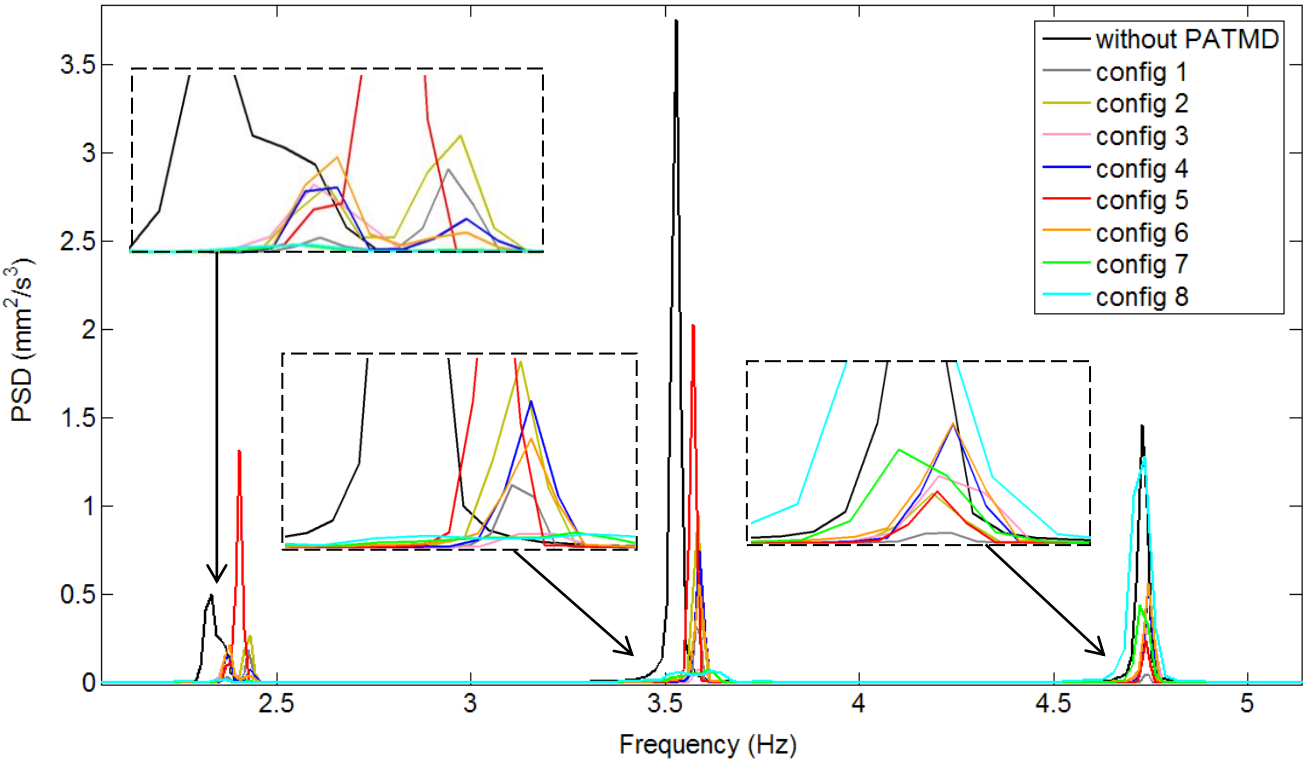

Figure 71. The PSD graphs for free coupled vibration (translation in the Y-direction and torsion) for the different connecting configurations of the PATMD.

8.2 Forced Vibration

8.2.1 Translational Vibration in the X-Direction

The model was placed on the shaking table for the forced vibration tests. As can be seen, the PATMD provided vibration attenuation for all of the connection configurations considered. Once again, configuration 5 provided the least control, however the PSD peak was still damped by 62% in this case.

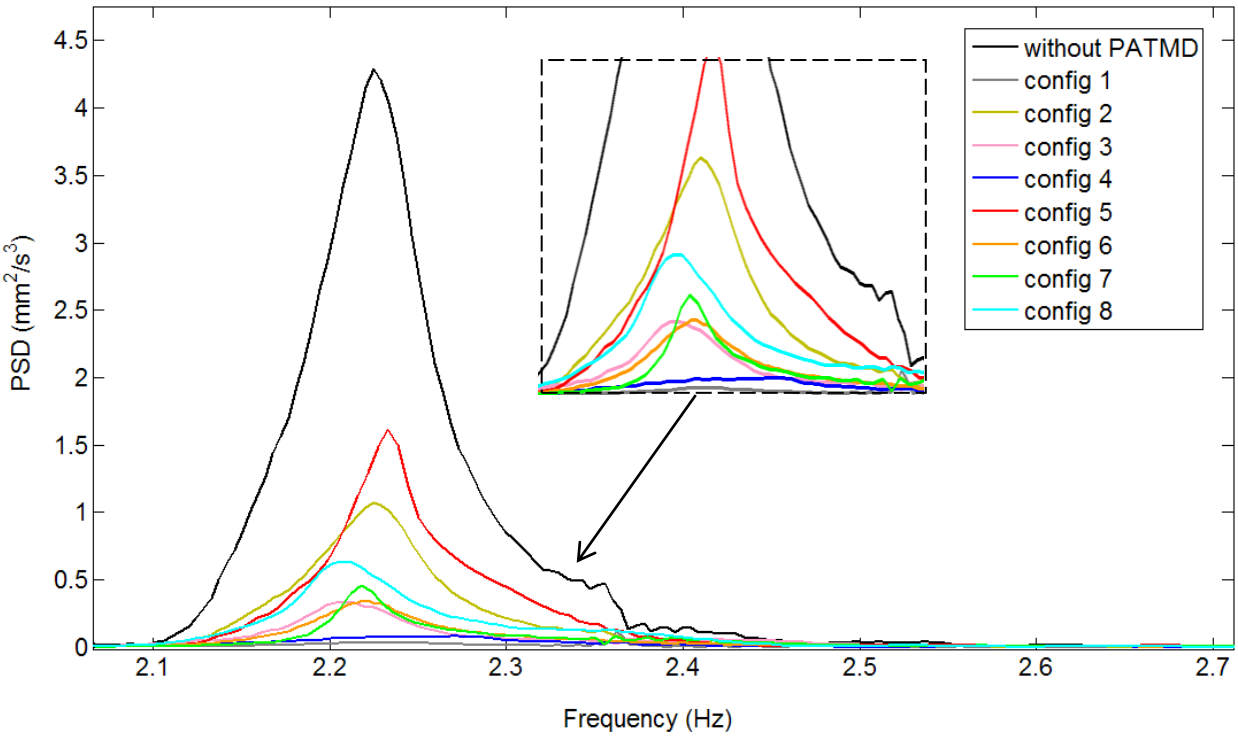

Figure 72. The PSD graphs for forced translational vibration in the X-direction for the different connecting configurations of the PATMD.

8.2.2 Translational Vibration in the Y-Direction

The model was placed on the shaking table in the Y-direction for these tests. As can be seen, the PATMD provided vibration attenuation for all of the connection configurations considered. Configuration 5 provided the least control with the PSD peak being damped to by 55% in this case.

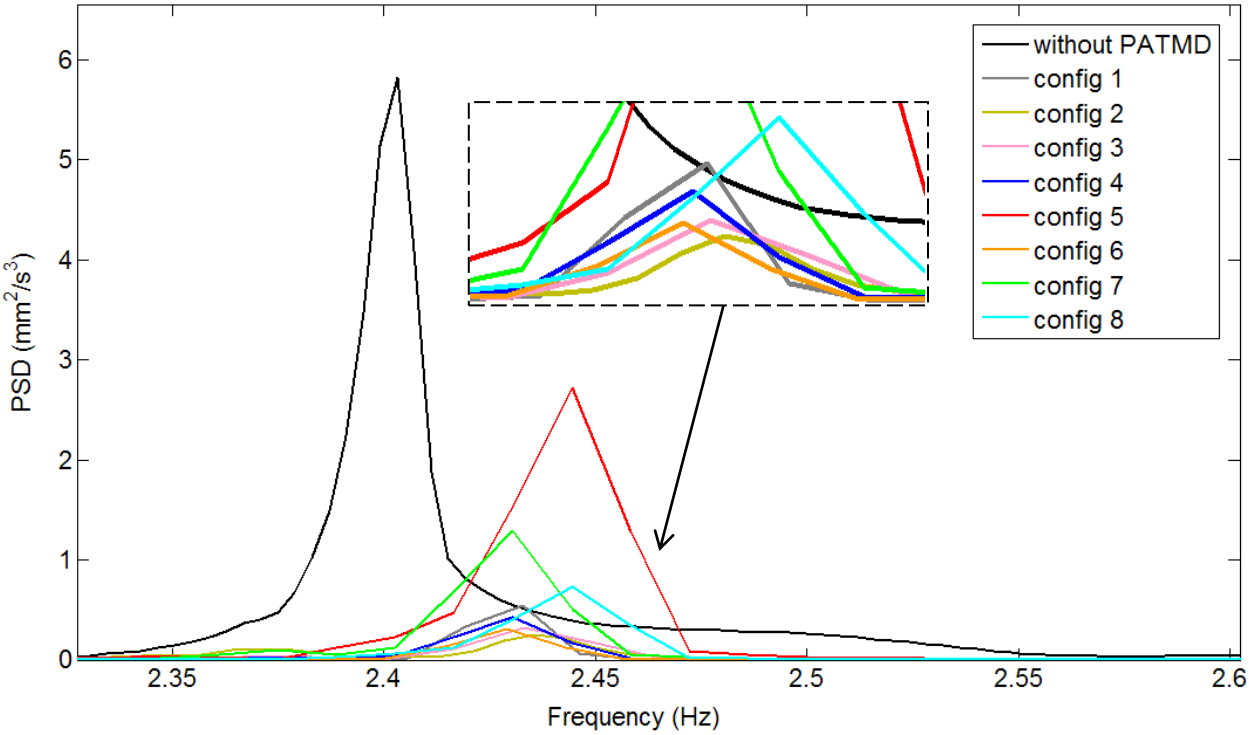

Figure 73. The PSD graphs for forced translational vibration in the Y-direction for the different connecting configurations of the PATMD.

8.3 Summary and Conclusions

Most of the connection configurations provided significant attenuation to the translational, torsional and coupled vibrations of the test model. It is clear from the results that the way in which the PATMD is connected to the primary structure has a large impact on the amount of vibration attenuation that takes place. Three of the configurations, 4,5 and 7 provided less control than the others in most of the tests. Configuration 4 represents the connection where only the two side ropes are connected, as shown in Figure 33. It is perhaps therefore understandable that the attenuation achieved is not very significant. Configuration 5 represents the case where all of the ropes are connected and they are pulled taut. Again, it is reasonable that this configuration did not provide high levels of attenuation as the PATMD was not free to move very much as it was connected so tightly, and therefore it could not dissipate large amounts of energy. Configuration 7 represents one of the 'random' connections.

Chapter 9

CONCLUSIONS

Ongoing advances in material science technology and structural analysis programs are the primary innovations allowing structures to be built taller and more slender. As these new technologies develop, structures are becoming more lightweight and flexible, and the problem of the vibrations in the floor systems of these buildings is becoming more of an issue to the inhabitants and designer. A number of vibration attenuation techniques have been researched and tested, and the emergence of vibration control devices has been an exciting engineering innovation that is still relatively new and shows a lot of promise as new devices are researched and developed. The TMD is the most common control device found in the literature and has been the most widely implemented auxiliary device. It has however, a few drawbacks that have generated the need for research into improvements. The vibration attenuation device proposed herein, the PATMD, therefore tackles the issues of torsional and coupled vibration control and the detuning of the TMD.

The free and forced vibration tests which were carried out, demonstrate the PATMD's capability of providing considerable vibration attenuation to structures such as the tall, flexible test model which has been tested. The PATMD efficiency tests revealed significantly positive attenuation for translational as well as torsional and coupled vibrations. The translational vibration PSD peaks were damped by at least 92% in the free and forced tests, whilst the torsional and coupled vibrations were damped by at least 77%. Generally,

TMDs have only been able to control a single frequency of the structure – the frequency to which they have been tuned. However, real-life structures contain more than one natural frequency as they can vibrate in a couple of translational directions (both with different frequencies), as well as in torsional and coupled directions (also with separate frequencies). Theoretically, each frequency to be controlled would require its own TMD, however the proposed PATMD is autonomously able to control multiple frequencies of the structure, as is demonstrated by its ability to control translational, torsional and coupled vibration. Furthermore, torsional and coupled vibration have, in the past, been more difficult to control than translational vibration and often multiple dampers or active dampers are needed. The proposed PATMD, although a singular passive damper, significantly reduced the torsional and coupled vibration of the test structure in the preceding tests.

The mass and stiffness of the test model were varied in the parameter tests, thereby altering the model's natural frequencies significantly. The experimental tests revealed that the PATMD continued to work effectively under the different conditions without being altered in any way; and it was therefore concluded that the PATMD is efficacious under a wide range of frequencies, without being tuned. This is a significant advantage over traditional TMDs which are often the subject of detuning due to changes in the structure's natural frequency, which can render the TMD ineffective.

The mass ratio of the PATMD and its connection to the test model were then altered in separate tests, while keeping the model's properties constant. Again, the PATMD worked effectively for all three of the mass ratios tested. The PATMD provided significant attenuation for most of the connecting configurations; however three of the eight configurations provided less vibration control. More research should be conducted into finding the optimum connecting conditions, as it seems to have a large effect on the level of attenuation achieved.

The preceding experimental results reveal that although the passive auto-tuning mass damper is a simple solution, it is robust, effective and versatile. It can effectively control translational, torsional and coupled vibration, without having been tuned, making it an attractive solution for many engineering applications.

Chapter 10

FURTHER RESEARCH

The attenuation provided by the PATMD in all cases reveals that specific tuning of the PATMD is not neccesary, however more research should be carried out to determine the PATMD connection configuration which provides the optimum amount of vibration control.

The test model considered consisted of only a single storey. The PATMD's effectiveness in a multiple storey structure should be investigated.

The research contained herein was based solely on experimentation of a test model. Further research needs to be carried out in order to develop practical design and optimisation guidelines in order for the PATMD to become a viable solution in real-life structures.

Although the test model was subjected to a frequency sweep during the forced vibration tests, it was not subjected to an earthquake signal. Perhaps the PATMD's effectiveness under earthquake loading should be a subject of further research.

BIBLIOGRAPHY

Abdelraheem Farghaly, A. (2012), 'Optimum design of TMD system for tall buildings', *The International Journal of Optimization in Civil Engineering,* 2(4), 511-532.

Ali, M.M. (2005). 'The skyscraper: epitome of human aspirations', *Proceedings of the 7th World Congress of the Council on Tall Buildings and Urban Habitat: Renewing the Urban Landscape.* Chicago.

Ali, M.M. and Moon, K.S. (2007), 'Structural developments in tall buildings: Current trends and future prospects', *Architectural Science Review*, 50(3), 205−223.

Amin, J.A. and Ahuja, A.K. (2010), 'Aerodynamic modifications to the shape of the buildings: A review of the state-of-the-art', *Asian Journal of Civil Engineering (Building and Housing),* 11(4), 433-450.

Bandivadekar, T.P. and Jangid, R.S. (2012), 'Optimization of multiple tuned mass dampers for vibration control of system under external excitation', *Journal of Vibration Control*.

Bergman, L.A., MacFarland, D.M and Kareem, A. (1991), 'Coupled passive control of buildings', Structural Abstracts, ASCE, New York, N.Y.

Carlisle, M and Li, K. (2013), 'A suspended mass damper for torsional and translational vibration control', *Proceedings of the 5th International Conference on Structural Engineering, Mechanics and Computation,* Cape Town.

Carlisle, M and Li, K. (2013), 'An experimental investigation into the use of a suspended mass damper to control translational and torsional vibration', Manuscript submitted for publication.

Carlisle, M and Li, K. (2013), 'An experimental investigation into a passive auto-tuning mass damper', Manuscript submitted for publication.

Clark, P., Aiken, I. and Kelly, J. (1997), 'Ongoing studies of the Foothill Communities Law and Justice Center', *Proceedings of the Structures Congress XV, Portland, Oregon.*

Datta, T.K. (2003), 'A state-of-the-art review on active control of structures', *ISET Journal of Earthquake Technology,* 41(1), 1-17.

Dyke, S.J., Spencer, B.F., Sain, M.K. and Carlson, J.D. (1996), 'Experimental verification of semi-active structural control strategies using acceleration feedback', *Proceedings of the 3rd International Conference on Motion and Vibration Control*, Chiba, Japan.

Feblowitz, J. (2010), *Confusing the Wind: The Burj Khalifa, Mother Nature, and the Modern Skyscraper*. [Online] Available at: http://www.studentpulse.com/articles/124/confusing-the-wind-the-burj-khalifa-mother-nature-and-the-modern-skyscraper (Accessed: 12 March 2013).

Gharib, M. and Ghani, S. (2012), 'Passive vibration control using a linear particle chain impact damper', *Proceedings of the Qatar Foundation Annual Research Forum*. Qatar.

Hazra, B. and Sadhu, A. (2013), 'Output-only de-tuning assessment of tuned mass dampers.' *Journal of Civil Structural Health Monitoring*, 3(1), 33−48.

Hoang, N., Fujino, Y. and Warnitchai, P. (2008) 'Optimal tuned mass damper for seismic applications and practical design formulas'. *Engineering Structures*, 30, 707-715.

Iwanami, K. and Seto, K. (1984), 'Optimum design of dual tuned mass dampers and their effectiveness', *Proceedings of the Japan Society of Mechanical Engineering*, 50, 44-52.

Jangid, R.S. (1995), 'Dynamic characteristics of structures with multiple tuned mass dampers', *Structural Engineering and Mechanics*, 28, 1041-1049.

Kareem, A., Kijewski, T. and Tamura, Y. (1999), 'Mitigation of motions of tall buildings with specific examples of recent applications', *Wind and Structures*, 2(3), 201-251.

Kareem, A. and Kline, S. (1995), 'Performance of multiple mass dampers under random loading', *Journal of Structural Engineering, ASCE*, 121, 348-361.

Kaynia, A.M., Veneziano, D. and Biggs, J.M. (1981), 'Seismic effectiveness of tuned mass dampers', *Journal of Structural Engineering-ASCE*, 107(8), 1465–1484.

Kobori, T., Takahashi, M. and Niwa, N. (1993), 'Seismic response controlled structure with active variable stiffness system', *Earthquake Engineering and Structural Dynamics*, 22(9), 925-941.

Kourakis, I. (2005) *Structural Systems and Tuned Mass Dampers of Super-Tall Buildings: Case Study of the Taipei 101*. Unpublished MSc thesis. Aristotle University of Thessaloniki.

Landau, S.B. and Condit, C.W. (1996), *The Rise of the New York Skyscraper 1865-1913*. Yale University Press, Connecticut.

Lewandowski, R. and Grzymisławska, J. (2009), 'Dynamic analysis of structures with multiple tuned mass dampers', *Journal of Civil Engineering and Management*, 15(1), 77-86.

Li, C. (2000), 'Performance of multiple tuned mass dampers for attenuating undesirable oscillations of structures under the ground acceleration', *Earthquake Engineering and Structural Dynamics*, 29, 1405-1421.

Li, H.N. and Ni, X.L. (2007), 'Optimization of non-uniformly distributed multiple tuned mass damper,' *Journal of Sound and Vibration*, 308(1-2), 80–97.

Li, K. and Darby, A.P. (2006), 'An experimental investigation into the use of a buffered impact damper', *Journal of Sound and Vibration*, 291, 844-860.

Lin, C.C., Ueng, J.M. and Haung, T.C. (1999), 'Sesimic response reduction of irregular buildings using passive tuned mass dampers', *Engineering Structures*, 22, 512-524.

Lourenco, R., Roffel, A. J. and Narasimhan, S. (2009), 'Adaptive pendulum mass damper for the control of structural vibrations', *Proceedings of Cansmart 2009 International Workshop*, Quebec, Canada.

Lynch, J. P. (1998), 'Active structural control research at Kajima Corporation.' *The National Science Foundation's Summer Institute in Japan Program*. Stanford University, U.S.A.

Matta, E., De Stefano, A. and Spencer, B.F. (2009), 'A new passive rolling-pendulum vibration absorber using a non-axial-symmetrical guide to achieve bidirectional tuning.' *Earthquake Engineering and Structural Dynamics*, 38, 1729 – 1750.

Mendis, P., Ngo, T., Haritos, N., Hira, A., Samali, B. and Cheung, J. (2007), 'Wind loadings on tall buildings', *EJSE Special Issue: Loading on Structures.*

Nagarajaiah, S. (2009), 'Adaptive passive, semiactive, smart tuned mass dampers: identification and control using empirical mode decomposition, hilbert transform, and short-term fourier transform', *Structural Control and Health Monitoring*, 16, 800–841.

Nagarajaiah, S. and Varadarajan, N. (2004), 'Short time fourier transform algorithm for wind response control of buildings with variable stiffness TMD', *Engineering Structures*, 27(3), 431–441.

Nawrotski, P. (2006), 'Earthquake protection for buildings and other structures', *Proceedings of the International Forum - Earthquake Prognostics*, Berlin, March.

Nazario, C. (2000), *The John Hancock Tower: Failures*. [Online] Available at http://matdl.org/failurecases/John_hancock_tower (Accessed 3 February 2013).

Ok, S.Y., Song, J. and Park, K.S. (2008), 'Optimal performance design of bi-tuned mass damper systems using multi-objective optimization', *KSCE Journal of Civil Engineering*, 12(5), 313–322.

Popplewell, N. and Semercigil, S.E. (1989), 'Performance of the bean bag impact damper for a sinusoidal external force', *Journal of Sound and Vibration*, 133(2), 193-223.

Sadhu, A. and Narasimhan, S. (2012), 'Identification of de-tuning level of tuned-mass-damper system using time-series analysis', *Journal of Mechanical Engineering and Automation*, 2(1), 1-8.

Sakamoto, M. and Kobori, T. (1996), 'Applications of structural response control (Reviews from the past and issues toward the future)', *Proceedings of the Second International Workshop on Structural Control*, Hong Kong.

Scheller, J. and Starossek, U. (2011), 'A versatile active mass damper for structural vibration control', *Proceedings of the 8th International Conference on Structural Dynamics EURODYN 2011*, Leuven, Belgium, July.

Schmidt, J.R. (2012), *The world's first skyscraper*. [Online] Available at http://www.wbez.org/blog/john-r-schmidt/2012-03-01/worlds-first-skyscraper-96741 (Accessed: 23 May 2013).

Shariatmadar, H. and Razavi, H. M. (2010), 'Multi-tuned mass dampers for seismic response reduction of mid and high-rise buildings', *Proceedings of 5th National Congress on Civil Engineering*, Masshad, Iran.

Soong, T.T. and Spencer, B.F. (2002), 'Supplemental energy dissipation: state-of-the-art and state-of-the-practice', *Engineering Structures*, 24(3), 243-259.

Spencer, B.F. and Sain, M.K. (1997), 'Controlling buildings: A new frontier in feedback', *IEEE Control Systems Magazine*, (17)6, 19-35.

Symans, M., Charney, F., Whittaker, A., Constantinou, M., Kircher, C., Johnson, M., and McNamara, R. (2008). 'Energy dissipation systems for seismic applications: Current practice and recent developments', *Journal of Structural Engineering.* 134, 3–21.

Taylor, D.P. (2003), *History, Design, and Application of Fluid Dampers in Structural Engineering.* Taylor Devices, Inc. [Online] Available at http://www.taylordevices.com/papers/history/design.htm (Accessed: 14 March 2013).

Xu, K. and Igusa, T. (1992), 'Dynamic characteristics of multiple substructures with closely spaced frequencies', *Earthquake Engineering and Structural Dynamics*, 21, 1059–1070.

Yamaguchi H. and Harnpornchai N. (1993), 'Fundamental characteristics of multiple tuned mass dampers for suppressing harmonically forced oscillations', *Earthquake Engineering and Structural Dynamics*, 22, 51–62.

Zuo, L. (2009), 'Effective and robust vibration control using series multiple tuned-mass dampers', *Journal of Vibration and Acoustics*, 131, 1-11.

APPENDIX A: PROKON SIMULATIONS

Changing the Model's Stiffness

The 1m Model

Translational Vibration in the X-direction

Natural frequency for
Mode no 1: 2.48 Hz

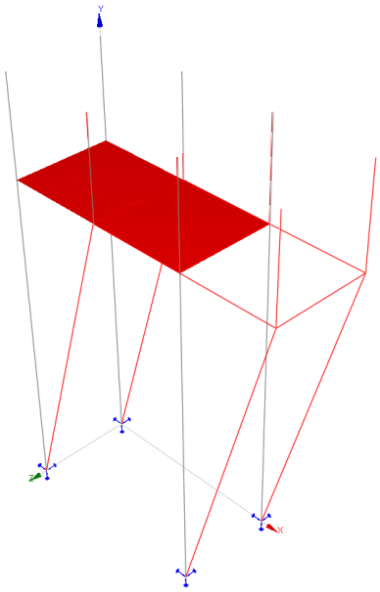

Translational Vibration in the Y-direction

Natural frequency for
Mode no 2: 2.55 Hz

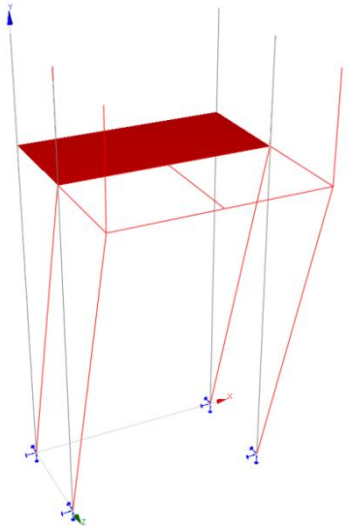

Torsional Vibration

Natural frequency for
Mode no 3: 4.29 Hz

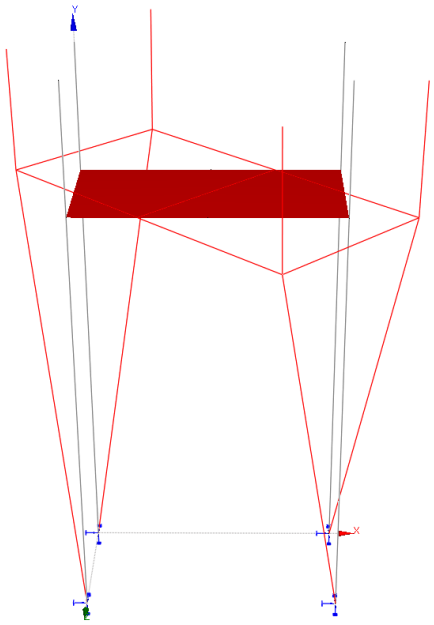

The 0.75m Model

Translational Vibration in the X-direction

Natural frequency for
Mode no 1: 3.77 Hz

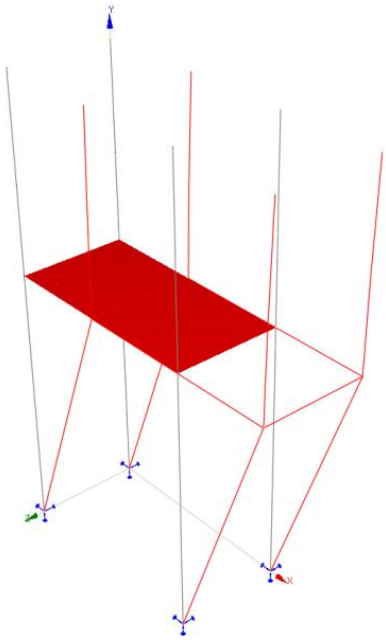

Translational Vibration in the Y-direction

Natural frequency for
Mode no 2: 3.79 Hz

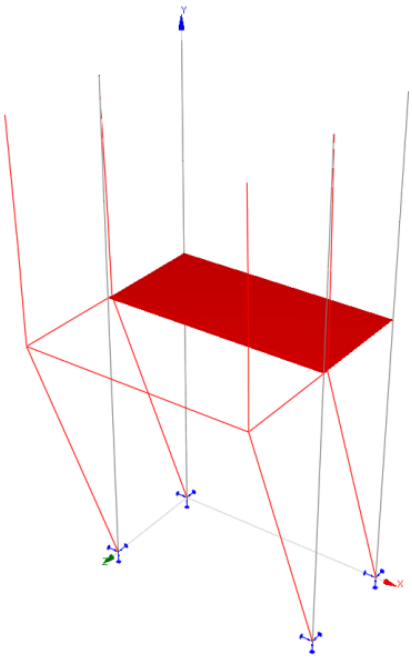

Torsional Vibration

Natural frequency for
Mode no 3: 5.83 Hz

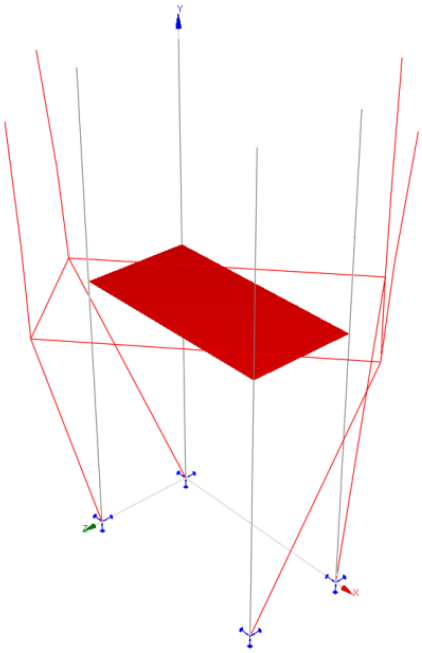

The 0.50m Model

Translational Vibration in the X-direction

Natural frequency for
Mode no 1: 6.65 Hz

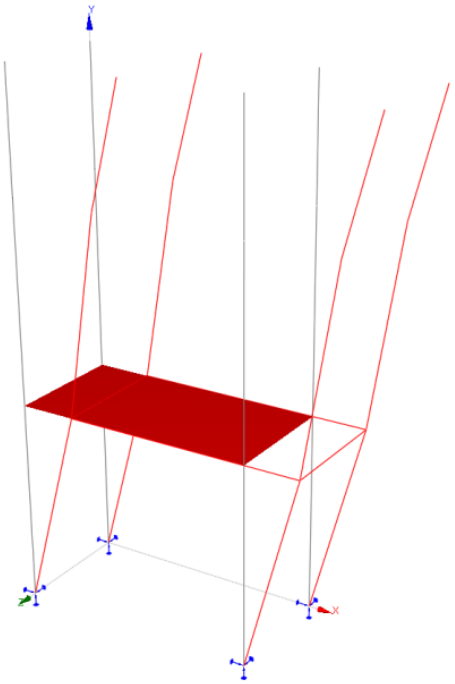

Translational Vibration in the Y-direction

Natural frequency for
Mode no 2: 6.72 Hz

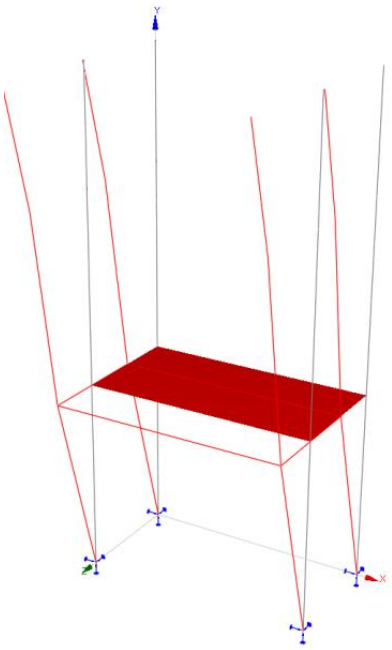

Torsional Vibration

Natural frequency for
Mode no 3: 12.44 Hz

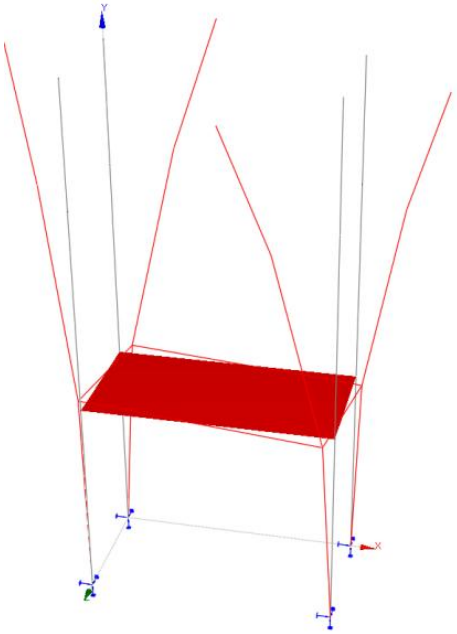

Changing the Model's Mass

The 14kg Model

Translational Vibration in the X-direction

Natural frequency for
Mode no 1: 2.48 Hz

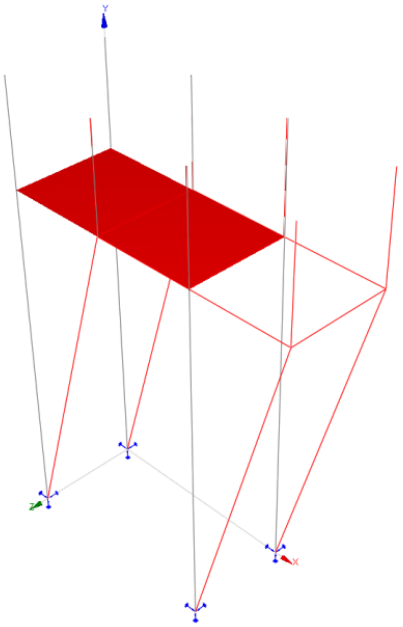

Translational Vibration in the Y-direction

Natural frequency for
Mode no 2: 2.55 Hz

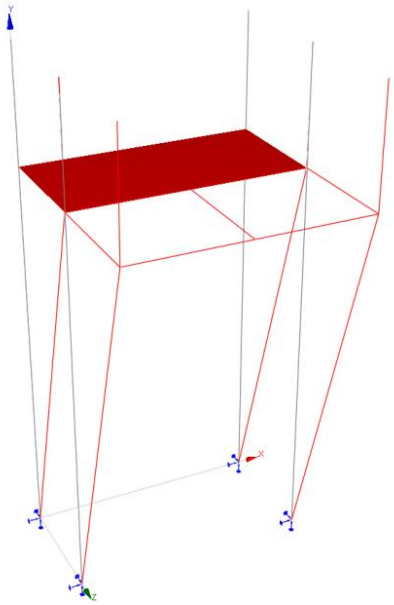

Torsional Vibration

Natural frequency for
Mode no 3: 4.29 Hz

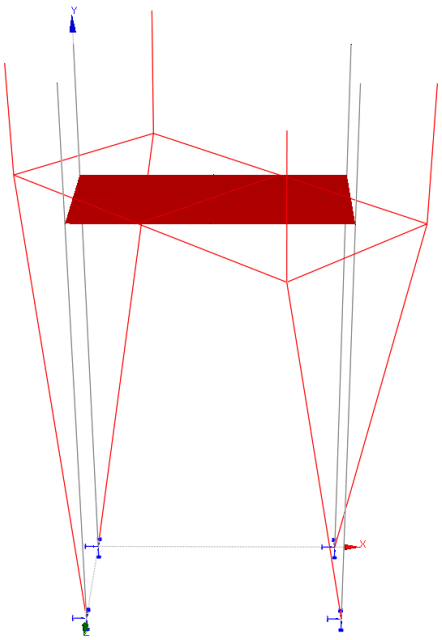

The 20kg Model

Translational Vibration in the X-direction

Natural frequency for
Mode no 1: 2.04 Hz

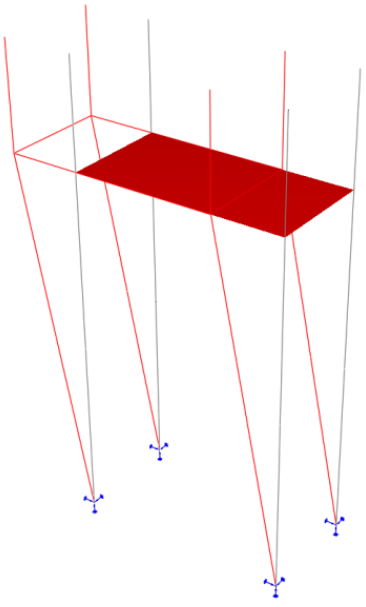

Translational Vibration in the Y-direction

Natural frequency for
Mode no 2: 2.13 Hz

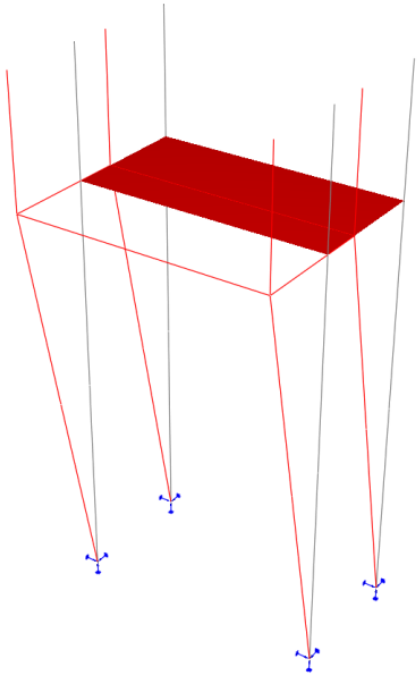

Torsional Vibration

Natural frequency for
Mode no 3: 4.47 Hz

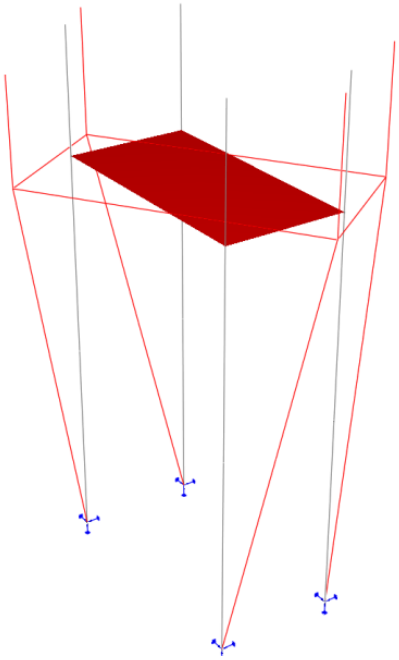

The 32kg Model

Translational Vibration in the X-direction

Natural frequency for
Mode no 1: 1.78 Hz

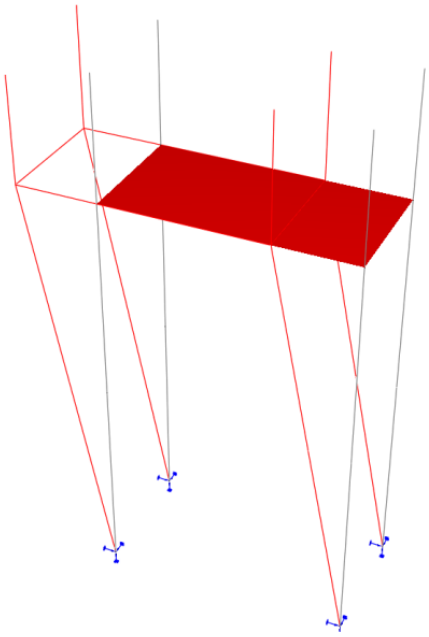

Translational Vibration in the Y-direction

Natural frequency for
Mode no 2: 1.88 Hz

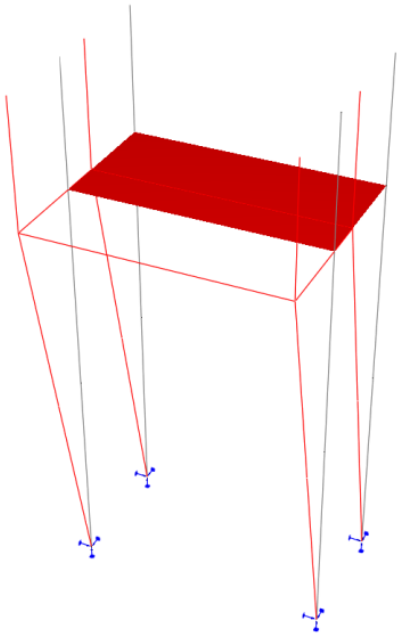

Torsional Vibration

Natural frequency for
Mode no 3: 3.41 Hz

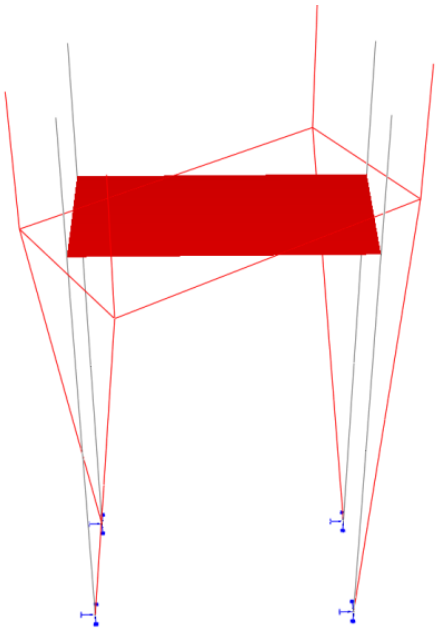

APPENDIX B: PHOTOGRAPHS

PATMD CONNECTION CONFIGURATIONS

Configuration 1

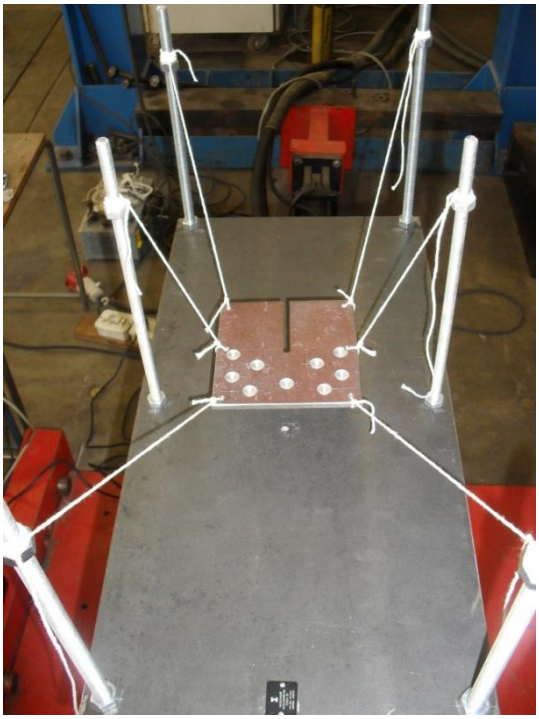

Configuration 2

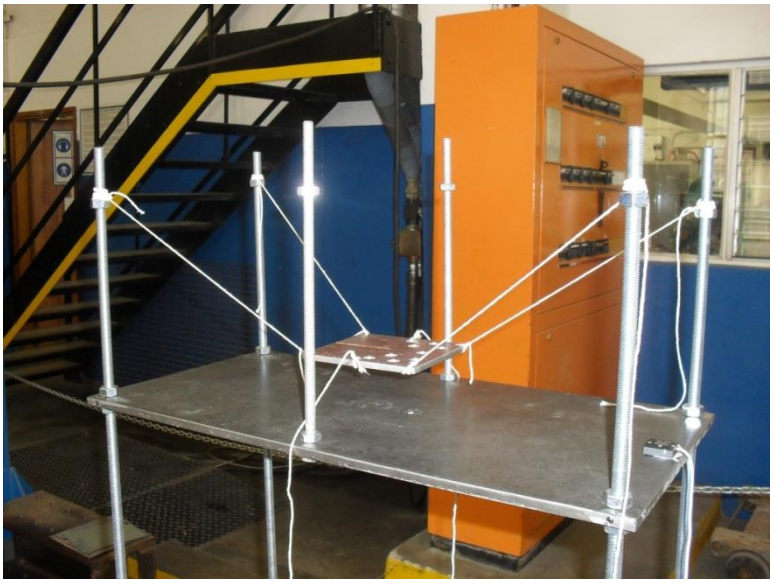

Configuration 3

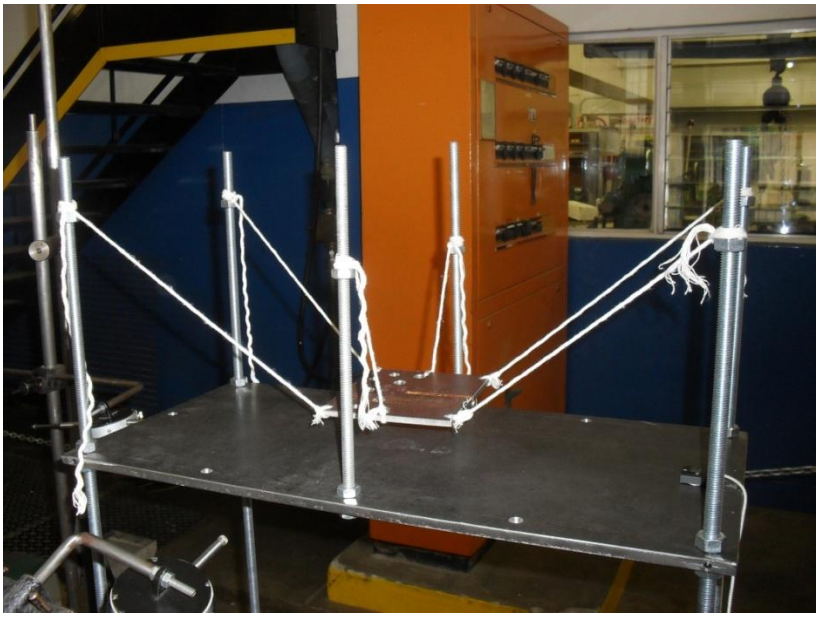

Configuration 4

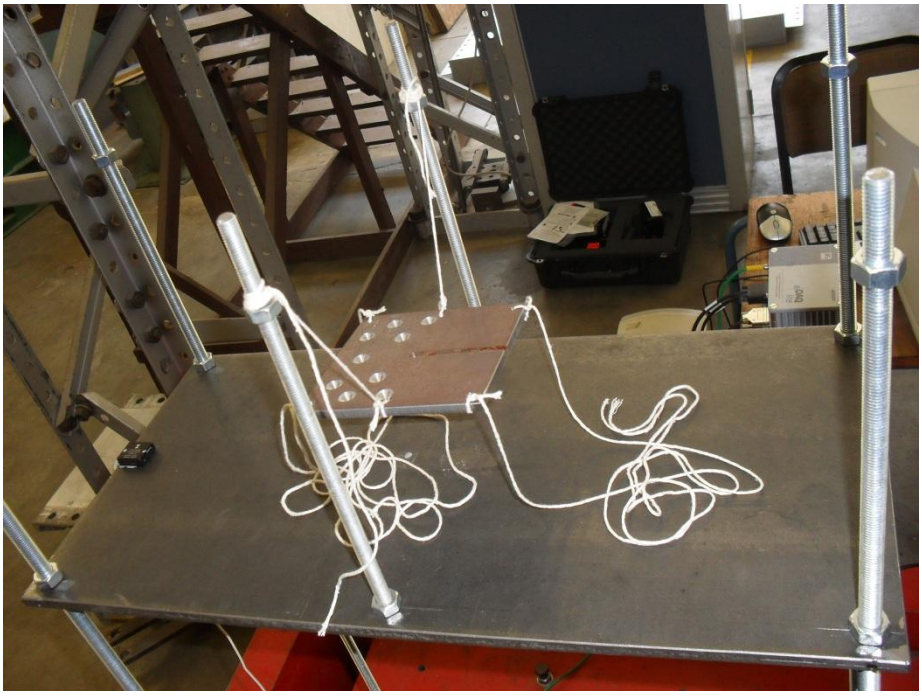

Configuration 5

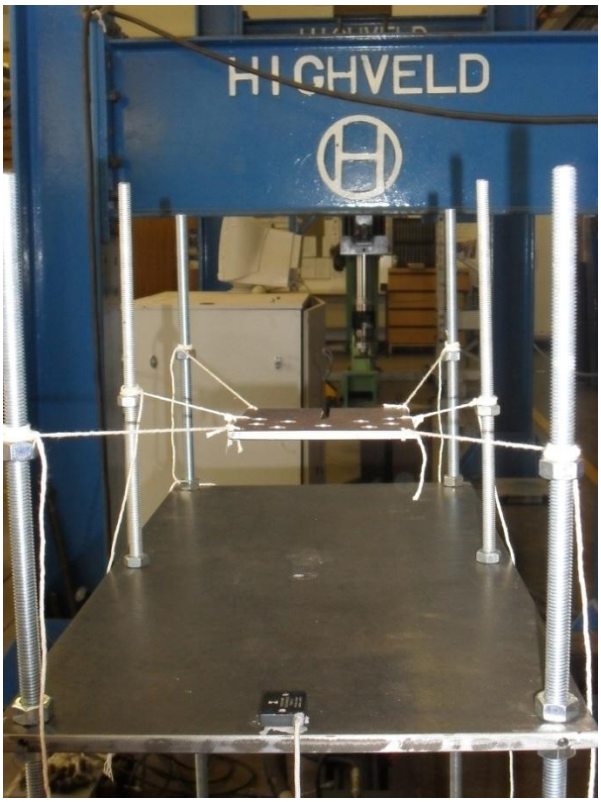

Configuration 6

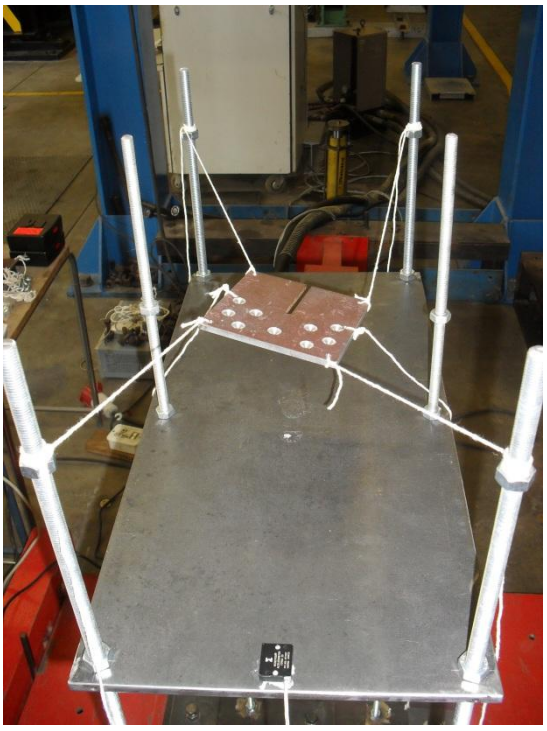

Configuration 7

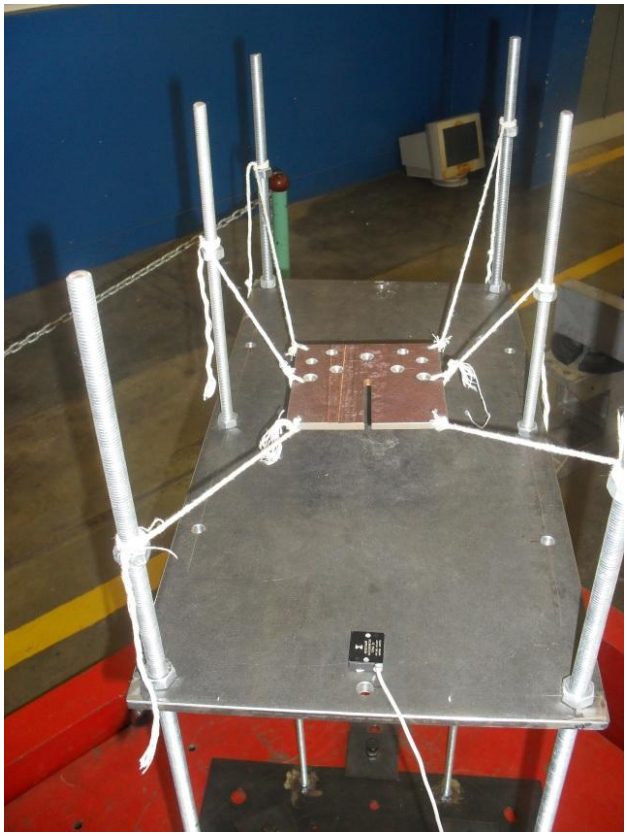

Configuration 8

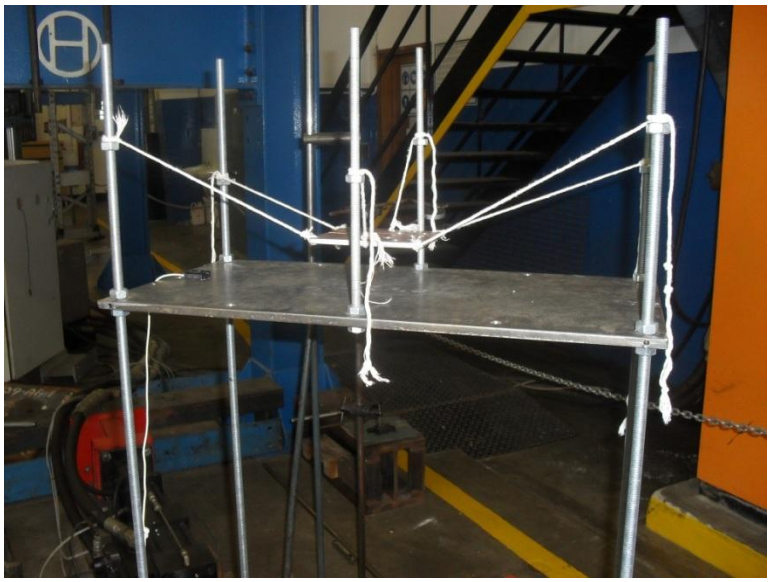

MISCELLANEOUS PHOTOGRAPHS

The Experimental Set-up: *The test model secured to the shaking table, with the computer used to analyse the data in the background.*



The Base Connection: *The test model is bolted to the shaking table.*

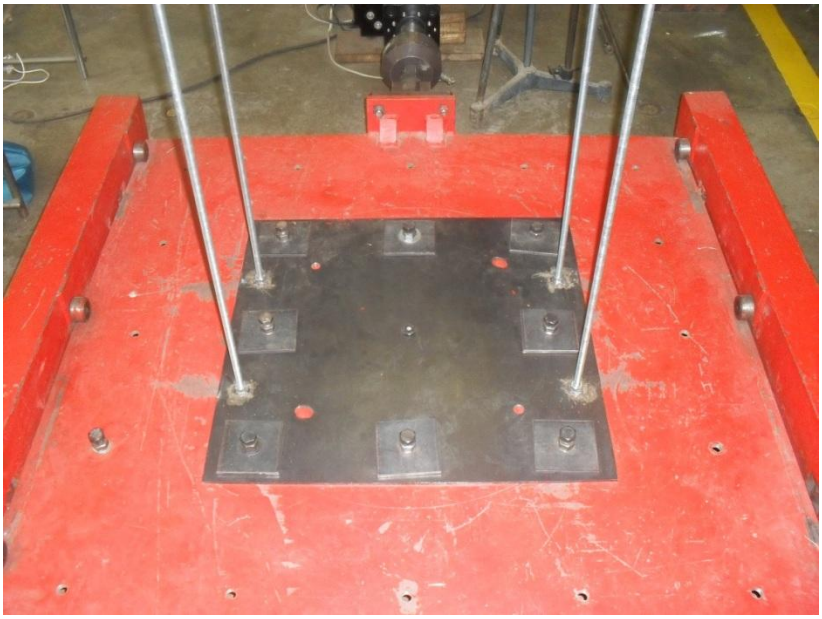

The Dial Gauges: *Dial gauges were used to measure the initial displacement in the free vibration tests.*

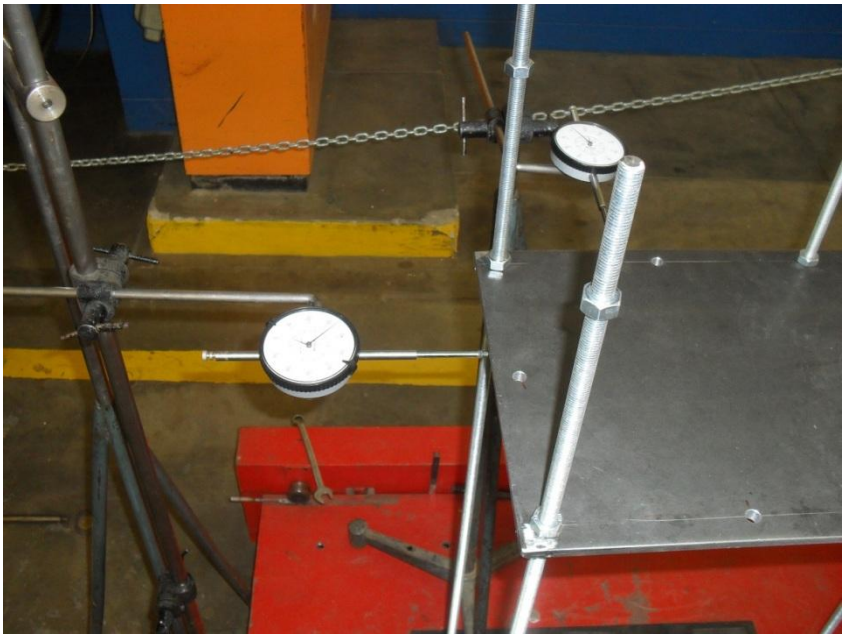

The Shaking Table : *The shaking table control system.*

